RELATIONSHIPS BETWEEN LABORATORY MEASURED CHARACTERISTICS

OF HMA AND FIELD COMPACTABILITY

Except where referenced is made to the work of others, the work described in this thesis is my own or was done in collaboration with my advisory committee. This thesis does not include proprietary or classified information.

_____

Fabricio Leiva-Villacorta

Certificate of Approval:

David Timm Assistant Professor Civil Engineering	Elton Ray Brown, Chair Director National Center for Asphalt Technology
Randy West Assistant Director National Center for Asphalt Technology	Joe F. Pittman Interim Dean Graduate School

RELATIONSHIPS BETWEEN LABORATORY MEASURED CHARACTERISTICS OF HMA AND FIELD COMPACTABILITY

Fabricio Leiva-Villacorta

A Thesis

Submitted to

the Graduate Faculty of

Auburn University

in Partial Fulfillment of the

Requirements for the

Degree of

Master of Science

Auburn University
December 17, 2007

RELATIONSHIPS BETWEEN LABORATORY MEASURED CHARACTERISTICS

OF HMA AND FIELD COMPACTABILITY

Fabricio Leiva-Villacorta

Signature of Author

Date of Graduation

VITA

Fabricio Leiva-Villacorta was born August 20, 1979, in Heredia, Costa Rica. He graduated with a Bachelors of Science Degree in Civil Engineering from the University of Costa Rica in 2003. After graduation he worked with the National Laboratory of Materials – University of Costa Rica for 2 years. He also graduated with a Masters Degree in Business Administration from the State University at Distance in 2005 while worked in Costa Rica. In fall 2005 he began his studies as a graduate student at Auburn University in pursuit of a Masters of Science degree in Civil Engineering.

THESIS ABSTRACT

RELATIONSHIPS BETWEEN LABORATORY MEASURED CHARACTERISTICS OF HMA AND FIELD COMPACTABILITY

Fabricio Leiva-Villacorta

Master of Science, December 17, 2007
(MBA, UNED-Costa Rica, 2005)
(B.S., University of Costa Rica, 2003)

159 Typed Pages

Directed by E. Ray Brown

Compactability of HMA mixtures is often used to describe how easy or difficult a mixture is to compact on a roadway. Several asphalt researchers have proposed laboratory measured parameters of mixtures and/or their components as indicators of HMA compactability and/or resistance to permanent deformation. However, most of these measured characteristics have not been validated with actual field performance.

The first part of this study includes a comparison between the laboratory compactability parameters Compaction Energy Index (CEI), number of gyrations to reach 92% of G_{mm} ($N@92\%G_{mm}$), Slope, Locking Point and Bailey Method ratios. The data used for this stage came from Superpave mixtures placed on the NCAT Test Track in the

first two cycles (quality control samples). It was found that CEI, N@92%G_{mm}, Slope, Locking Point can be used to represent the applied energy to reach a level of compaction in the SGC.

The second part of this study includes the determination of a field compactability indicator based on rolling operation (Accumulated Compaction Pressure – ACP) and correlation between this indicator and laboratory parameters. When all the combined data were used to correlate ACP and lab compactability parameters, the values of simple linear correlation (R-value) were always near zero. The results showed that t/NMAS and temperature significantly affected the applied compactive effort to reach the post-construction density level.

The third part of this project includes compaction of specimens using the SGC at to meet the 8% air voids at thicknesses equal to those in the field. A multiple regression analysis showed that eighty two percent of the variability in the ACP can be explained by four predictors: PCSI, FAc ratio, lift temperature and number of gyrations to reach the post construction density level at lift thickness (N@field-density).

The last part of this study involved density testing during the rolling operation. The purpose of this part was to determine the field compaction energy required to produce the same level of density as samples compacted in the laboratory and correlate that energy with laboratory compaction parameters. A multiple regression analysis provided a model with ACP@92%G_{mm} as the response, while ninety two percent of the variability in the response can be explained by the interaction temperature*thickness, % passing No 200 sieve, actual PG grade, slope, locking point/Slope ratio, FAc ratio and PCSI square.

ACKNOWLEDMENTS

The author would like to thank Dr. Randy West and Dr. E. Ray Brown for all of their support in this endeavor. Also the author would like to express his gratitude for all the support he received from the staff at the National Center for Asphalt Technology. Finally, to his wife Adriana, very special thanks are given for all of her patience and hard work.

Style manual used: Proceedings, Association of Asphalt Paving Technologists

Computer software used: Microsoft Word, Microsoft excel, Minitab, Pine Pave.

TABLE OF CONTENTS

LIST OF TABLES xiii

LIST OF FIGURES xv

CHAPTER 1. INTRODUCTION 1

1.1 BACKGROUND 1

1.2 OBJECTIVES 2

1.3 SCOPE 3

CHAPTER 2. LITERATURE REVIEW 5

2.1 FIELD COMPACTION 5

2.1.1 Introduction 5

2.1.2 Aggregate characteristics 6

2.1.3 Environmental conditions 7

2.1.4 Binder characteristics 7

2.1.5 Compaction equipment and roller operation 8

2.1.6 Gradation 9

2.1.7 Lift thickness 11

2.2 LABORATORY COMPACTION 15

2.2.1 Introduction 15

2.2.2 Potential effect of the internal angle of gyration 16

2.3 LABORATORY MIX PARAMETERS USED TO DESCRIBE COMPACTABILITY 16
2.3.1 Introduction 16
2.3.2 The percentage of maximum theoretical specific gravity at N_{ini} ($\%G_{mm}@N_{ini}$). 17
2.3.3 Compaction Energy Index (CEI) 17
2.3.4 Compaction slope determined from compaction in the Superpave Gyratory Compactor (SGC). 18
2.3.5 The number of gyrations with the SGC to reach the Locking Point of the mixture. 20
2.3.6 Other densification indices 21
2.4 AGGREGATE CHARACTERISTICS RELATED TO COMPACTABILITY 23
2.4.1 Introduction 23
2.4.2 Bailey Method ratios 24
2.4.3 Primary Control Sieve Index PCSI 28
2.5 STUDIES THAT RELATE LABORATORY CHARACTERISTICS AND FIELD COMPACTABILITY 29
2.5.1 C-value method 29
2.5.2 The modified Mohr method 31
2.5.3 The k-factor method 32
2.6 SUMMARY OF FINDINGS 33
CHAPTER 3. RESEARCH PLAN 36
3.1 OVERVIEW 36
3.2 ANALYSIS OF TEST TRACK MIXES 39

3.2.1 Material and Mixture Properties 39
3.2.2 Test Track construction 39
3.3 Accumulated Compaction Pressure (ACP) as a field compactability indicator 43
3.4 Laboratory compaction parameters 45
3.5 Correlation of ACP and laboratory parameters 46
3.6 Material and Mixture Properties for Validation Analysis 50
CHAPTER 4. RESULTS AND ANALYSES 52
4.1 Conceptual hypothesis for explaining expected trends 52
4.2 Laboratory compaction parameters 53
4.2.1 Parameters obtained from Densification Curve 54
4.2.2 Gradation parameters as indicators of compactability 61
4.2.3 Comparison between laboratory measured characteristics of HMA 64
4.2.4 Effect of physical properties on the SGC parameters 68
4.2.5 Assessment of variability among observations (multivariate statistical analysis) 72
4.3 Field compaction 79
4.3.1 Conceptual hypothesis for explaining expected trends 80
4.3.2 Analysis of the Accumulated compaction Pressure 82
4.3.3 Analysis of pairs 88
4.4 Correlations between ACP and laboratory compaction parameters 92
4.5 Compaction of specimens using the SGC at field thickness 97
4.6 Correlations between ACP@92%Gmm and lab compaction parameters 102

4.7 SUMMARY OF FINDINGS 105

4.8 APPLICABILITY OF THE ACP CONCEPT FOR VALIDATION PURPOSES 108

CHAPTER 5. CONCLUSIONS AND RECOMMENDATIONS 111

REFERENCES 114

APPENDIX A. MATERIAL PROPERTIES 118

APPENDIX B. COMPACTION INFORMATION 132

APPENDIX C. INFORMATION OF FIELD AND LABORATORY STUDY 136

LIST OF TABLES

Table 2.1: Definition of Fine- and Coarse-Graded Mixes *(9)* 10

Table 2.2: Recommended lift thickness for HMA mixes *(9)*..... 11

Table 2.3: Summary of minimum t/NMAS to provide 7 % air voids in laboratory *(2)* ... 13

Table 2.4: Recommended ranges of aggregate Ratios..... 27

Table 2.5: Recommended ranges of aggregate Ratios for SMA mixes..... 28

Table 2.6: Control sieves 28

Table 3.1: Summary of the experimental plan..... 38

Table 3.2: Summary of mix types evaluated 40

Table 3.3: Compaction Pressure per Pass (psi)..... 45

Table 3.4: Properties of NCAT Test Track mixtures 2nd and 3rd cycle 48

Table 3.5: Data from NCHRP 9-27 mixtures 51

Table 4.1: Single correlation among parameters 65

Table 4.2: Principal effects - MANOVA analysis. 71

Table 4.3: Canonical functions on canonical correlation (*). 74

Table 4.4: Factorial experiment analysis 76

Table 4.5: Cluster separation and properties..... 78

Table 4.6: Post-construction density level (%G_{mm}) sorted by Gradation Type and Test Track cycle..... 80

Table 4.7: Description of levels per factor used in analysis of variance 86

Table 4.8: ANOVA for ACP 87

Table 4.9: Comparison of ACP by various subjects 89

Table 4.10: Comparison of CEI by various subjects 91

Table 4.11: Single correlation between ACP and some parameters 93

Table 4.12: Correlation and expected trend between ACP and compactability parameters including mix properties (Tangents only, cycle 1) 94

Table 4.13: Correlation and expected trend between ACP@92% of G_{mm} and compactability parameters 103

Table 4.14: Summary of models used to correlate field and laboratory compactability 107

Table 4.15: Single correlation among laboratory parameters based on NCHRP 9-27 mixtures..... 109

LIST OF FIGURES

Figure 2.1: 9.5 mm NMAS Superpave Gradations (2). 10

Figure 2.2: Relationships of t/NMAS and Air Voids for Superpave Mixes (2). 12

Figure 2.3: Relationships of Gradations and laboratory Air Voids for Superpave Mixes (2). 13

Figure 2.4: Relationship of Air Voids and Thickness for 19.0 mm Coarse-Graded with Modified Asphalt (2) 14

Figure 2.5: Schematic of the Superpave Gyratory Compactor. 15

Figure 2.6: Illustration of CEI and TDI Indices (4) 18

Figure 2.7: Illustration of Compaction Slope (14). 19

Figure 2.8: Effect of mixture properties on compaction slope (15). 20

Figure 2.9: Energy Indices CEI and TDI; CFI and TFI (18). 22

Figure 2.10: Correlation between CEI and CFI; TDI and TFI (18). 23

Figure 2.11: Illustration of the PCSI for 12.5 mm NMAS gradations 29

Figure 2.12: The compaction process according to the C-value method. 30

Figure 3.1: Frequency distribution of test track layer thicknesses. 43

Figure 3.2: Contact arc of the drum on the mat 45

Figure 3.3: Relationship between nuclear density (pcf), lift temperature, compaction time and roller pattern. 49

Figure 3.4: Relationship between ACP and density (%G_{mm}). 49

Figure 3.5: Illustration of the model used to fit field compaction data. 50

Figure 4.1: %G_{mm}@N_{ini} sorted by Gradation Type. 55

Figure 4.2: Relationship between %G_{mm}@N_{ini} and asphalt content. 56

Figure 4.3: Relationship between %G_{mm}@N_{ini} and PCSI. 56

Figure 4.4: Compaction Energy Index (CEI) sorted by Gradation Type. 57

Figure 4.5: Relationship between PCSI and %G_{mm}@N_{ini} and PCSI and CEI for SMA mixtures..... 58

Figure 4.6: Traffic Densification Index (TDI 92-96) sorted by Ndes. 59

Figure 4.7: Compaction Slope sorted by Gradation Type. 60

Figure 4.8: N @ Locking Point sorted by Gradation Type. 61

Figure 4.9: CA Ratio sorted by Gradation Type.....63

Figure 4.10: FAc Ratio sorted by Gradation Type. 63

Figure 4.11: Relationship between %Gmm@Nini and CEI.....67

Figure 4.12: Relationship between N@92%Gmm and CEI 67

Figure 4.13: Post-construction density level (%G_{mm}) sorted by Gradation Type. 79

Figure 4.14: ACP sorted by Gradation Type. 83

Figure 4.15: ACP sorted by Gradation Type and cycle. 84

Figure 4.16: Thickness and T/NMAS ratio for each cycle. 85

Figure 4.17: Temperature measured at different compaction stages. 85

Figure 4.18: Main Effects Plot (fitted means) for ACP. 87

Figure 4.19: Interaction Plot (fitted means) for ACP. 88

Figure 4.20: Comparison of ACP by various subjects. 90

Figure 4.21: Comparison of CEI by various subjects. 91

Figure 4.22: Effect of thickness on ACP. 93

Figure 4.23: Relationship between ACP and N@92%G_{mm}. 95

Figure 4.24: Relationship between ACP and number of cycles to reach 92%Gmm and field density. 98

Figure 4.25: Compaction of lab specimens at 50 mm. 99

Figure 4.26: Compaction of lab specimens at 100 mm. 99

Figure 4.27: Effect of reducing thickness on lab specimens 100

Figure 4.28: Comparison of predicted ACP for test track sections and NCHRP 9-27 projects using Equation 18 110

CHAPTER 1. INTRODUCTION

1.1 Background

Meeting the specified density of HMA is often cited as a difficult challenge for asphalt pavement construction *(1).* Since the introduction of Superpave designed mixtures this challenge has become a bigger issue. Overall, Superpave designed mixes have been cited as more difficult to compact than Marshall/Hveem mixes and greater compactive efforts have been needed to achieve similar density levels *(1).* Data from research projects such as NCHRP 9-27 *(2)* and NCHRP 9-9 *(3)* have also shown that density was less than desirable for many field projects.

The importance of achieving a well compacted pavement is crucial to avoiding problems with numerous types of distresses including permanent deformation, moisture damage, and cracking. Numerous factors affect the contractor's ability to achieve the target density for HMA mixtures, including weather, support of underlying layers, layer thickness, compaction equipment, experience of roller operators and mixture characteristics.

Compactability of HMA mixtures is often used to describe how easy or difficult a mixture is to compact on a roadway. Several asphalt researchers *(4, 5)* have proposed laboratory measured parameters of mixtures and/or their components as indicators of

HMA compactability and/or resistance to permanent deformation. However, most of these measured characteristics have not been validated with actual field performance.

1.2 Objectives

The primary objective of this research was to evaluate a variety of mixture characteristics and determine if they are correlated to compactability in the field. The mixture characteristics included in the evaluation were:

1. The percentage of maximum theoretical specific gravity at N_{ini} ($\%G_{mm}$ @ N_{ini}).
2. Compaction slope determined from compaction in the Superpave Gyratory Compactor (SGC).
3. Number of gyrations to achieve 92% of the maximum theoretical specific gravity ($N@92\%G_{mm}$).
4. The Compaction Energy Index determined from the SGC compaction process as recommended by Bahia *(4).*
5. The number of gyrations with the SGC to reach the Locking Point of the mixture.
6. The Coarse and Fine Aggregate Ratios as determined using the Bailey Method recommended by Pine *(5).*
7. Mix parameters such as gradation, aggregate shape, binder grade, and mix volumetric properties.
8. The Primary Control Sieve Index PCSI, which is the difference in percent passing from gradation to primary control sieve. It represents the relative coarseness or fineness of the gradation.

A second objective was to explain why some mixtures are more compactable than others using basic mix parameters such as gradation, aggregate shapes, binder grade, and mix volumetric properties. This analysis included parameters obtained from quality control samples and specimens compacted to the field lift thickness.

The underlying goal of this study was to identify a practical method to evaluate the compactability of an HMA mixture in the laboratory for use by mix designers and quality control technicians to help them achieve suitable levels of density in the field.

1.3 Scope

To accomplish the objectives of this study, a literature review was completed to understand the different parameters used to measured compactability in the lab. HMA mixtures placed on the NCAT Test Track in the first two cycles were used to calculate those parameters (Thirty-five different surface mixtures and seven binder mixtures placed on the track in 2000, seventeen surface mixtures and twenty-two binder mixtures placed in 2003 were used in this analysis).

The data used to determine the laboratory measured mix characteristics were obtained from quality control samples taken during track construction. Triplicate gyratory samples were compacted for each section. Compaction operations at the track were well documented and provided good information about the compactability of the mixtures in the field. These data were used to determine the total compaction energy applied by the rollers during construction.

Each of the mixture parameters listed in the objectives were calculated from the quality control samples taken during construction. Statistical analyses were used to describe the relationships among these parameters. The effect of different mix properties over these parameters was also evaluated. Regression between these parameters and the field compaction energy were analyzed. The laboratory measured parameters which yield the best correlations were analyzed further by performing multiple stepwise regressions with basic mixture properties.

CHAPTER 2. LITERATURE REVIEW

This chapter presents an overview of the research that has been conducted in the following areas:

1. Factors affecting field compaction,
2. Laboratory compaction,
3. Laboratory mix parameters used to describe compactability,
4. Aggregate characteristics related to compactability,
5. Studies that relates laboratory characteristics and field compactability

2.1 Field compaction

2.1.1 Introduction

Compaction is the process by which the volume of air in an HMA mixture is reduced by the application of external forces to reorient the constituent aggregate particles into a more closely spaced arrangement. The reduction of air voids in a mixture produces an increase in HMA unit weight (6). HMA compaction is influenced by many factors; some related to the environment, some determined by mix and structural design and some under contractor and agency control during construction. Some of the most important

factors that affect field compaction include aggregate characteristics, environmental conditions, compaction equipment and roller operation, gradation and lift thickness.

2.1.2 Aggregate characteristics

Aggregate gradation influences key HMA parameters such as stiffness, stability, durability, permeability, workability, fatigue resistance, frictional resistance and resistance to moisture damage. The maximum aggregate size can be influential in compaction and lift thickness determination *(6).*

Coarse aggregate (aggregate retained in the No. 4 sieve). Surface texture, particle shape and the number of fractured faces can affect compaction. Rough surface texture, cubical or block shaped aggregate and highly angular particles will all increase the required compactive effort to achieve a specific density *(6).*

Midsize fine aggregate (between the 0.60 and 0.30-mm (No. 30 and No. 50) sieves). High amounts of midsize fine, rounded aggregate cause a mix to displace laterally or shove under roller loads. This occurs because the excess midsize fine, rounded aggregate results in a mix with insufficient voids in the mineral aggregate (VMA). This provides only a small void volume available for the binder to fill. Consequently, if the binder content is slightly high, it completely fills the voids and the excess binder serves to resist compaction by forcing the aggregate apart and lubricate the aggregate making it easy for the mix to laterally displace *(6).*

Fines or dust (aggregate passing the 0.075-mm (No. 200) sieve). Generally, a mix with high fines content will be more difficult to compact than a mix with low fines content. Gradations with excessive fines cause distortion because the large amount of fine

particles tend to push the larger particles apart and act as lubricating ball-bearings between these larger particles *(6).*

2.1.3 Environmental conditions

HMA temperature has a direct effect on the viscosity of the asphalt binder and thus compaction. As HMA temperature decreases, its asphalt cement binder becomes more viscous and resistant to deformation for a given compactive effort.

The major environmental conditions affecting field compactability are *(6):*

- Initial mat temperature. Higher initial mat temperatures require more time to cool down, which means more time available for compaction, but to high temperatures may damage the binder and make the mix tender during compaction.
- Temperature of the surface on which the mat is placed. Cooler surfaces will remove heat from the mat at a faster rate, decreasing the time available for compaction.
- Ambient temperature. Hotter air temperatures will remove heat from the mat at a slower rate, increasing the time available for compaction.
- Wind speed. Lower wind speeds will decrease mat heat loss by convection, which will increase the time available for compaction.

2.1.4 Binder characteristics

Asphalt binders with lower PG grade tend to deform more easily under load. Modified asphalt binders tend to have higher shear stiffness and lower permanent shear strain; in other words, they tend to increase resistance to permanent deformation.

The asphalt binder grade affects compaction through its viscosity. A binder that has higher viscosity will generally result in a mix that is more resistant to compaction *(6).* Mixes with low asphalt content are generally difficult to compact because of inadequate lubrication, whereas mixes with high asphalt content will be easier to compact. Since the viscosity of asphalt is highly temperature dependent, the temperature of the mix therefore affects its compactability.

2.1.5 Compaction equipment and roller operation

Compaction is done by any of several types of compactors or rollers, which reduce the volume of air in the mix and increase in HMA unit weight or density. There are three basic pieces of equipment available for HMA compaction: 1) the paver screed, 2) the steel wheeled roller (including vibratory rollers) and 3) the pneumatic tire roller.

The type and operational characteristics of rolling equipment can affect the level of density obtained in the asphalt concrete mix. For steel wheel rollers, a greater roller mass will result in more change in the degree of density per roller pass. Vibratory rollers use dynamic force to increase the compaction energy per pass. For pneumatic tire rollers, the compactive effort applied to the mix is a function of the wheel load and the tire pressure *(7, 8).*

In terms of roller operations, a number of variables affect the ability of the compaction equipment to adequately densify the mix. Operating at lower speeds allows the roller to remain in contact with a particular mat location longer than it would at higher speeds. Lowering equipment speed increases the shearing stress. Higher shearing stresses are more capable of rearranging aggregate into more dense configurations *(7).*

Earlier roller passes over hotter (as long as not too hot) HMA will increase density (decrease air voids) more than later passes over cooler HMA. Adding rollers can be used to increase the number of roller passes in a given time.

2.1.6 Gradation

Gradation is one of the most influential aggregate characteristics affecting HMA properties and performance. The aggregate size distribution influences almost every important property of asphalt mixes including volumetrics, stiffness, stability, durability, permeability, workability, fatigue resistance, frictional resistance and resistance to moisture damage *(1)*.

The simplest definition of fine and coarse gradations establishes a gradation that, when plotted on the 0.45 power gradation graph, falls mostly above (fine) or below (coarse) the 0.45 power maximum density line. These terms generally apply to dense graded aggregate. Dense or well-graded refers to a gradation that is near the 0.45 power curve for maximum density.

Many research studies, involving HMA gradations, have identified fine-graded and coarse-graded mixtures based on the definition given by the National Asphalt Pavement Association (NAPA) *(9)*. Percent passing certain sieve sizes for a given Nominal Maximum Aggregate Size (NMAS) is used to define fine-graded and coarse-graded mixes as shown in Table 2.1.

Other studies have used definitions based on the location of the gradation curve with respect to the maximum density line and the restricted zone *(3)*. Figure 2.1 illustrates 9.5 mm NMAS Superpave gradations where BRZ, ARZ and TRZ stand for below, above

and through the restricted zone, respectively. However, since the restricted zone has been eliminated from AASHTO specifications; coarse, fine and intermediate-graded (medium-graded) mixtures are more commonly used *(2)*.

Table 2.1: Definition of Fine- and Coarse-Graded Mixes *(9)*

Mixture NMAS	Coarse-Graded	Fine-Graded
37.5 mm (1 1/2")	< 35% Passing 4.75mm Sieve	> 35% Passing 4.75mm Sieve
25.0 mm (1")	< 40% Passing 4.75mm Sieve	> 40% Passing 4.75mm Sieve
19.0 mm (3/4")	< 35% Passing 2.36mm Sieve	> 35% Passing 2.36mm Sieve
12.5 mm (1/2")	< 40% Passing 2.36mm Sieve	> 40% Passing 2.36mm Sieve
9.5 mm (3/8")	< 45% Passing 2.36mm Sieve	> 45% Passing 2.36mm Sieve
4.75 mm (No. 4 Sieve)	N/A (No Standard Superpave Gradation)	

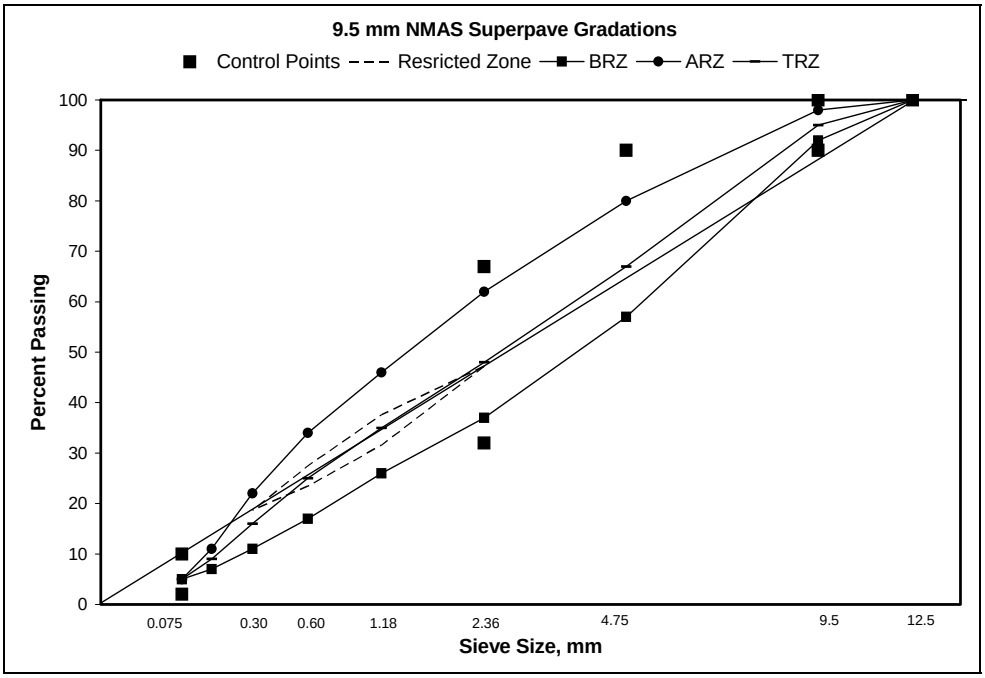

Figure 2.1: 9.5 mm NMAS Superpave Gradations *(2)*.

2.1.7 Lift thickness

Prior to Superpave implementation, the rule of thumb for lift thickness was two times the maximum aggregate size which is approximately equivalent to three times the NMAS. Table 2.2, from the "HMA Pavement Mix Type Selection Guide" *(9),* presents the recommended minimum lift thickness for various mixes. Overall, for fine-graded mixes the recommended t/NMAS ratio is from 2.4 to 5.0 and for coarse-graded mixes a range from 3.0 to 6.0. Dense-graded is in an intermediate range between fine-graded and coarse-graded mixes. In terms of minimum thickness, thicker layers are recommended for coarse-graded mixes than for fine-graded mixes.

Table 2.2: Recommended lift thickness for HMA mixes *(9)*

Mix	Minimum t/NMAS	Minimum Thickness, mm
4.75 mm dense-graded	2.6 – 4.0	12.5 – 19.0
9.5 mm fine-graded	2.6 – 3.9	25.0 – 37.5
9.5 mm coarse-graded	3.4 – 5.3	32.0 – 50.0
12.5 mm fine-graded	2.4 – 5.0	30.0 – 62.5
12.5 mm coarse-graded	3.0 – 6.0	37.5 – 75.0
19.0 mm fine-graded	2.6 – 3.7	50.0 – 70.0
25.0 mm dense-graded	3.0 – 4.0	75.0 – 100.0
37.5 mm dense-graded	2.7 – 4.0	100.0 – 150.0
9.5 mm SMA	2.6 – 3.9	25.0 – 37.5
12.5 mm SMA	3.0 – 4.0	37.5 – 50.0
19.0 mm SMA	2.6 – 3.9	50.0 – 75.0

Figure 2.2 was obtained from the NCHRP 9-27 study *(2)* and shows the impact t/NMAS on the air voids using the gyratory compactor. The figure indicates that as the

t/NMAS increases, the air voids decrease for a given NMAS. Figure 2.3 shows a general trend for Superpave mixtures for a given NMAS. ARZ mixes (Above the Restriction Zone mixes – Fine-Graded mixes) had the lowest air voids compared to the TRZ and BRZ mixes. This result suggested that fine-graded mixes are easier to compact compared to coarse-graded.

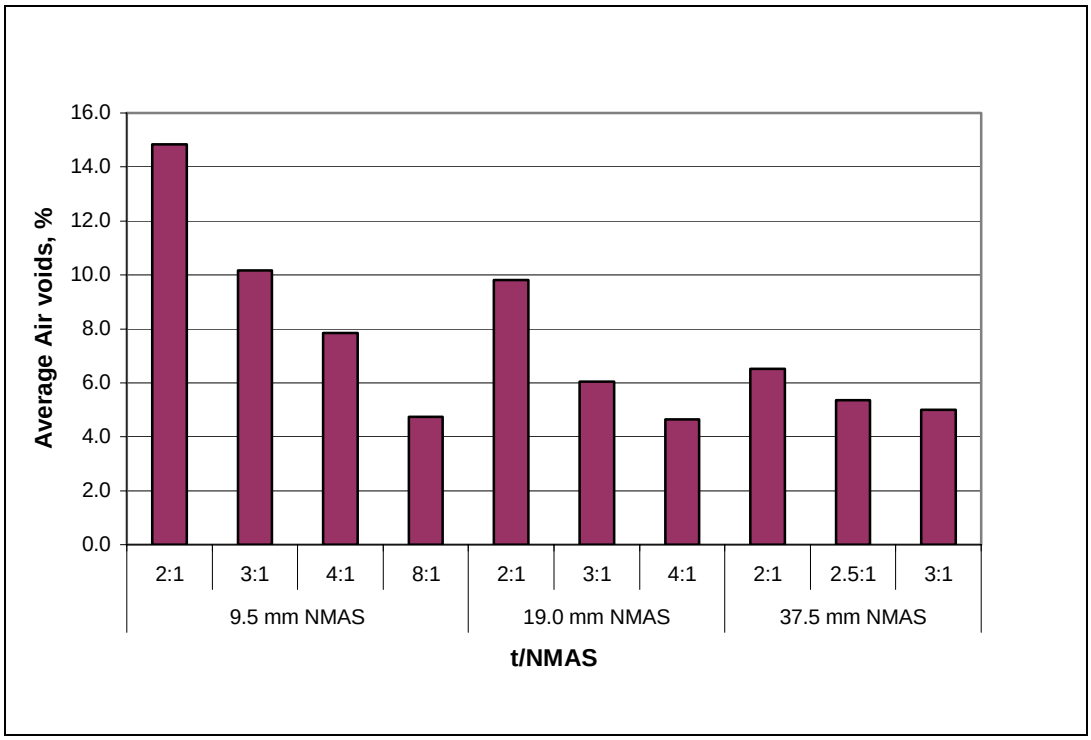

Figure 2.2: Relationships of t/NMAS and Air Voids for Superpave Mixes *(2)*.

Table 2.3 is the summary of minimum t/NMAS to provide 7 % air voids using the SGC for NCHRP 9-27 study. The results show that as the NMAS increases the minimum t/NMAS decreases and fine-graded mixes have lower desired t/NMAS values than the coarse-graded mixes.

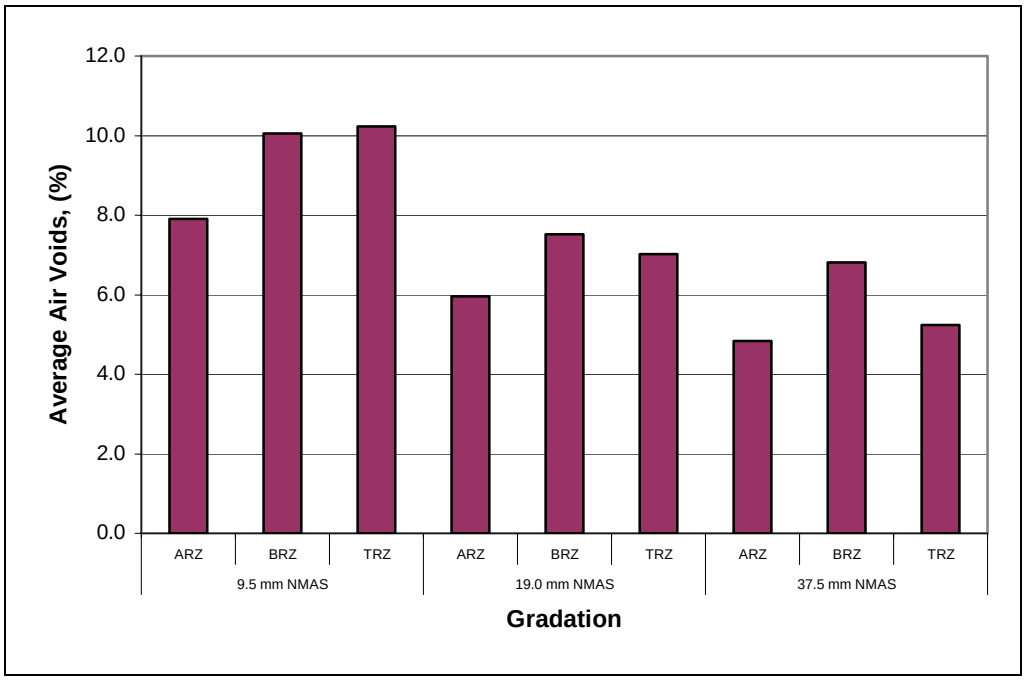

Figure 2.3: Relationships of Gradations and laboratory Air Voids for Superpave Mixes *(2)*.

Table 2.3: Summary of minimum t/NMAS to provide 7 % air voids in laboratory *(2)*

Mix	Minimum t/NMAS	Minimum Thickness, mm
9.5 mm ARZ	3.9	37
9.5 mm BRZ	5.2	49
9.5 mm TRZ	5.4	51
19.0 mm ARZ	2.4	46
19.0 mm BRZ	3.0	57
19.0 mm TRZ	2.8	53
37.5 mm ARZ	2.0	75
37.5 mm BRZ	2.4	90
37.5 mm TRZ	2.0	75
9.5 mm SMA	7.3	69
12.5 mm SMA	7.5	94
19.0 mm SMA	4.4	84

Figure 2.4 represents the general trend observed in NCHRP study for field compaction of a 19.0 mm coarse-graded mixture. The best fit lines indicate that as the thickness increased the air voids decreased until a point where excessive thickness resulted in an increase in air voids. This figure also pointed out the difference in the results due to types of rollers used which may indicate that minimum field t/NMAS criteria should include other factors besides density.

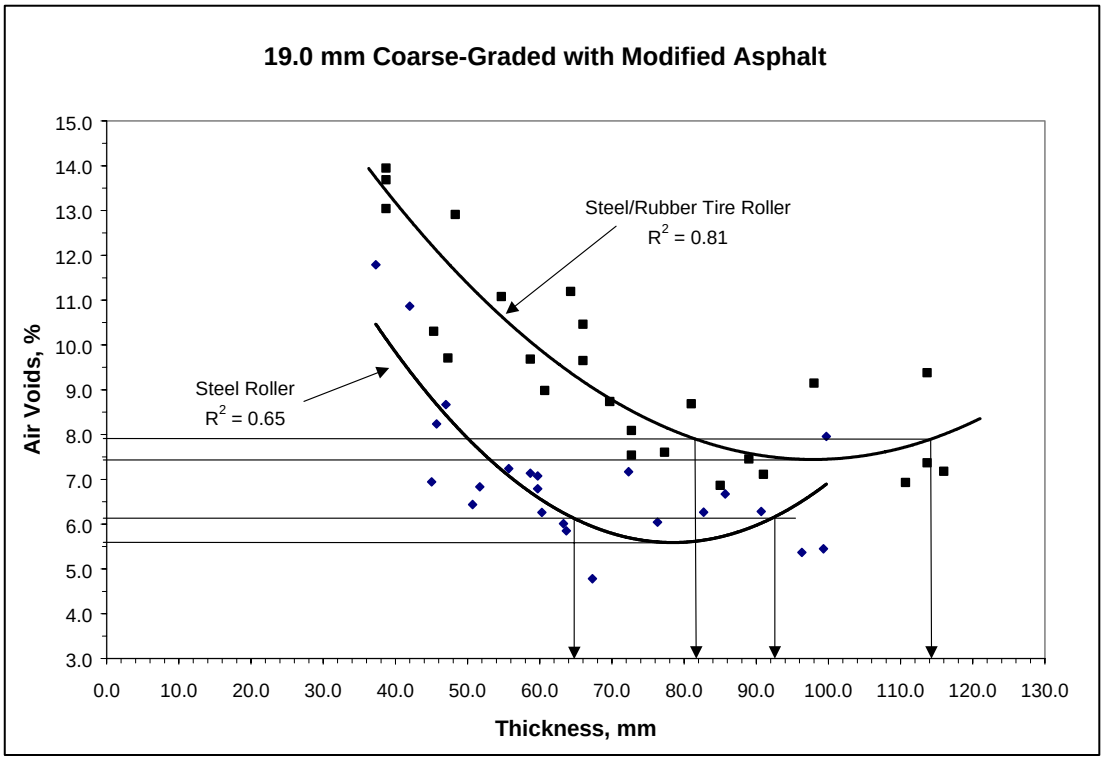

Figure 2.4: Relationship of Air Voids and Thickness for 19.0 mm Coarse-Graded with Modified Asphalt *(2)*.

2.2 Laboratory Compaction

2.2.1 Introduction

Superpave mix design method accounts for traffic loading and environmental conditions. One of the biggest differentiating aspects of the Superpave method compared to other methods such as Hveem and Marshall is the use of the gyratory compactor to simulate field compaction.

The Superpave gyratory compactor was developed to improve the ability to compact samples for mix design to simulate actual field particle orientation (6). A compaction pressure of 600 kPa (87 psi) is applied to the sample top. The sample is inclined at 1.25° and rotates at 30 revolutions per minute as the load is continuously applied (see Figure 2.5). This helps achieve a sample particle orientation that is somewhat like that achieved in the field after roller compaction. Initially, compactors from different manufactures provided different results (densities). Lack of control of the internal angle was the main reason for the difference between brands of compactors *(10).*

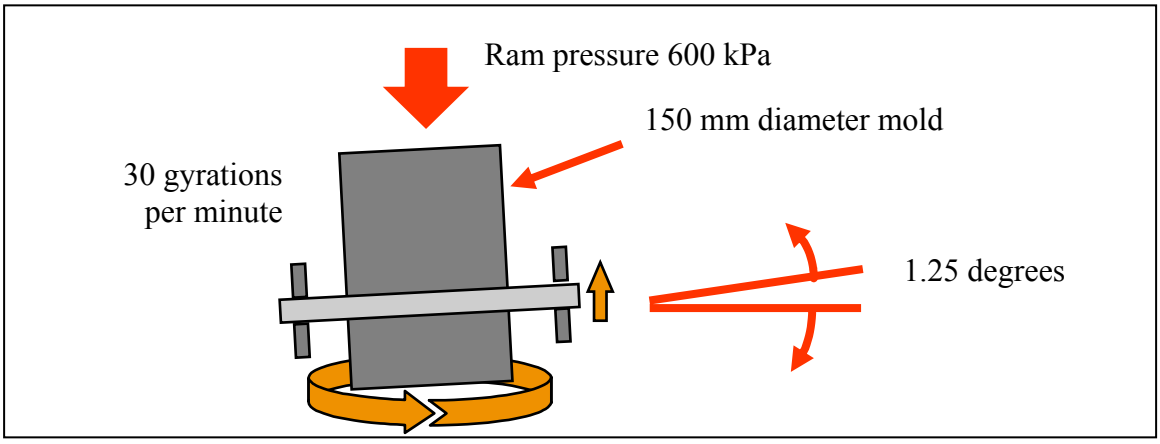

Figure 2.5: Schematic of the Superpave Gyratory Compactor.

2.2.2 Potential effect of the internal angle of gyration

One influencing factor that has been identified to explain the differences in sample density produced by different models and units of gyratory compactors is the dynamic internal angle (DIA) of gyration. Prowell et al. *(10)* measured the DIA on 112 different SGCs in Alabama (seven different models) and it was found that on average a change in 0.1 degrees of internal angle will result in a change of 0.010 G_{mb} units or a difference in air voids of approximately 0.4 percent. FHWA conducted a study to determine the target and tolerance for the DIA of 1.16 ± 0.03 degrees *(11).*

The difference of DIA affects the number of gyrations necessary to reach a required level of density. In theory, the compacted sample density from a compactor has to be adjusted to that which would have been produced if it had been set to a DIA of 1.16 degrees. Another study conducted by Prowell *(12)* suggested that the locking point of the mixture (the first instance of two consecutive gyrations resulting in the same sample height) was approximately the same number of gyrations for two different gyratory compactors, without any adjustments. However, the density at a given definition of the locking point was higher for the Pine compactor, compared to the Troxler compactor, when the data were not corrected to a DIA of 1.16 degrees.

2.3 Laboratory mix parameters used to describe compactability

2.3.1 Introduction

Several asphalt researchers have proposed laboratory measured parameters of mixtures and/or their components as indicators of HMA compactability and/or resistance to

permanent deformation. Some of the parameters used to describe lab compactability are the percentage of maximum theoretical specific gravity at N_{ini} ($\%G_{mm}$ @ N_{ini}), the Compaction Energy Index determined from the SGC compaction process as recommended by Bahia *(4)* and the Coarse and Fine Aggregate Ratios as determined using the Bailey Method recommended by Pine *(5).* Compaction slope and the number of gyrations to reach the Locking Point of the mixture are related to resistance to permanent deformation.

2.3.2 The percentage of maximum theoretical specific gravity at N_{ini} ($\%G_{mm}@N_{ini}$)

The Superpave mix procedure *(13)* suggests that the compactability of a mixture can be indicated by its relative density at $N_{initial}$ which is an early point in the gyratory compaction process. According to the Superpave mix procedure *(13)*, mixes that compact too quickly (air voids at $N_{initial}$ are too low) may be tender during construction and unstable when subjected to traffic. This is an indication of aggregate quality. Mixes with excess natural sand will frequently fail the $N_{initial}$ requirement *(6).*

2.3.3 Compaction Energy Index (CEI)

The Compaction Energy Index (CEI) was defined by Bahia *(4)* as the area beneath the compaction curve from percent of G_{mm} at the 8^{th} gyration to 92% of G_{mm} as shown in Figure 2.6. Bahia reasoned that this index is analogous to the work applied by the roller to compact the mixture to the required density during construction. It is reasoned that mixtures with lower values of CEI are easier to compact; while a very low value of CEI could be an indication of a tender mixture and should be avoided.

Bahia also introduced the Traffic Densification Index (TDI) which is defined as the area beneath the compaction curve from 92% to 98% of G_{mm} (Figure 2.6). This index represents the energy required by traffic to densify the mixture from 92% G_{mm} to a terminal density of 98% of G_{mm}. 98% of G_{mm} is considered a critical density, at which the mixture is approaching the plastic failure zone. Mixtures with lower values of CEI and higher values of TDI will have better constructability and performance *(4).*

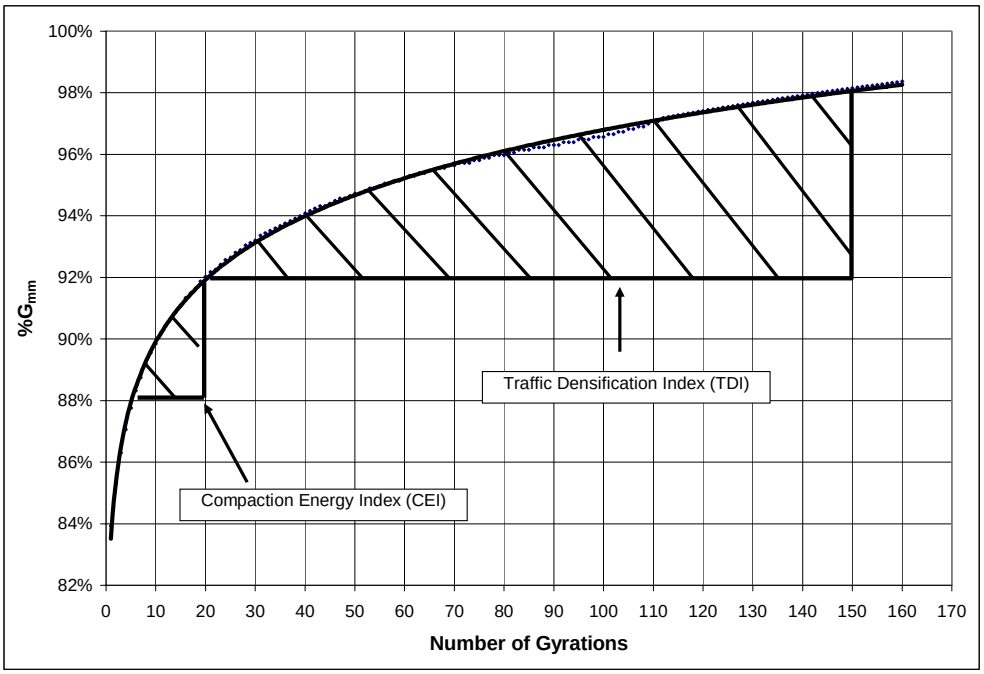

Figure 2.6: Illustration of CEI and TDI Indices *(4)*

2.3.4 Compaction slope determined from compaction in the Superpave Gyratory Compactor (SGC).

Figure 2.7 shows the percentage of maximum theoretical density versus the log of gyrations and the equation used to calculate the compaction slope *(14).* Figure 2.8 is an

illustration of the effect of different mixture properties on compaction slope: a) Higher compaction slopes are associated with higher asphalt content for the same mixture. It can be seen that a mixture asphalt content of 4.7% resulted in a slope of 8.02 while the same mixture with an asphalt content of 6.2% ended with a slope of 8.3. b) Finer gradations tend to have lower compaction slopes (slope of 6.6 for the finest gradation and 9.93 for the coarsest). c) More rounded aggregates, or those with less internal friction (gravel2 with a slope of 6.14), also tend to produce lower compaction slopes than more angular aggregates (limestone2 with a slope of 8.84). d) Higher compaction slope mixtures tend to have higher shear stiffness and lower permanent shear strain. A good correlation was obtained between compaction slope and mixture stiffness ($R^2 = 0.69$) for a mixture placed on Mississippi US 61 in 1994 *(15).*

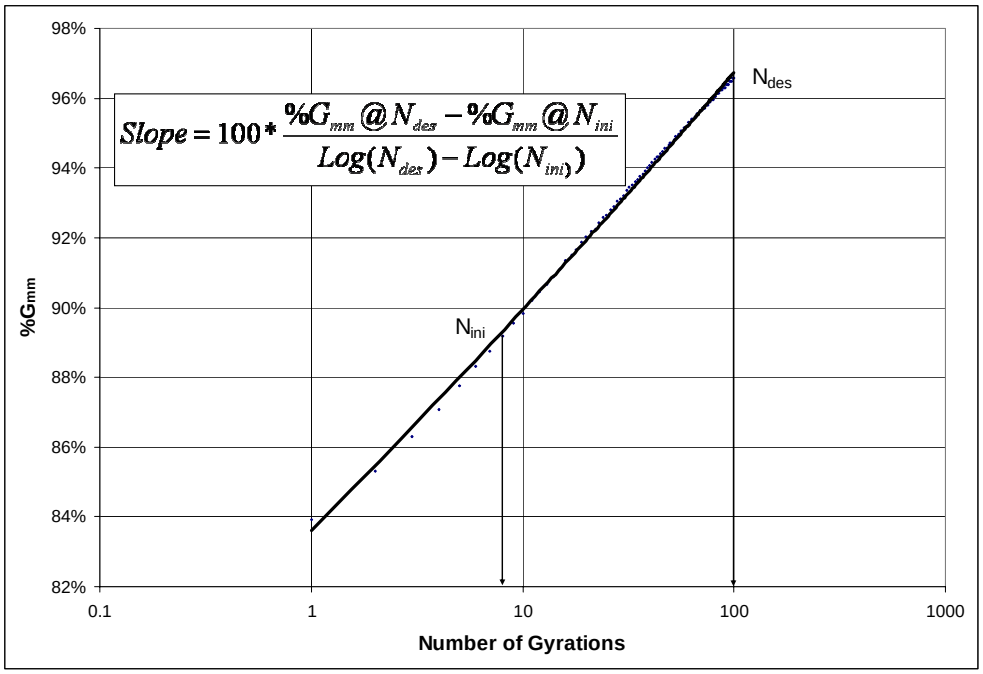

Figure 2.7: Illustration of Compaction Slope *(14).*

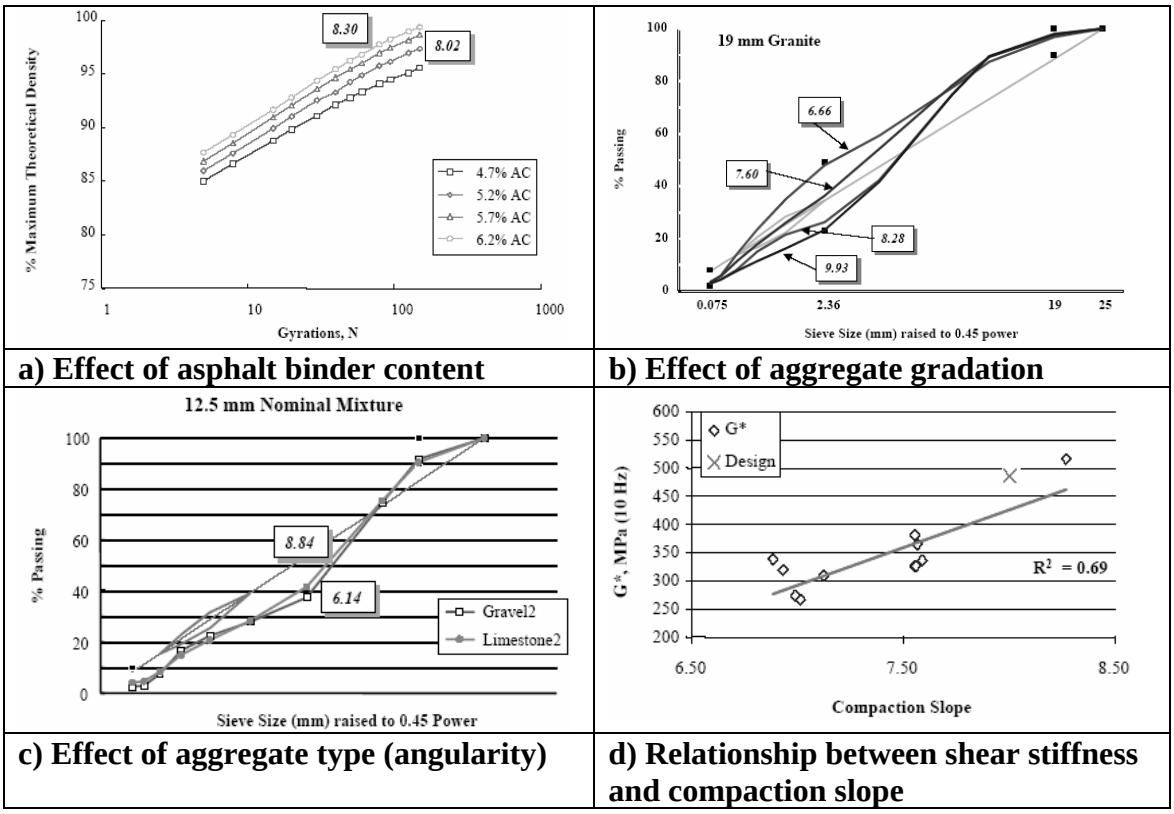

a) Effect of asphalt binder content | **b) Effect of aggregate gradation**

c) Effect of aggregate type (angularity) | **d) Relationship between shear stiffness and compaction slope**

Figure 2.8: Effect of mixture properties on compaction slope *(15)*.

2.3.5 The number of gyrations with the SGC to reach the Locking Point of the mixture.

Initially, the locking point was defined as the first of three gyrations at the same height which were preceded by two gyrations of the same height *(16)*. Vavrick and Carpenter *(17)* refined the definition of the locking point as the first gyration in the first occurrence of three gyrations of the same height proceeded by two sets of two gyrations with the same height. Since its development, other agencies have altered the definition of the locking point. Other values used include: first instance of two consecutive gyrations resulting in the same sample height (locking point 2-1), second instance of two

consecutive gyrations resulting in the same sample height (locking point 2-2), the third instance of two consecutive gyrations resulting in the same sample height (locking point 2-3).

In this study, the first instance of two consecutive gyrations resulting in the same sample height (locking point 2-1) was used as the locking point of the mixture. The trend is similar to the compaction slope; higher locking point mixtures tend to have higher shear stiffness and lower permanent shear strain *(14).*

2.3.6 Other densification indices

Since the CEI and TDI are derived from densification (volume change) only, they could be considered incomplete in representing the resistance of mixtures to distortion under traffic *(4).* Another method was developed to directly measure the shear resistance of mixtures. Delage *(18)* proposed analyzing data from SGC testing with the Gyratory Load-Cell Plate Assembly (GLPA) and the introduction of two more indices based on resistive effort curve, which is similar to the densification curve. The GLPA is placed on top of an HMA specimen during compaction in the SGC *(19).* In this configuration, the GLPA is able to record the resultant force on the sample and the radial eccentricity throughout the compaction. The resultant force and the eccentricity are used to estimate the resistive effort of compaction. To quantify the resistive efforts above and below 92% G_{mm}, Figure 2.9 shows that the area under the resistive effort curve between N_{ini} and 92% G_{mm} is calculated and named the compaction force index (CFI), and the area between 92% and 98% G_{mm} is calculated and named the traffic force index (TFI).

Delage also suggested that the CEI relating to the compaction curve be renamed the construction densification index (CDI). This study also showed that CDI and CFI are well correlated (see Figure 2.10). Therefore, hypothetically both indices equally represent the effort applied by the rollers to compact the mix to the required density during construction.

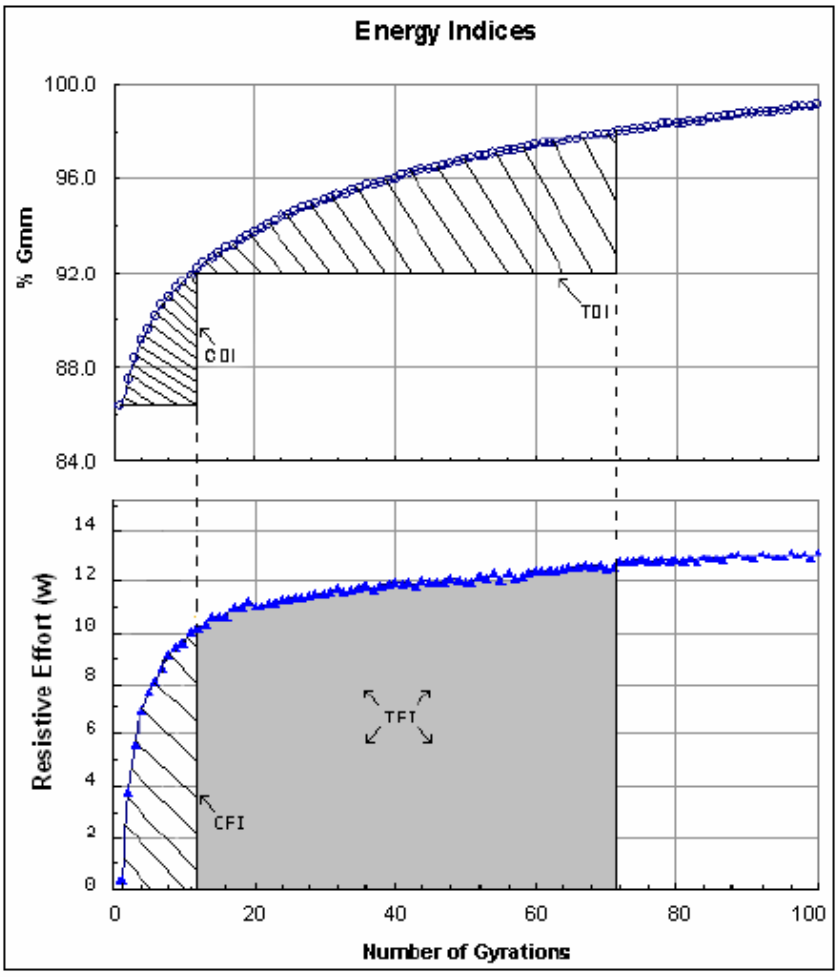

Figure 2.9: Energy Indices CEI and TDI; CFI and TFI *(18)*.

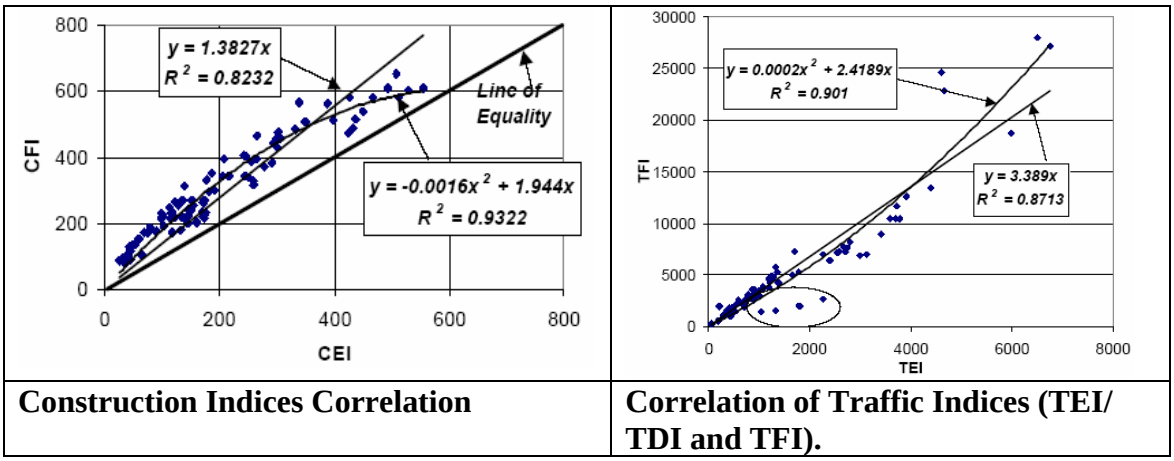

Construction Indices Correlation	Correlation of Traffic Indices (TEI/ TDI and TFI).

Figure 2.10: Correlation between CEI and CFI; TDI and TFI *(18)*.

2.4 Aggregate characteristics related to compactability

2.4.1 Introduction

Changing the aggregate gradation of a mixture alters the particle size distribution which in turn influences the packing of the aggregate skeleton. Pine says that the Bailey Method of Gradation Analysis can be used as an indicator of HMA compactability *(20).* The Bailey Method involves the following approach:

- Evaluates packing of coarse and fine aggregates separately
- Defines a gradation as either fine-graded, coarse-graded, or an SMA
- Evaluates the ratio of percentages of different size particles (indicators of HMA compactability used in this study)
- Evaluates the individual aggregates and the combined blend by volume

2.4.2 Bailey Method ratios

Four sieves are defined to quantify the shape of the gradation curve and the determination of the ratio of different size particles.

- The primary control sieve (PCS) is designated as the split between coarse aggregate and fine aggregate.
- The half sieve is designated as an intermediate sieve in the coarse aggregate
- The secondary control sieve (SCS)
- The tertiary control sieve (TCS)

The primary control sieve is determined as the sieve size closest to the size defined by:

$$PCS = NMPS \times 0.22 \quad [1]$$

Where,

PCS = primary control sieve for the overall blend

NMPS = nominal maximum particle size for the overall blend

The value 0.22 is the factor that gives the average size opening between the coarse particles, considering the different shapes of aggregates.

The Half sieve is determined as follows to find the closest sized sieve:

$$Half\ sieve = NMPS \times 0.5 \quad [2]$$

The secondary and tertiary control sieves are defined as follows:

$$SCS = 0.22 \times PCS \quad [3]$$

$$TCS = 0.22 \times SCS \quad [4]$$

Three ratios define the shape of the gradation curve. One ratio defines the shape of the coarse aggregate portion of the gradation. The second ratio defines the shape of the coarse portion of the fine aggregate, and the third ratio defines the shape of the fine portion of the fine aggregate.

The CA ratio is used to represent the packing characteristics of the coarse aggregate fraction of the combined blend. For coarse gradations this ratio is defined as follows:

CA Ratio = (% passing half sieve - % PCS) / (100 - % half sieve) [5]

Where,

% half sieve = percent passing the half sieve

% PCS = percent passing the primary control sieve

This ratio describes how the coarse aggregate particles pack together and, consequently, how these particles compact the fine aggregate portion of the aggregate blend that fills the voids created by the coarse aggregate.

The FA_C ratio of the fine aggregate is used to estimate the packing characteristics of the coarse portion of the fine aggregate. For coarse gradations this ratio is defined as follows:

FA_C *= % passing SCS / % PCS* [6]

This ratio describes how the coarse portion of the fine aggregate packs together and, consequently, how these particles compact the material that fills the voids it creates.

The FA_F ratio of the fine aggregate is used to estimate the packing characteristics of the fine portion of the fine aggregate. For coarse gradations this ratio is defined as follows:

$$FA_F = \%\ passing\ TCS / \%\ FAIB \quad [7]$$

This ratio describes how the fine portion of the fine aggregate packs together. It also influences the voids that will remain in the overall fine aggregate portion of the blend because it represents the particles that fill the smallest voids created.

For fine gradations, new factors are necessary to apply equations 5, 6 and 7 and those factors are given as follows:

$$New\ NMPS = PCS \quad [8]$$

$$New\ Half\ sieve = 0.5 \times New\ NMPS \quad [9]$$

$$New\ PCS = 0.22 \times New\ NMPS \quad [10]$$

$$New\ SCS = 0.22 \times New\ PCS \quad [11]$$

$$New\ TCS = 0.22 \times New\ SCS \quad [12]$$

Pine describes how the three ratios affect mixture compactability of dense gradations:

- As the CA Ratio increases, the mixes are more difficult to compact in the field.
- In general, as the FA_c ratio increases towards 0.55, compactability of the overall fine fraction increases. And as the ratio decreases, compactability of the mixture increases.

- In general, as the FA_f Ratio increases towards 0.55, compactability of the overall fine fraction increases. And as the ratio decreases, compactability of the mixture increases.
- For SMA mixtures a value of 0.65 may be used instead of 0.55.

Tables 2.4 and 2.5 show the recommended ranges of aggregate ratios for conventional and SMA mixtures, respectively. It can be seen that the CA ratio is the only parameter that is clearly affected by the aggregate size. The CA ratio decreases as the nominal particle size decreases for coarse-graded and SMA mixes and varies from 0.30 to 0.95 for coarse-graded and 0.15 to 0.50 for SMA. The remaining parameters are mostly contained in a reduced range. Table 2.6 shows the controls sieves used to calculate aggregate ratios *(5)*.

Table 2.4: Recommended ranges of aggregate Ratios

NMPS, mm	37.5	25.0	19.0	12.5	9.5	4.75
CA Ratio Coarse-graded mixes	0.80-0.95	0.70-0.85	0.60-0.75	0.50-0.65	0.40-0.55	0.30-0.45
CA Ratio Fine-graded mixes	0.60-1.0					
FA_C Ratio	0.35-0.50					
FA_f Ratio	0.35-0.50					

Table 2.5: Recommended ranges of aggregate Ratios for SMA mixes

NMPS, mm	19.0	12.5	9.5
CA Ratio	0.35-0.50	0.25-0.40	0.15-0.30
FA_C Ratio	0.60-0.85		
FA_f Ratio	0.65-0.90	0.60-0.85	0.60-0.85

Table 2.6: Control sieves

Nominal size, mm	**Primary Control Sieve**	**Half Sieve**	**Initial Break**	**Secondary Break**
4.75	1.18	2.36	0.30	0.075
9.5	2.36	4.75	0.6	0.15
12.5	2.36	4.75	0.6	0.15
19.0	4.75	9.5	1.18	0.30

2.4.3 Primary Control Sieve Index PCSI

The Primary Control Sieve Index PCSI is defined as the difference of percentage passing from the mixture's gradation to primary control sieve. It represents the relative coarseness or fineness of the gradation. Figure 2.11 shows an example of the PCSI for 12.5 mm NMAS fine and coarse gradations. Coarse gradations will have negative values and fine gradations will have positive values of PCSI.

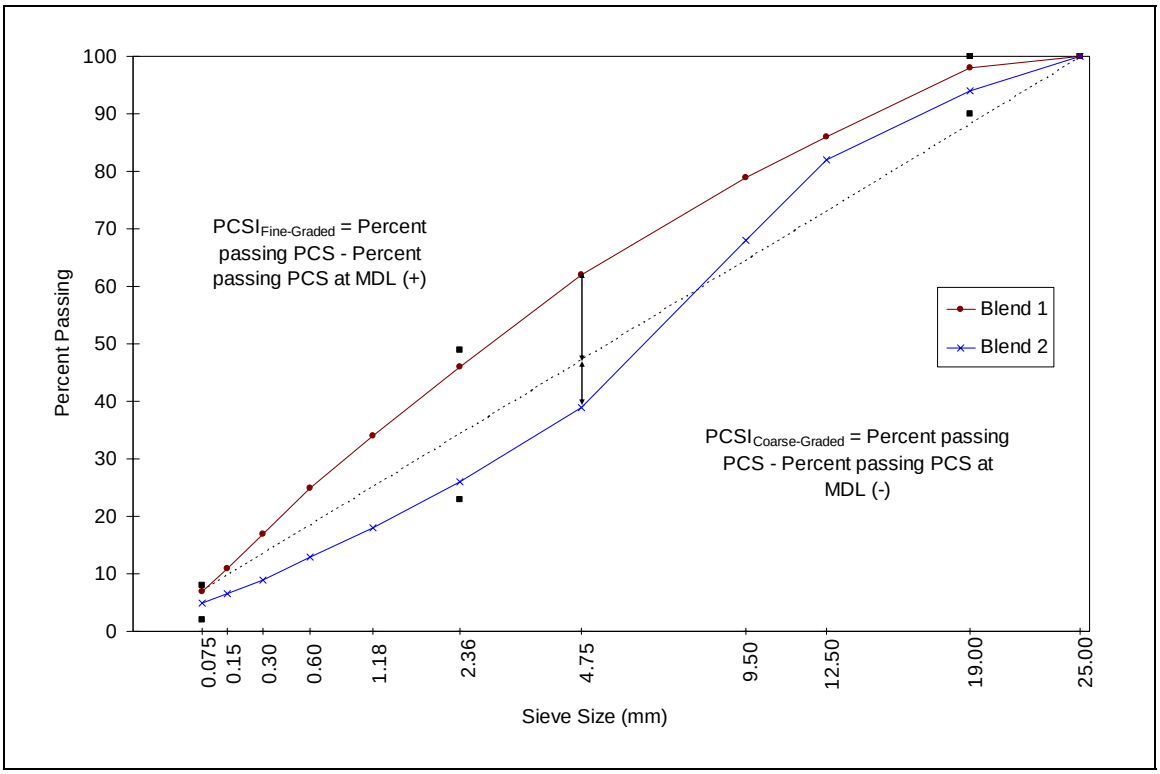

Figure 2.11: Illustration of the PCSI for 12.5 mm NMAS gradations.

2.5 Studies that relate laboratory characteristics and field compactability

In the literature, several methods for measuring compactability can be found and some of them relate laboratory and field compaction. Three methods are discussed here:

2.5.1 C-value method

The *C*-value method is the most frequently used method to measure compactability. It describes the progress in compaction by using an exponential formula. Kezdi and other researchers *(21)* developed this principle. The model is based on the assumption that the progress of compaction, expressed in terms of increase in density (ρ),

due to an added amount of compaction energy (*S)*, depends on the difference between the current density state and the maximum density (ρ_∞). Where ρ_0 is the density at the start of the compaction process. The concept of Kezdi can be formulated as:

$$\rho_A(S) = \rho_{A\infty} - (\rho_{A\infty} - \rho_{A0}) \cdot e^{\frac{S}{C}} [kg/m^3] \qquad [13]$$

The *C* value in the formula is a measure of the rate at which the density approaches the asymptotic value ρ_∞ and thus also for the rate of the compaction progression (see Figure 2.12). Analyzing the equation above, one can see that materials with lower *C*-values are easier to compact compared to materials with higher *C*-values. For asphalt concrete mixtures commonly used in Germany during the 1980's typical values were between 10 and 30, and in the Netherlands *C*-values ranged from 18 to 38 *(21).*

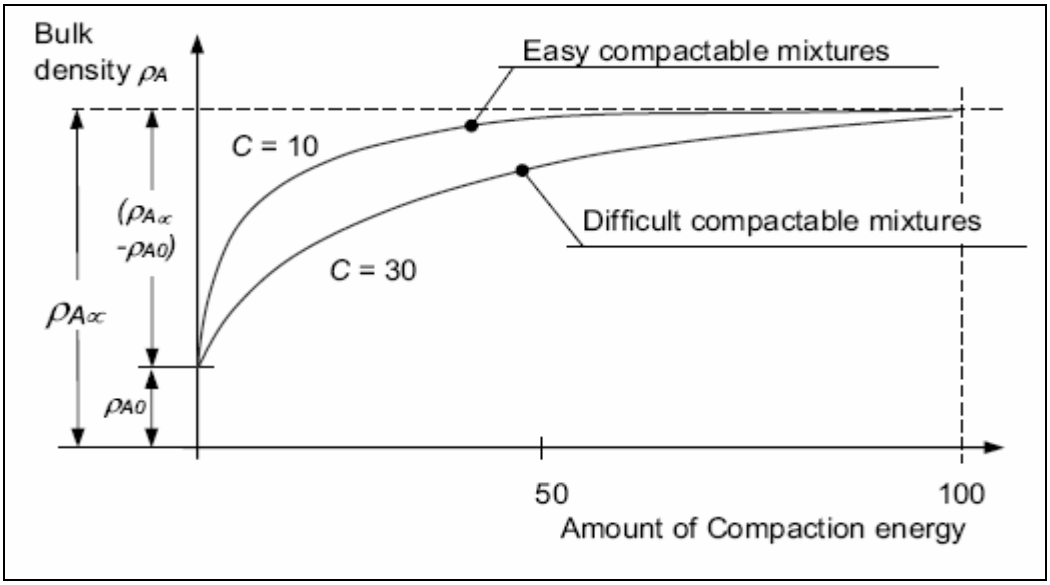

Figure 2.12: The compaction process according to the C-value method.

2.5.2 The modified Mohr method

Based on the similarity between HMA and granular materials, Nijboer *(21)* characterized HMA mixes by means of the parameters τ and ϕ which follows the Mohr theory to characterized granular materials. In addition, he introduced the parameter η to capture the viscous component of HMA. Nijboer assumed that the resistance against deformation of "bituminous mineral aggregate mixtures" could be represented by three physical quantities:

- the angle of internal friction, ϕ,
- the initial resistance, τ,
- the viscosity of the mass, η, which denotes the influence of the viscosity on the shear resistance of the bitumen aggregate mixture.

Nijboer studied the plastic behavior of bituminous aggregate mixtures for developing his "rolling theory". He made an inventory of all parameters of which he thought that they were relevant for the progress of bituminous mixtures compaction. As a result of Nijboer's investigation is the R_f factor which is a parameter that should indicate how far the compaction process of HMA is progressed.

$$R_f = \frac{\frac{P}{ID} - C\tau_{cb}}{\eta_m} \cdot n \cdot \left(\frac{h}{v}\right)^{0.4} \qquad [14]$$

Where:

P = the weight of the roller drum, N

l = the width of the roller drum, mm

D = the diameter of the roller drum, mm

C = factor for the roller type (i.e. 2.5 for static steel rolling)

τ_{cb} = the initial resistance of the bituminous mixture, N/mm^2

η_m = the viscosity of the mass of the compacted mixture, poise

n = the number of roller passes applied

h = thickness of the layer, mm

v = speed of the compactor, mm/sec

The method is in principle not a "pure" method to measure compactibility but rather a method to describe the plastic deformation of HMA's. During material measurements in the tri-axial apparatus, the governing stress conditions cause the material to shear. During compaction, excessive shear stresses must be avoided because when granular materials shear, they dilate, producing lower densities and even cracks can develop. This inconsistency makes the method, in the author's opinion, not fully suitable for modeling bituminous aggregate mixtures compaction behavior.

2.5.3 The k-factor method

This study was conducted in France and this included bituminous concrete layer thicknesses between 30 and 120 mm. The laboratory samples were compacted using a gyratory compactor developed in France called gyratory shear compacting press (PCG). The field samples were compacted using a type of pneumatic compactor in the laboratory. The number of gyratory revolutions corresponding to the number of passes by the pneumatic compactor was found to be reasonably accurate by the formula *(22):*

$$Ng = k \cdot e \cdot Np \quad [15]$$

Where:

Ng = number of PCG revolutions

e = layer thickness (mm)

Np = number of compactor passes.

k = 0.0625

The k-factor depends essentially on the nature of the compactor and increases with compactor efficiency. For a vibratory roller with a linear static load of 3.5 N/mm and a frequency of 25 to 30 Hz the k-factor value was determined to be about 0.25.

When the thickness of a layer is known, this expression makes it possible to calculate the number of PCG revolutions for which the void content obtained in the laboratory will be equal to the void content obtained on the job site for a given number of passes of the compactor. Thus, if the intended job site thickness is 100 mm and the number of passes of the roller in the field is 16, the reference number of revolutions is 100. Therefore, it is possible to predict whether the void content in situ will be acceptable and to adjust the mix composition if necessary.

2.6 Summary of findings

Literature suggests that field compactability of asphalt mixtures has become a major concern since the adoption of Superpave designed mixes. Many factors have been identified affecting the compaction on the field including material properties, environmental conditions, gradation, lift thickness and roller operations. In general,

rough surface texture, cubical or block shaped aggregate and highly angular particles all decrease mix compactability. Mixes with mixes with high asphalt content will be easier to compact. Higher initial mat temperatures require more time to cool down, which means more time available for compaction. The desired density is difficult to obtain on thin lifts (layers less than 50 mm) because of the mix's rapid decline in temperature *(8).*

With respect to laboratory compaction, literature suggests that the factors mentioned above are under control during the compaction process. Laboratory compaction using the gyratory compactor is characterized by samples with one and only height (thickness), confined in mold, compacted to a relatively high density, not sensitive to temperature and rapid compaction process (<3 min.). The dynamic internal angle (DIA) of gyration is probably the only influencing factor that has been identified to produce differences in sample density *(10).*

Several asphalt researchers *(4, 5)* have proposed laboratory measured parameters of mixtures and/or their components as indicators of HMA compactability. Bahia *(4)*, for example, proposed the Compaction Energy Index (CEI) which simulates the field compaction process to obtain an air voids content of 8%. Meanwhile, Pine *(5)* developed a set of parameters, called Bailey Method ratios, based on particle packing in a determined gradation. According to Pine the compactability of a mixture in the field can be predicted by observing how the aggregate particles are packed together. In general, the mixes are more difficult to compact in the field when the Bailey Method ratios increase.

Literature also suggests that other researchers *(14, 16)* have developed laboratory measured parameters of mixtures and/or their components as indicators of resistance to

permanent deformation. Because of this resistance to permanent deformation the compaction slope determined by Anderson *(14)* and the number of gyrations with the SGC to reach the Locking Point of the mixture developed by Pine *(16)* have a potential used to predict field compactability of a mixture.

Literature shows that some studies have been conducted to relate laboratory characteristics and field compactability *(21, 22);* the modified Mohr method by Nijboer, C-value method by Kezdi and the K-factor method. The applicability of these methods is yet questionable.

In summary, literature suggests that there is a significant need to evaluate the factors affecting mix compactability in the laboratory and in the field. Most of the parameters mentioned above that have been used to measure mix compactability have not been validated with actual field performance and have been developed considering only laboratory compaction.

CHAPTER 3. RESEARCH PLAN

3.1 Overview

The first part of this study included a comparison between laboratory measured characteristics of HMA ($\%G_{mm}@N_{ini}$, $N@92\%G_{mm}$, CEI, Slope, Locking Point and Bailey Method ratios), an evaluation of the effect of physical properties on the SGC parameters and an assessment of variability among observations. The data used for this stage came from the Superpave mixtures placed on the NCAT Test Track in the first two cycles (2000 and 2003). This data set is well suited for this analysis because of the wide variety of mixtures included in the test track and the uniformity in construction operations at the track. This analysis included thirty-five different surface mixtures and seven binder mixtures placed on the track in 2000, and seventeen surface mixtures and twenty-two binder mixtures placed in 2003. The data used to determine the laboratory measured mix characteristics were obtained from quality control samples taken during track construction. Triplicate gyratory samples were compacted for each section.

The second part of this study included the determination of a field compactability indicator based on the rolling operation: the Accumulated Compaction Pressure (ACP) that is defined in section 3.3. Compaction operations at the track were well documented and provide good information about the compactability of the mixtures in the field. These data were used to determine the total compaction energy applied by the rollers

during construction. Regressions between the laboratory compaction parameters and the field compaction energy were analyzed. The laboratory compaction parameters which yielded the best correlations were analyzed further by performing multiple regression analysis with basic mixture properties.

The third part of this project included laboratory compaction of specimens using the SGC at the field lift thickness. The specimens were compacted to determine the number of gyrations to reach 92 percent of G_{mm} ($N@92\%G_{mm}$). The $N@92\%G_{mm}$ for the field lift thickness specimens were compared to the $N@92\%G_{mm}$ of normal height (115 ± 5 mm) specimens. Initially 25 mixtures were included but only 23 met the target air void content. For the remaining two mixtures, which have thicknesses below 30 mm, it was impossible to obtained an air voids content of 8% and the target thickness at the same time.

The fourth part of this study involved eleven mixtures placed on the Test Track in 2006 and twelve mixes placed in 2003. These mixes were used to evaluate the field compactability indicator by conducting nuclear density tests and surface temperature measurements after each roller pass. Surface temperatures were obtained with an infrared temperature gun. The purpose of this part was to obtain the field compaction energy at 92 percent of G_{mm} and correlate that energy with the laboratory compaction parameters.

The last part of this project involved validation of one of the final compaction models using information from the NCHRP 9-27 study. The data set includes a variety of compaction equipment and mixtures. Table 3.1 shows a summary of the experimental plan.

Table 3.1: Summary of the experimental plan

Section	Number of observations (mixtures)	Description
Analysis of laboratory compaction parameters	81	Variety of mixes including fine, coarse, intermediate-graded and SMA. Nominal maximum size aggregate of 9.5, 12.5 and 19.0 mm. Parameters analyzed: $\%G_{mm}@N_{ini}$, $N@92\%G_{mm}$, CEI, Slope, Locking Point and Bailey Method ratios.
Correlation of ACP and laboratory parameters	71	Mix and materials properties used to correlate with ACP: air voids, VMA, VFA, microdeval, FAA, CAA, F&E 3:1, %pass 0.075mm, lift thickness, mix temperature and density level. Laboratory parameters analyzed: $\%G_{mm}@N_{ini}$, $N@92\%G_{mm}$, CEI, Slope, Locking Point and Bailey Method ratios.
Correlation of ACP and laboratory parameters for SGC specimens compacted at lift thickness	25	Variety of mixes including fine, coarse, intermediate-graded and SMA. Nominal maximum size aggregate of 9.5, 12.5 and 19.0 mm. A variety of lift thicknesses from 35 to 65 mm.
Correlation of ACP obtained at 92% of G_{mm} and laboratory parameters	23	Density testing was conducted on 11 mixes placed in 2006 and formation of 12 mixes was used to complete the analysis. Lift thickness and mix temperature were also used as predictor variables.
Analysis of NCHRP mixes for validation purposes	16	A variety of mixes including fine, coarse, intermediate-graded and SMA. Nominal maximum size aggregate of 9.5, 12.5 and 19.0 mm. Variety of lift thicknesses from 30 to 100 mm. Variety of equipment, roller operation and environmental conditions.

3.2 Analysis of Test Track mixes

3.2.1 Material and Mixture Properties

The HMA mixtures used in the first part of this study are shown in Table 3.2, which includes surface and some binder layer mixtures constructed on the NCAT Test Track in 2000 and 2003. This data set is well suited for this analysis because of the wide variety of mixtures included in the test track and the uniformity in construction operations at the track.

3.2.2 Test Track construction

Several aggregate types were used on the track including limestone, granite, Florida limestone, gravel, and slag. Reclaimed asphalt pavement (RAP) was also used in a few sections. Each section on the test track had the same structural pavement foundation and used the same rollers and operator within each cycle. Weather condition was another similitude for each section within each cycle.

In order to obtain the target density, each section was rolled with different number of roller passes with a combination of rollers. Each roller type applies a specific compactive effort – vibratory force, static force and pneumatic tire kneading action.

Table 3.2: Summary of mix types evaluated

Quad	Sec	Cycle*	Sublot **	Aggregate Type	Prod. NMAS	Binder Grade	Mod. Type	Grad. Type	N_{des}
E	1	1	S	quartzite	9.5	67-22	NEAT	Fine	100
E	2	1	S	granite	12.5	67-22	NEAT	Coarse	100
E	3	1	S	granite	12.5	76-22	SBR	Coarse	100
E	4	1+2	S	granite	12.5	76-22	SBS	Coarse	100
E	5	1+2	S	granite	12.5	76-22	SBS	Intermediate	100
E	6	1+2	S	granite	12.5	67-22	NEAT	Intermediate	100
E	7	1+2	S	granite	12.5	76-22	SBR	Intermediate	100
E	8	1+2	S	granite	12.5	67-22	NEAT	Fine	100
E	9	1+2	S	granite	12.5	76-22	SBS	Fine	100
E	10	1	S	granite	12.5	76-22	SBR	Fine	100
N	1	1	S	lms/slag	9.5	76-22	SBS	Fine	100
N	2	1	S	lms/slag	9.5	76-22	SBS	Fine	100
N	3	1	S	lms/slag	9.5	67-22	NEAT	Fine	100
N	4	1	S	lms/slag	9.5	67-22	NEAT	Fine	100
N	5	1	S	lms/slag	12.5	67-22	NEAT	Coarse	100
N	6	1	S	lms/slag	12.5	67-22	NEAT	Coarse	100
N	7	1	S	lms/slag	12.5	76-22	SBR	Coarse	100
N	8	1	S	lms/slag	12.5	76-22	SBR	Coarse	100
N	9	1	S	lms/slag	12.5	76-22	SBS	Coarse	100
N	10	1	S	lms/slag	12.5	76-22	SBS	Coarse	100
N	11	1+2	S	granite	12.5	76-22	SBS	Intermediate	100
S	1	1	S	granite	12.5	76-22	SBS	Coarse	100
S	2	1+2	S	gravel	9.5	76-22	SBS	Coarse	100
S	3	1+2	S	gvl/lms	9.5	76-22	SBS	Coarse	100
S	4	1	S	limestone	12.5	76-22	SBS	Fine	125
S	5	1	S	gravel	12.5	76-22	SBS	Intermediate	125
S	6	1+2	S	lms/RAP	12.5	67-22	NEAT	Fine	100
S	7	1+2	S	lms/RAP	12.5	67-22	NEAT	Coarse	100
S	8	1+2	S	mar. schist	9.5	76-22	SBS	Coarse	100
S	9	1+2	S	granite	12.5	67-22	NEAT	Coarse	100
S	10	1+2	S	granite	12.5	67-22	NEAT	Fine	100
S	11	1+2	S	mar. schist	9.5	76-22	SBS	Coarse	100
W	6	1	S	lms/slag	12.5	67-22	NEAT	Intermediate	100
W	9	1	S	gravel	12.5	67-22	NEAT	Coarse	100
W	10	1+2	S	gravel	12.5	76-22	SBR	Coarse	100
E	1	2	S	lms	12.5	76-22	SBS	SMA	50
E	2	2	S	marine lms	9.5	67-22	NEAT	Fine	100
E	3	2	S	marine lms	9.5	76-22	SBS	Fine	100
N	1	2	S	grn/lms/snd	9.5	76-22	SBS	Fine	80
N	3	2	S	grn/lms/snd	9.5	70-22	NEAT	Fine	80
N	4	2	S	grn/lms/snd	9.5	76-22	SBS	Fine	80

* Cycle 1 = 2000 Test track experiment, cycle 1+2 = 2000 and 2003, cycle 2 = 2003 only.
** S = surface mixture, B = binder or bottom mixture.

Table 3.2 (continued): Summary of mix types evaluated

Quad	Sec	Cycle*	Sublot **	Aggregate Type	Prod. NMAS	Binder Grade	Mod. Type	Grad. Type	N_{des}.
N	5	2	S	grn/lms/snd	9.5	76-22	SBS	Fine	80
N	6	2	S	grn/lms/snd	9.5	70-22	NEAT	Fine	80
N	9	2	S	lms	12.5	70-22	SBS	SMA	75
N	10	2	S	lms/chert	12.5	70-22	SBS	SMA	75
N	13	2	S	granite	12.5	76-22	SBS	SMA	50
S	1	2	S	granite	12.5	76-22	SBS	SMA	50
S	5	2	S	gvl/lms/snd	12.5	76-22	SBS	Intermediate	75
W	2	2	S	porph/lms	19.0	70-22	SBS	SMA	75
W	3	2	S	lms	9.5	67-22	NEAT	Fine	50
W	6	2	S	lms/gvl/snd	4.75	76-22	SBS	Fine	50
W	9	2	S	granite	9.5	67-22	NEAT	Fine	100
S	1	1	B	Granite	19.0	76-22	SBS	Coarse	100
S	2	1+2	B	Gravel	19.0	76-22	SBS	Coarse	100
S	3	1+2	B	Limestone	19.0	76-22	SBS	Coarse	100
S	4	1	B	Lms/RAP	19.0	76-22	SBS	Fine	125
S	5	1	B	Lms/Grv/RAP	19.0	76-22	SBS	Coarse	125
S	11	1+2	B	Marble-Schist	19.0	67-22	NEAT	Coarse	100
N	11	1+2	B	Granite	19.0	67-22	NEAT	Coarse	100
N	2	2	B	grn/lms/snd	19.0	67-22	NEAT	Fine	80
N	3	2	B	grn/lms/snd	19.0	67-22	NEAT	Fine	80
N	3	2	B	grn/lms/snd	19.0	67-22	NEAT	Fine	80
N	3	2	B	grn/lms/snd	19.0	67-22	NEAT	Fine	80
N	3	2	B	grn/lms/snd	19.0	67-22	NEAT	Fine	80
N	4	2	B	grn/lms/snd	19.0	70-22	SBS	Fine	80
N	4	2	B	grn/lms/snd	19.0	70-22	SBS	Fine	80
N	5	2	B	grn/lms/snd	19.0	70-22	SBS	Fine	80
N	5	2	B	grn/lms/snd	19.0	70-22	SBS	Fine	80
N	5	2	B	grn/lms/snd	19.0	70-22	SBS	Fine	80
N	6	2	B	grn/lms/snd	19.0	67-22	NEAT	Fine	80
N	6	2	B	grn/lms/snd	19.0	67-22	NEAT	Fine	80
N	6	2	B	grn/lms/snd	19.0	67-22	NEAT	Fine	80
N	7	2	B	grn/lms/snd	19.0	67-22	NEAT	Fine	80
N	7	2	B	grn/lms/snd	19.0	67-22	NEAT	Fine	80
N	7	2	B	grn/lms/snd	19.0	67-22	NEAT	Fine	80
N	8	2	B	grn/lms/snd	19.0	67-22	NEAT	Fine	80
N	8	2	B	grn/lms/snd	19.0	67-22	NEAT	Fine	80
N	9	2	B	lms	12.5	70-22	SBS	SMA	75
N	10	2	B	lms	12.5	70-22	SBS	SMA	75
N	13	2	B	Granite	19.0	67-22	NEAT	Intermediate	100
S	1	2	B	Granite	19.0	67-22	NEAT	Intermediate	100

* Cycle 1 = 2000 Test track experiment, cycle 1+2 = 2000 and 2003, cycle 2 = 2003 only.
** S = surface mixture, B = binder or bottom mixture.

The breakdown roller utilized in the 2000 experiment was a 10-ton steel double drum roller HYPAC C778B with 78 inch drum width, which could operate in vibratory or static mode. The rubber tire roller was a HYPAC C560B with a tire pressure of 83 psi. For most segments, the initial rolling was performed using vibratory mode at low amplitude and high frequency (3400 vpm). This was followed by a variable number of passes of static mode. In a few cases the rubber tire roller was incorporated at the end of the compaction process.

In the 2003 experiment, a 13-ton double drum roller HYPAC C784 with 84 inch drum width, which could operate in vibratory or static mode, was used as the breakdown roller using vibratory mode at low amplitude and high frequency (4000 vpm). This was followed by a variable number of passes of static mode using either, double drum roller HYPAC C784 or HYPAC C778B. In some cases a rubber tire roller (HYPAC C560B with a tire pressure of 83 psi) was used at the end of the compaction process.

Figure 3.1 shows the distribution of thicknesses placed in the test track in both cycles for either binder or surface mixes. It can be observed that the mean thickness was around 50 mm and the majority of the layers (47 layers) were constructed with the same thickness (50 mm).

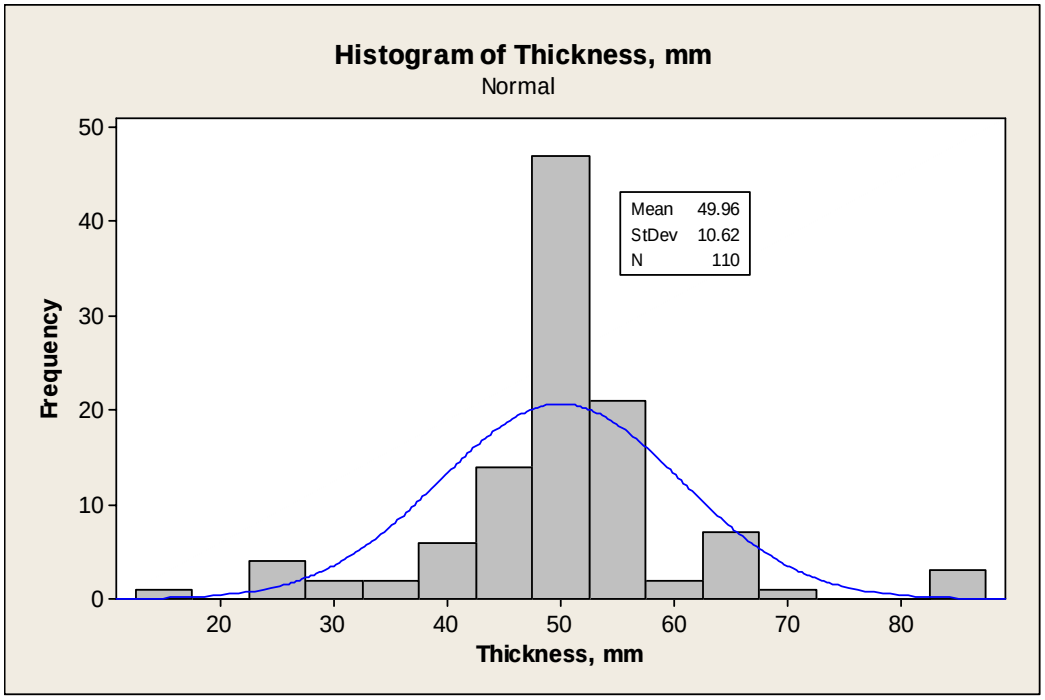

Figure 3.1: Frequency distribution of test track layer thicknesses.

3.3 Accumulated Compaction Pressure (ACP) as a field compactability indicator

Accumulated Compaction Pressure (ACP) was defined to quantify the total applied compactive effort to the HMA mat. It is the summation of the force applied by each pass of each roller in the field compaction process. For any roller type and any number of passes made by each roller type, the ACP is calculated using Equation 16.

For steel wheel rollers in vibratory mode, the total applied load in pounds per linear inch (pli) is the sum of centrifugal force plus the unsprung drum weight of both vibratory drums, divided by drum width. The compaction pressure was calculated using pli divided by the small contact arc of the drum on the mat (Figure 3.2). The contact arc decreases with each drum pass as mix densifies. According to the roller manufacturer, the contact arc for vibratory mode after the third pass will be nearly constant. For steel wheel

rollers in static mode, each pass will produce similar pressure and for pneumatic rollers the contact pressure is similar to tire pressure.

$$ACP = \sum_{r=1}^{m} \sum_{p=1}^{n} CP_{rp} \qquad [16]$$

Where,

r = roller type

p = pass number

CP = compaction pressure

Equation 17 shows an example of the model if vibratory mode is used for initial breakdown rolling followed by static mode. In this model was assumed that each pass made with the roller in vibratory mode provides a different compactive energy to the mat while each pass made with the roller in static mode provides the same amount of energy to the mat.

$$ACP = \sum_{p=1}^{n_V} CP_V + n_S \cdot CP_S \qquad [17]$$

Where,

CP_V = compaction pressure for vibratory mode

CP_S = compaction pressure for static mode

n_V = total number of passes in vibratory mode

n_S = total number of passes in static mode

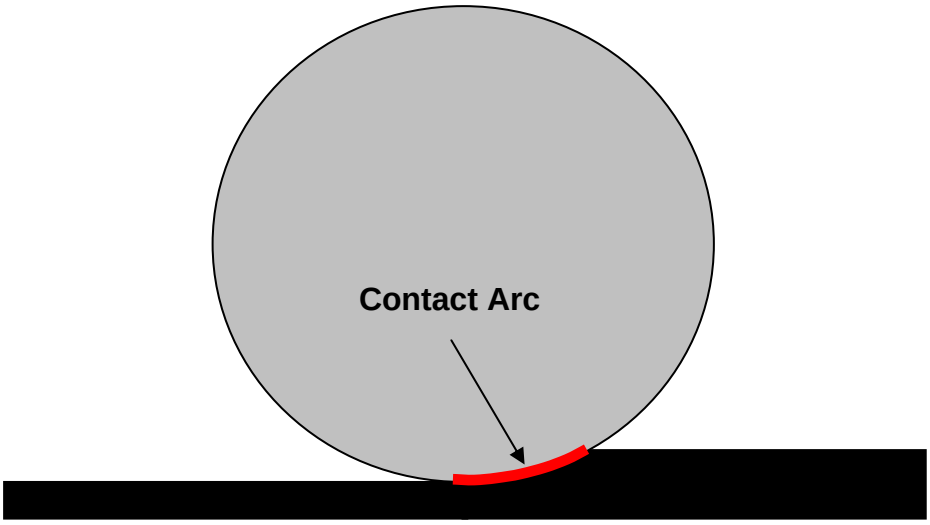

Figure 3.2: Contact arc of the drum on the mat.

Table 3.3 shows the data used to calculate the compaction pressure per roller pass for the test track in the first two cycles. The roller manufacturer provided the contact arc for vibratory mode.

Table 3.3: Compaction Pressure per Pass (psi)

Passes	Contact arc (in)	C778			C784		
		Low amp.	High amp.	Static	Low amp.	High amp.	Static
1	6.92	100	112	NA*	109	120	NA*
2	4.90	141	159		153	169	
3	3.46	200	225	87	217	240	97
>3	3.46	200	225		217	240	

* If used as breakdown roller it would be necessary to calculate pressure for the first two passes

3.4 Laboratory compaction parameters

Quality control data were used to calculate the different laboratory compaction parameters: $\%G_{mm}@N_{ini}$, $N@92\%G_{mm}$, CEI, Slope, Locking Point and Bailey Method ratios. The results for eighty one mixtures were then compared and several statistical

analyses were conducted to identify correlations and trends among lab compaction parameters. Overall, it was expected that all these parameters would follow the same trend that coarser mixes are more difficult to compact than finer mixes *(4).* The effect of PCSI, as a measurement of the relative coarseness or fineness of the gradation, on the compactability of the mix with the gyratory compactor was a key factor to identify the expected trend.

3.5 Correlation of ACP and laboratory parameters

Seventy one mixtures placed on the test track were used for this analysis. These mixes corresponded to surface and binder layers placed on top of HMA. The remaining ten mixes were excluded from this analysis because they were placed directly on top of unbound material.

The ACP represents the total compactive effort during the compaction process. However, the resulting density from the compaction operations varied somewhat from section to section. Nevertheless, single and multiple linear regression analyses were conducted to evaluate possible relationships between ACP and laboratory compaction parameters. For the multiple regression analysis, the following parameters were used as predictor variables: asphalt content, actual PG grade, compaction slope, Compaction Energy Index (CEI), $\%G_{mm}@ N_{ini}$, $N@92\%G_{mm}$, locking point (2-1) as defined in section 2.3.4, coarse and fine aggregate ratios, lift temperature, t/NMAS ratio, PCSI, fine aggregate angularity (FAA), the effective asphalt content (Vbe), and Micro Deval abrasion loss which is a measure of aggregate toughness and abrasion resistance.

Specimens were compacted to meet 8% air voids and obtain the number of gyrations at 92 percent of G_{mm} (N@92%G_{mm}-lift thickness). The original objective of this part of the study was to compare the N@92%G_{mm} obtained from these specimens with those calculated in the first part and to evaluate the effect of using field thickness. The correlation between ACP and this new parameter (N@92%G_{mm}-lift thickness) was also analyzed. Due to limited material availability, only twenty five mixtures were used in this stage and included a variety of mat thicknesses from 35 mm to 65 mm for coarse, fine and intermediate gradations.

Finally, twenty three mixes (Table 3.4) were used to compare the ACP at 92% of G_{mm} with different laboratory compaction parameters, mix properties and field conditions to try to improve any model obtained in previous stages. Density testing was performed on eleven surface mixtures placed on the 2006 Test Track to determine the compaction curve. Figure 3.3 is an illustration of one of the studied mixes that shows the relationship among density (pcf), lift temperature (°F), compaction time and roller pattern (V-vibratory, R-pneumatic, S-static). Figure 3.3 is another illustration that shows the relationship between corrected density (nuclear density expressed as %G_{mm} once corrected by core density) and ACP for mixtures with different gradations. A Weibull model was used to fit these curves and obtain ACP at 92% of G_{mm}. Figure 3.5 is an example of the Weibull model used to fit field compaction data. The remaining mixtures used in this analysis were taken from the 2003 experiment and only those mixes which had complete information were selected.

Table 3.4: Properties of NCAT Test Track mixtures 2nd and 3rd cycle

Cycle	Quad.	Sec.	NMAS	AC%	Temp 1st pass, F	Thickness (mm)	ACP@92% G_{mm}
2003	E	1	12.5	6.3	251	46	144
	N	1	19	4.5	228	53	353
	N	4	19	4.3	230	43	350
	N	5	9.5	6.1	168	23	1200
	N	6	9.5	6.2	162	28	750
	S	1	12.5	5.1	226	43	314
	N	9	12.5	6.6	249	46	328
	N	10	12.5	6.2	245	51	353
	W	3	9.5	6.2	221	33	840
	W	9	9.5	5.8	158	25	750
	E	3	9.5	7.9	168	56	353
	E	2	9.5	7.8	217	50	216
2006	N	1	12.5	5.7	198	47	406
	N	2	12.5	5.3	246	45	445
	N	5	12.5	6.2	212	50	125
	N	10	19	4.4	263	44	410
	E	5	12.5	5.2	195	54	118
	E	6	12.5	5.1	183	51	465
	E	7	12.5	5.2	199	54	545
	S	2	9.5	7.0	215	41	765
	W	3	12.5	6.1	240	50	48
	W	4	12.5	6.0	225	56	47
	W	5	12.5	5.1	205	52	99

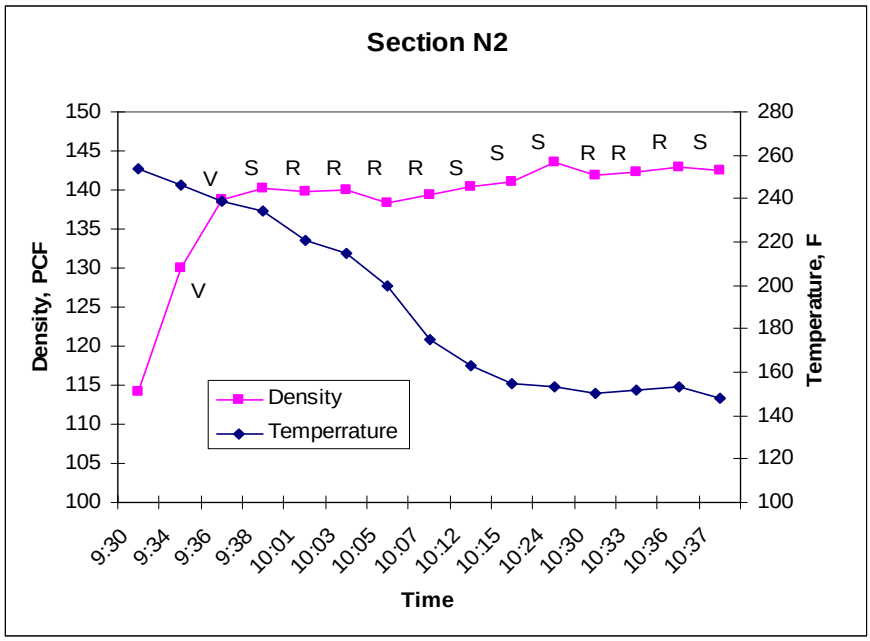

Figure 3.3: Relationship between nuclear density (pcf), lift temperature, compaction time and roller pattern.

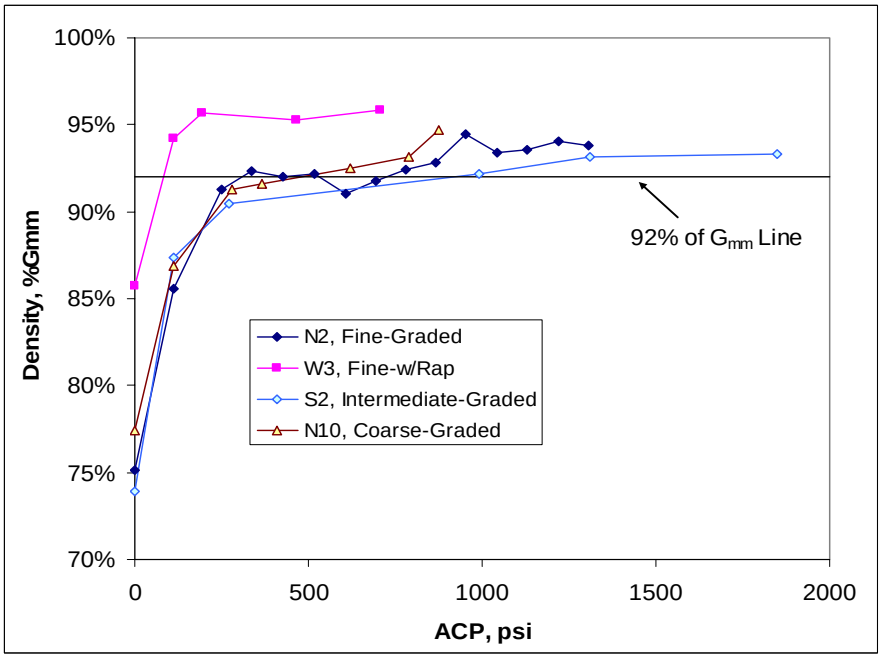

Figure 3.4: Relationship between ACP and density (%G_{mm}).

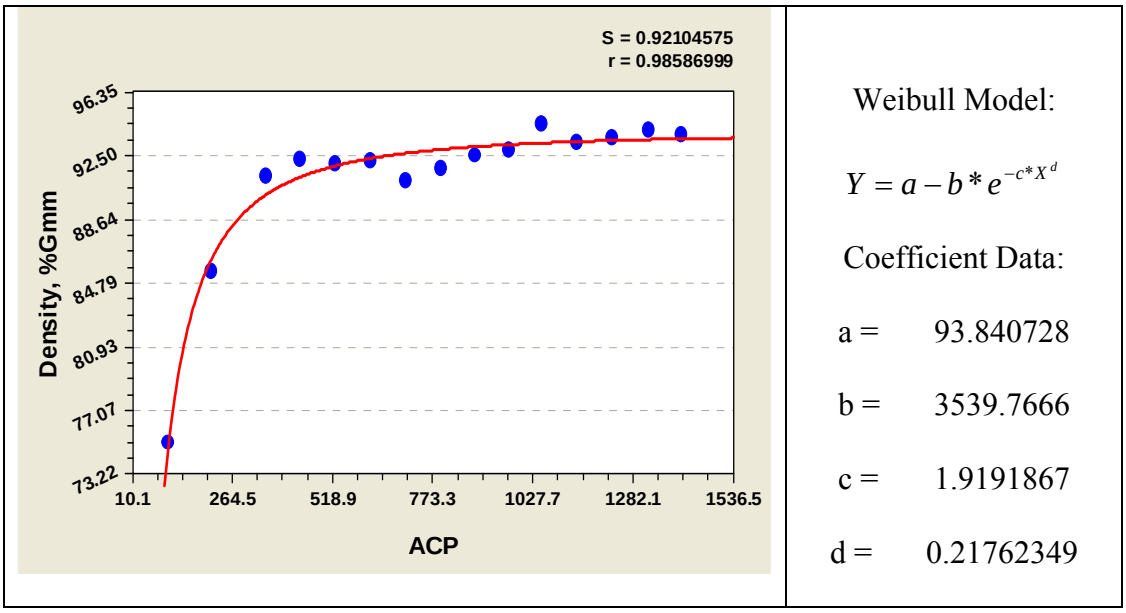

Figure 3.5: Illustration of the model used to fit field compaction data.

3.6 Material and Mixture Properties for Validation Analysis

The HMA mixtures used for this part of the study are shown in Table 3.5. This includes surface mixtures placed in different states as part of the NCHRP 9-27 study. These data were used to compare the results obtained from the analyses of the Test Track mixes. NCHRP 9-27 projects are characterized by a variety of equipment, roller operations and locations with a variety of environmental conditions.

Table 3.5: Data from NCHRP 9-27 mixtures

Section	Prod NMAS	PG Grade	Grad Type	$N_{des.}$	Average field thickness, mm
VA-1	9.5	70-22	Fine	65	38.1
VA-2	19.0	64-22	Coarse	65	63.5
VA-3	9.5	64-22	Coarse	65	38.1
NC-1	9.5	70-22	Fine	100	31.8
CO-1	12.5	58-28	Coarse	75	57.2
MO-1	19.0	64-22	Coarse	100	50.8
MO-2	19.0	64-22	Coarse	100	101.6
UT-2	19.0	64-34	Coarse	125	38.1
AL-1	25.0	76-22	SMA	50	60.9
AL-2	25.0	67-22	Fine	100	69.9
AL-4	19.0	76-22	Coarse	100	57.2
AL-5	12.5	67-22	Coarse	86	38.1
FL-2	12.5	64-22	Fine	75	37.5
GA-1	12.5	67-22	Coarse	75	38.1
GA-2	9.5	67-22	Fine	75	31.8
MS-1	12.5	67-22	Fine	80	38.1

CHAPTER 4. RESULTS AND ANALYSES

4.1 Conceptual hypothesis for explaining expected trends

The following concepts were used to explain expected trends in terms of laboratory compactability using the Superpave gyratory compactor:

- Rough surface texture, cubical or block shaped aggregate and highly angular particles will all increase the required compactive effort to achieve a specific density *(8).*
- Strength of the aggregate particles directly affects the amount of degradation that occurs in the SGC. Softer aggregates typically degrade more than strong aggregates and allow denser aggregate packing to be achieved.
- Modified asphalt binders tend to have higher shear stiffness and lower permanent shear strain; in other words, they tend to increase resistance to permanent deformation and decrease compactability *(8).*
- Asphalt binder lubricates the aggregate during compaction and therefore, mixes with low asphalt content are generally difficult to compact because of inadequate lubrication, whereas mixes with high asphalt content will be easier to compact *(6)*.
- According to Bahia *(4),* it is possible that during the initial stage of compaction (from $N_{initial}$ to $N@92\%G_{mm}$), the initial density of coarse mixes is relatively low because of the larger voids that can be entrapped under the initial compaction.

This can explain the higher compaction energy indices expected for coarser mixes.

- The amount of compactive energy applied to a mix (number of gyrations) indirectly affects compactability. It is expected that mixes compacted at low N_{des} (i.e. 50 gyrations) require higher asphalt content to reach 4% air voids than mixes compacted at high N_{des} (i.e. 125 gyrations). Therefore, mixes with low N_{des} (higher asphalt content) are expected to be easy to densify *(6).*

4.2 Laboratory compaction parameters

The parameters used to describe laboratory compactability are the percentage of maximum theoretical specific gravity at N_{ini} ($\%G_{mm}@N_{ini}$), the Compaction Energy Index and the Coarse and Fine Aggregate Ratios as determined by the Bailey Method. The first two parameters are obtained from a densification curve using the SGC, the Bailey Method ratios are computed from the gradation. Compaction slope and the number of gyrations to reach the Locking Point of the mixture are also obtained from a Superpave densification curve and because these parameters are related to resistance to permanent deformation they were also used to describe laboratory compactability.

When analyzing the data, presenting the information using box plots was the best approach to study and compare the characteristics of a different batch of observations *(24).* A box plot allows identifying the center and how spread out the data are about this central value. A box plot also allows investigating extreme values (referred to as outliers) or study the distribution of the data values (the pattern of the data values along the

measurement axis). Box plots are useful for assessing symmetry, presence of outliers, general equality of location, and equality of variation and usually are a better way to visualize the results of comparisons using analysis of variance (ANOVA) or t-tests.

A box plot is made up of a box with various lines and points added to it. The top and bottom of the box are the 25th and 75th percentiles. The length of the box is the interquartile range (IQR). Thus, the box represents the middle 50% of the data. Values outside the upper and lower adjacent values are called outside or extreme values. Values that are under three IQRs from the 25th and 75th percentiles are called mild outliers (shown as whiskers). Those outside three IQRs are called severe outliers (shown as asterisks). Mild outliers are not unusual, but severe outliers are.

4.2.1 Parameters obtained from Densification Curve

Figure 4.1 shows a comparison of the percentage of maximum theoretical density at the number of initial gyrations ($\%G_{mm}@N_{ini}$) in terms of four types of gradations (fine, intermediate, coarse and SMA) using box plots. It can be seen that the coarser the gradation the lower the $\%G_{mm}@N_{ini}$. It was found a strong evidence to conclude that the mean values of $\%G_{mm}@N_{ini}$ for the four groups are different (p-value < 0.0001; analysis of variance F-test) for a significance level alpha = 5%. This result suggests that coarser mixes are tougher to compact, at least in the gyratory compactor. When using a two-sample t-test to compare two groups, only the fine-graded and the intermediate-graded groups resulted not significant (p-value = 0.52) which means that there is no evidence that intermediate-graded mixes have lower values of $\%G_{mm}@N_{ini}$ than fine-graded mixes. Table A.3 of Appendix A contains the complete data set.

It was found that higher values of $\%G_{mm}@N_{ini}$ for each category (fine, intermediate, coarse and SMA) are associated to mixes with lower asphalt contents as shown in Figure 4.2. It was determined that the reason why these results went contrary to the expected trend is the fact that gradations relatively finer tended to have lower initial air voids and therefore, higher values of $\%G_{mm}@N_{ini}$. On the other hand, gradations relatively coarser tended to have lower values of $\%G_{mm}@N_{ini}$ because of the larger voids that can be entrapped under the initial compaction, as shown in Figure 4.3.

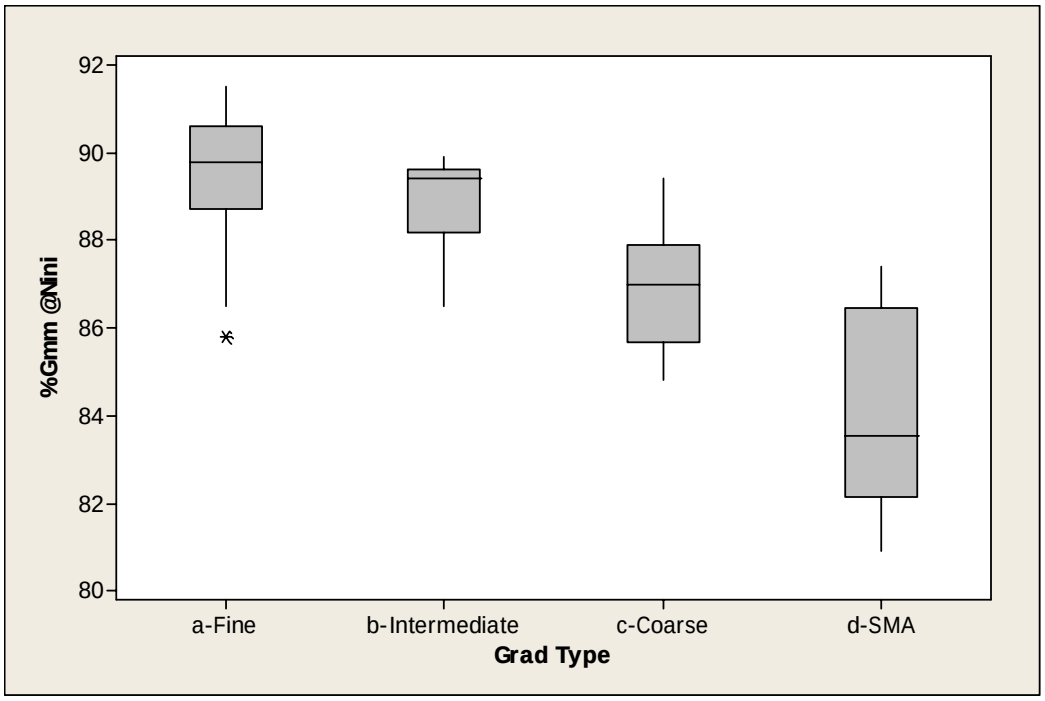

Figure 4.1: $\%G_{mm}@N_{ini}$ sorted by Gradation Type.

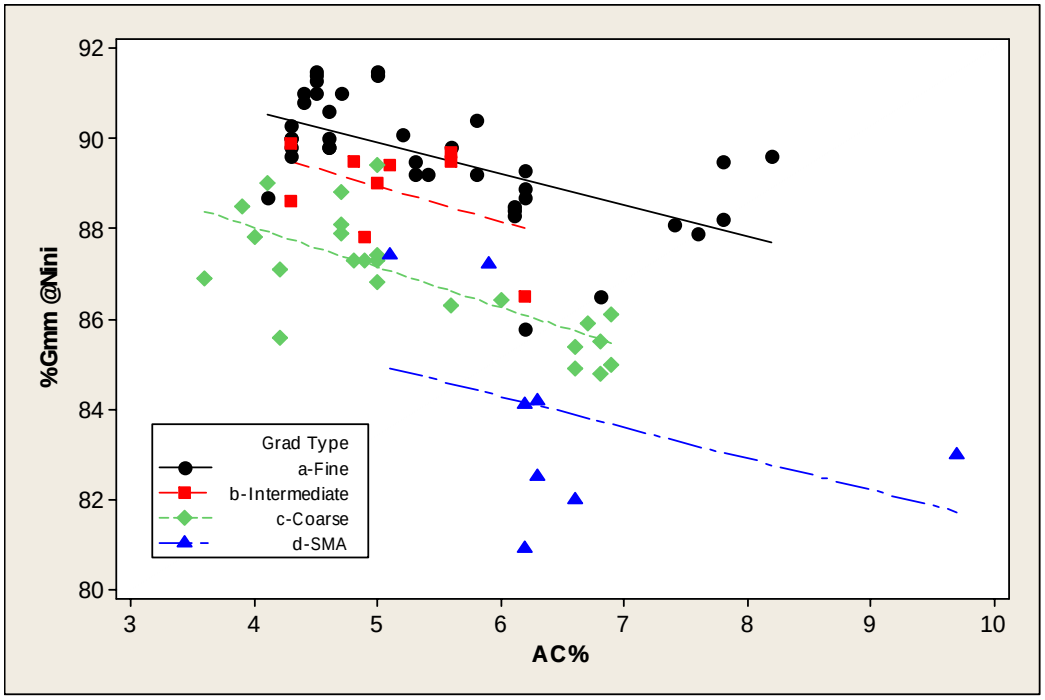

Figure 4.2: Relationship between $\%G_{mm}@N_{ini}$ and asphalt content.

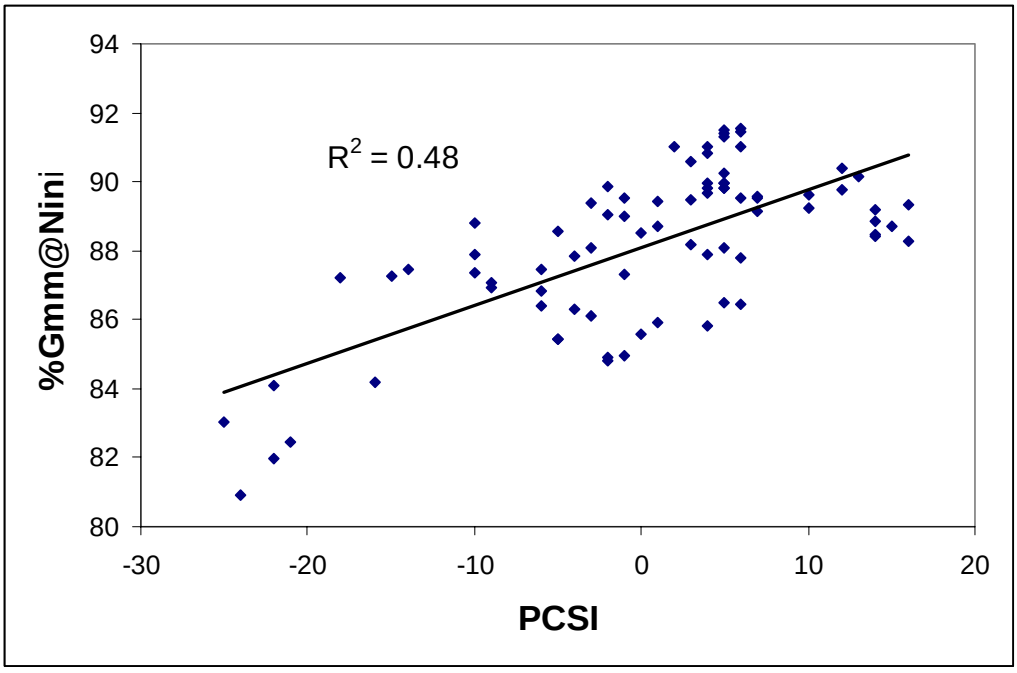

Figure 4.3: Relationship between $\%G_{mm}@N_{ini}$ and PCSI.

The Compaction Energy Index is another indicator of mixture compactability. According to Bahia *(4)* low values of CEI represent mixtures easy to compact, and in this case, fine and intermediate mixtures require less energy to achieve the desired density, while SMA mixtures cover a wide range of required energy (see Figure 4.4). It was found that there is a strong evidence to conclude that the mean CEIs in the four groups are different (p-value < 0.0001; analysis of variance F-test) for a significance level alpha = 5%. Once again only the fine-graded and the intermediate-graded groups resulted not significant (p-value = 0.99, two sample t-test) which means that there is no evidence that intermediate-graded mixes have lower values of CEI.

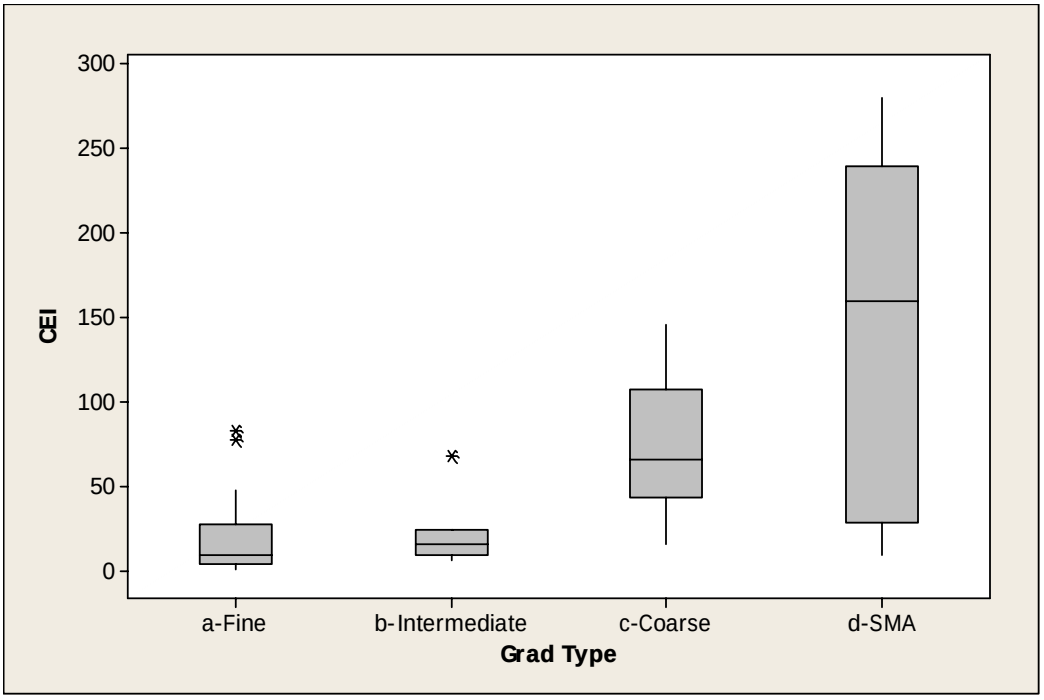

Figure 4.4: Compaction Energy Index (CEI) sorted by Gradation Type.

The greater spread observed for SMA mixtures can be explained by a difference in compactive effort (N_{des}) and the relative coarseness expressed by the PCSI. It was

found that SMA mixes compacted at N_{des} = 50 gyrations presented CEI values below 70, while SMA mixes compacted at N_{des} = 75 presented CEI values up to 280. Figure 4.5 shows a strong correlation between PCSI and $\%G_{mm}@N_{ini}$ and PCSI and CEI which indicates that coarser SMA mixtures also tended to be difficult to compact in the laboratory and also explains the greater spread observed for SMA in Figure 4.1. This suggests that SMA mixtures are very sensitive to the relative coarseness of the gradation and the compactive effort.

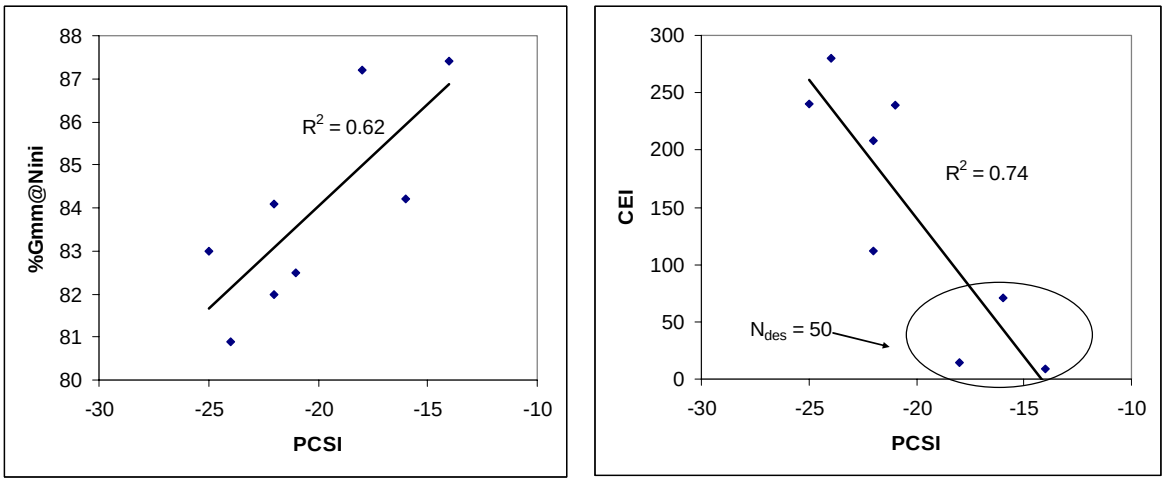

Figure 4.5: Relationship between PCSI and $\%G_{mm}@N_{ini}$ and PCSI and CEI for SMA mixtures.

Figure 4.6 shows the traffic densification index measured from the number of gyrations to compact samples from 92 to 96% G_{mm} ($TDI_{92\text{-}96}$). TDI has been described as an indicator of the potential of the mixture to consolidate under traffic. It can be noticed how this parameter tends to increase for mixtures designed with higher number of gyrations. This trend was expected because mixes compacted at higher N_{des} are designed

to resist higher permanent deformations which also requires increased compaction effort to obtain a desired density.

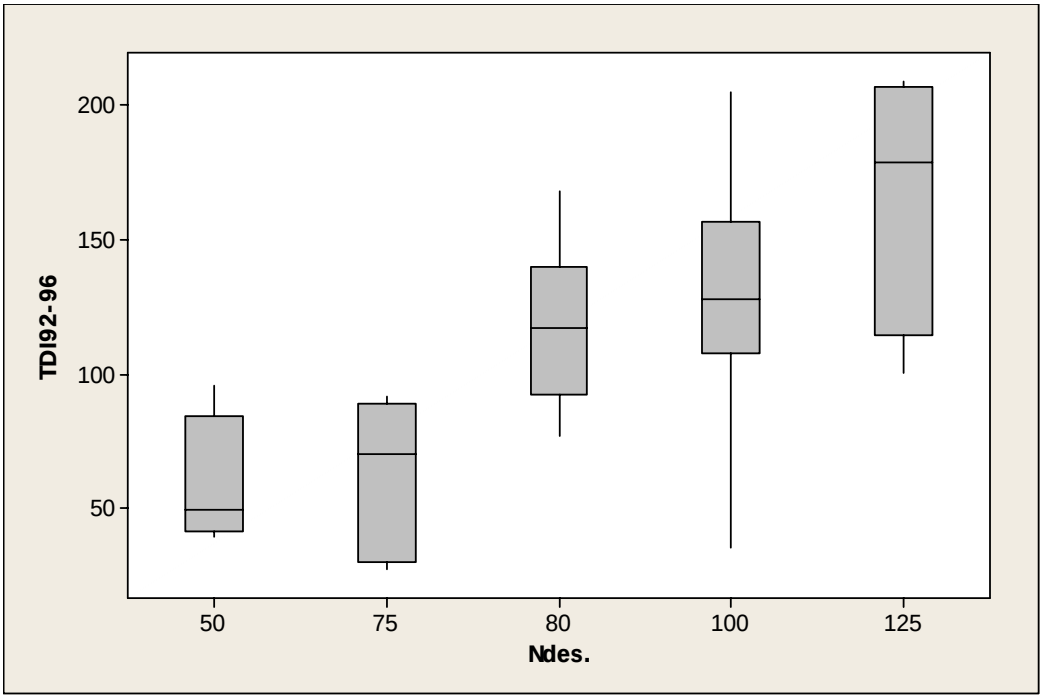

Figure 4.6: Traffic Densification Index (TDI 92-96) sorted by Ndes.

It can be seen in Figure 4.7 that the parameter compaction slope increases as the mixture becomes coarser. There is significant evidence that the mean slopes for the four groups are different (p-value < 0.0001; analysis of variance F-test) for a significance level of alpha = 5%. Since high slope values have been associated with mixtures resistant to permanent shear strain *(15)* therefore, the coarser the gradation the more resistance to deformation the mixture is. In this case it was found that there is no evidence that intermediate-graded and coarse-graded mixes have different mean values of slope (p-value = 0.065, two sample t-test) at significance level of 5%.

A group of possible outliers can be seen for fine-graded mixes. That group corresponds to mixes with high asphalt contents (above 7%) as part of the 2000 test track study to compare low versus high asphalt contents.

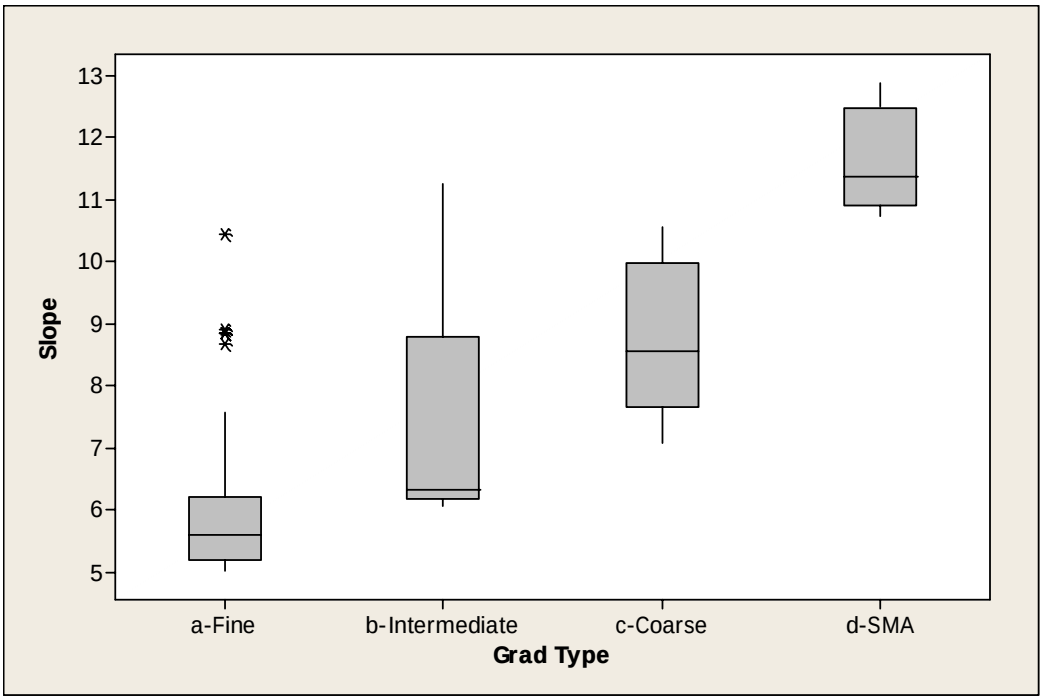

Figure 4.7: Compaction Slope sorted by Gradation Type.

The number of gyrations to achieve the locking point (LP 2-1) of the mixture indicates that fine aggregate mixtures tend to compact easily while SMA mixes present the opposite trend (Figure 4.8). It can be seen that the plots of slope and locking point have similar shapes. It was found that there is significant evidence that the mean values of LP 2-1 for the four groups are different (p-value < 0.0001; analysis of variance F-test) for a significance level of alpha = 5%. In this case it was found that there is no evidence that fine-graded and intermediate-graded mixes have different mean values of LP 2-1 (p-

value = 0.17, two sample t-test). The same conclusion was obtained for coarse-graded and SMA mixes (p-value = 0.18, two sample t-test) at significance level of 5%.

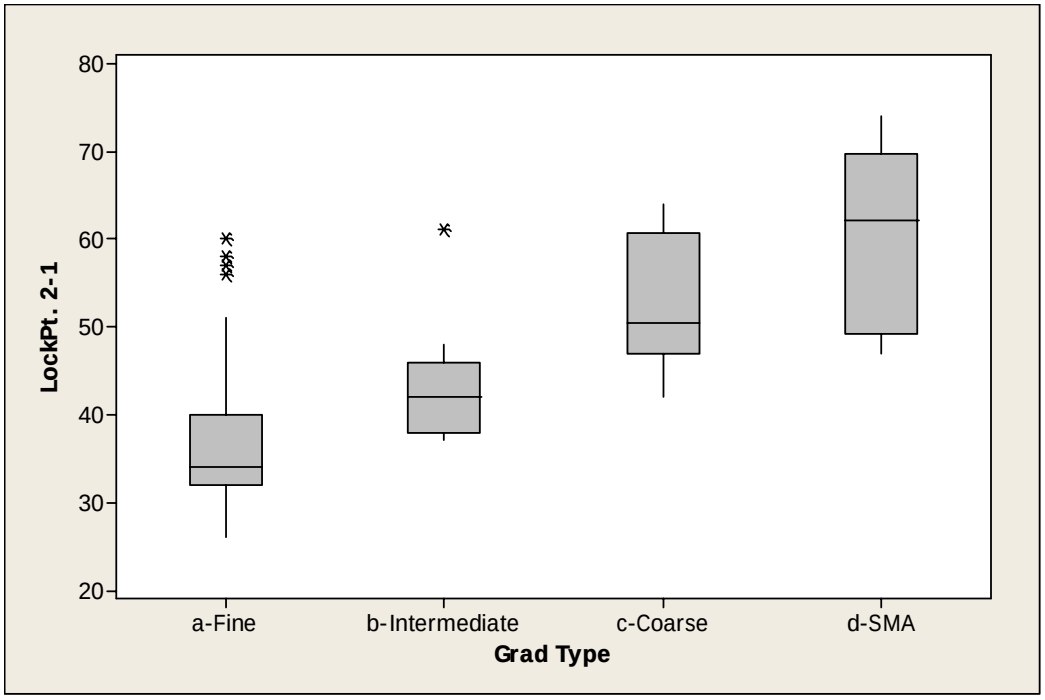

Figure 4.8: N @ Locking Point sorted by Gradation Type.

4.2.2 Gradation parameters as indicators of compactability

According to the Bailey Method Coarse Aggregate Ratio, Fine Aggregate (coarse portion) Ratio and Fine Aggregate (fine portion) Ratio are indicators of compactability. As the ratios increase the overall compactability of mixture decreases.

When evaluating the compactability using the CA ratio, the results indicate that an opposite trend from CEI and $\%G_{mm}@N_{ini}$ as gradations go from fine to coarse (Figure

4.9). This is indicating that the fine portion of the mix predominates over the coarse portion. On the other hand, FA_c ratio has the same trend as CEI and $\%G_{mm}@N_{ini}$ for gradation type (Figure 4.10). It was found strong evidence that the mean values of CA ratio are different for the four groups (p-value < 0.0001; analysis of variance F-test) and even for pair comparisons using a t-test for a significance level of alpha = 5%.

According to Pine *(5)*, altering the FA_c ratio normally involves a change in particle shape, strength and texture, as well as a change in gradation. It was found that this ratio has the most influence on altering VMA or air voids in a coarse-graded mix. Therefore, the assumption that packing characteristics of the coarse particles of the fine portion of the mix predominates over the packing of coarse portion may be valid at least for coarse-graded mixes. It was found that there is significant evidence to conclude that the four groups have different mean FA_c ratios (p-value < 0.0001; analysis of variance F-test) for a significance level of alpha = 5%. In this case it was found that there is no evidence that intermediate-graded and coarse-graded mixes have different mean values of FA_C ratio (p-value = 0.065, two sample t-test) at significance level of 5%.

Only the CA Ratio and the FA_C Ratio were included in this study. FA_f Ratios could only be calculated for coarse gradations which produced too few observations with respect to the other two parameters. Table A.3 of Appendix A contains the complete data set of the computed parameters.

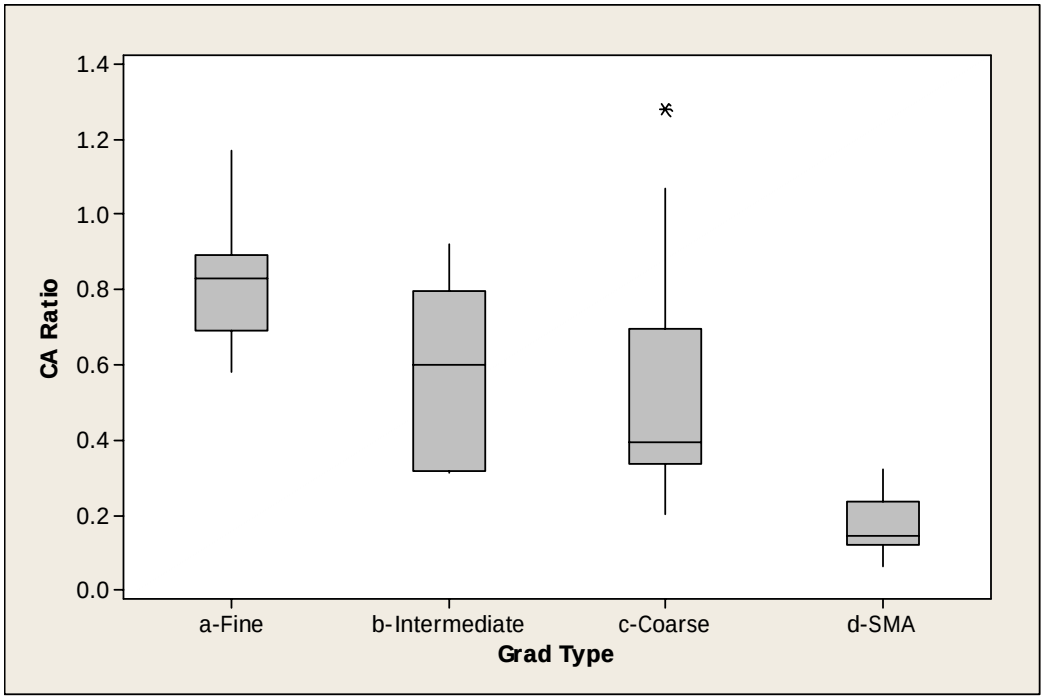

Figure 4.9: CA Ratio sorted by Gradation Type.

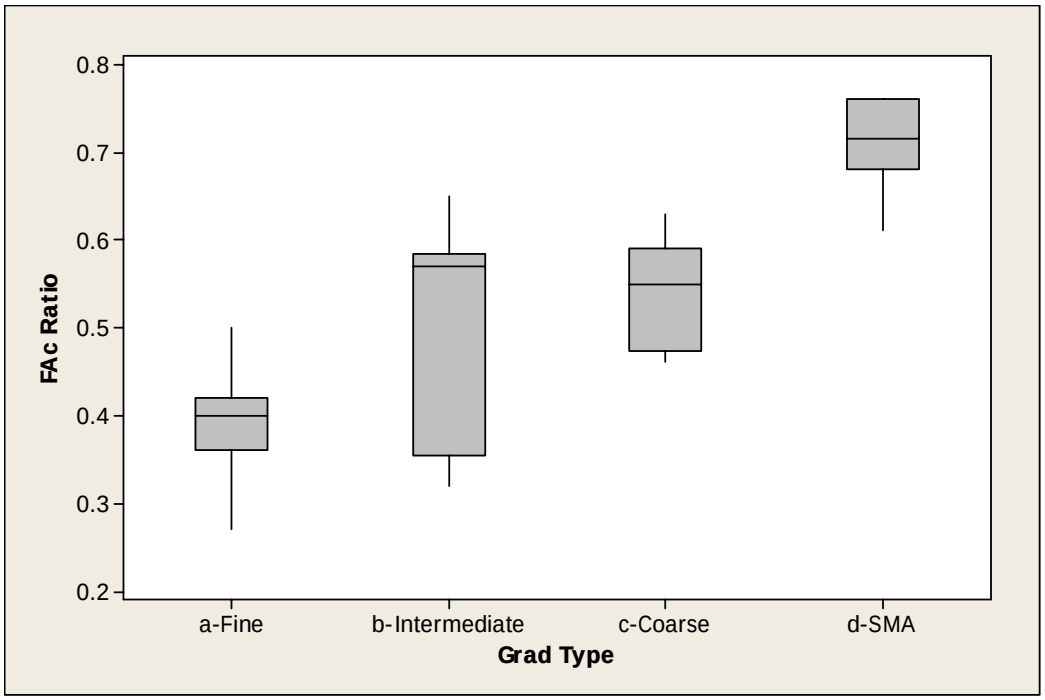

Figure 4.10: FAc Ratio sorted by Gradation Type.

4.2.3 Comparison between laboratory measured characteristics of HMA

Correlations were performed in order to compare mixture parameters. Table 4.1 shows the single correlation (R-value) calculated for each pair of variables, the shaded cells indicate a better correlation (above 0.6), and a letter "C" indicates that the expected trend was correct.

Compaction Energy Index correlates well with $\%G_{mm}@N_{ini}$ (R = -0.92) and indicates how as the compaction energy increases the initial air voids content of the mixture increases. Mixtures with low CEI and high $\%G_{mm}@N_{ini}$ tend to compact easily in the SGC.

Superpave compaction slope and locking point of the mixture are strongly correlated (R = 0.92), and both are correlated with $\%G_{mm}@N_{ini}$ (R = -0.90 and R = -0.91 respectively). These results indicate that mixes with higher values of slope and locking point are difficult to compact in the lab.

It can be noticed how the PCSI has good correlations with the mix compaction parameters as well. The relationship between PCSI and $\%G_{mm}@N_{ini}$ (R = -0.63) indicates that fine gradations tend to have low air void content at $N_{initial}$ and are mixes that compact rapidly in the SGC.

Table 4.1: Single correlation among parameters

	PCSI	Lab Voids	%Gmm @Nini	N @ 92%Gmm	CEI	TDI92-96	TDI92-Ndes	N @ 96%Gmm	Slope	LockPt.	CA Ratio	FAc Ratio
PCSI	1		C	C	C				C	C	C	C
Lab Voids	-0.01	1					C					
$\%G_{mm}$ @N_{ini}	0.69	-0.26	1	C	C				C	C	U	U
N @ 92%G_{mm}	-0.54	0.21	-0.91	1	C			C	C	C	U	U
CEI	-0.64	0.07	-0.91	0.95	1				C	C	U	U
TDI92-96	0.42	0.14	0.39	0.16	0.04	1		C				
TDI92-Ndes	0.28	-0.79	0.51	-0.25	-0.21	0.27	1					
N @ 96%Gmm	0.08	0.53	-0.25	0.66	0.50	0.70	-0.18	1				
Slope	-0.73	-0.14	-0.90	0.62	0.69	-0.55	-0.28	-0.09	1	C		C
LockPt1	-0.63	-0.09	-0.91	0.78	0.82	-0.38	-0.19	0.14	0.92	1		C
CA	0.70	0.00	0.55	-0.29	-0.28	0.17	0.18	-0.06	-0.58	-0.54	1	
FAc	-0.83	-0.07	-0.58	0.20	0.22	-0.41	-0.24	-0.13	0.67	0.56	-0.71	1
AC%	-0.12	0.10	-0.50	0.39	0.39	-0.21	-0.23	0.10	0.45	0.49	-0.24	0.01

C = correct (expected) trend.

U = unexpected trend

Blank = not considered in the analysis or poor correlation

Previously, the potential effect of the internal angle of gyration due to the use of different gyratory compactors was discussed. For the first group of mixes (Test Track cycle 1) a Troxler gyratory compactor was used for design and quality control; and for the second group (cycle 2) a Pine SGC was used. The internal angle of gyration of each device was not determined at the time the data was collected. This factor can be a source of significant error, especially for those parameters which are computed based on specific gravity of specimens.

For example, Figure 4.11 shows the difference in comparisons of CEI and $\%G_{mm}@N_{ini}$ resulting from the use of two different gyratory compactors. On the other hand, Figure 4.12 shows the relationship between $N@92\%G_{mm}$ and CEI, which indicates that the results are not affected much by compactor type. These results follow the findings made by Prowell *(12),* where the data suggest that parameters expressed in terms of number of gyrations seem to be less affected by the dynamic internal angle (DIA) of gyration than parameters expressed in terms of density.

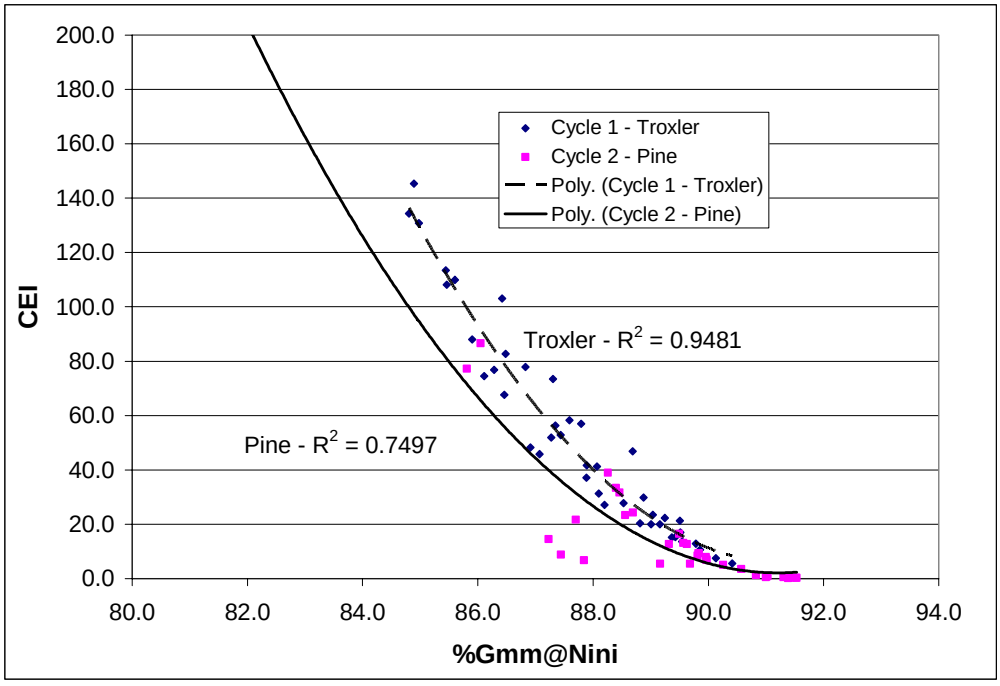

Figure 4.11: Relationship between $\%Gm_m@N_{ini}$ and CEI.

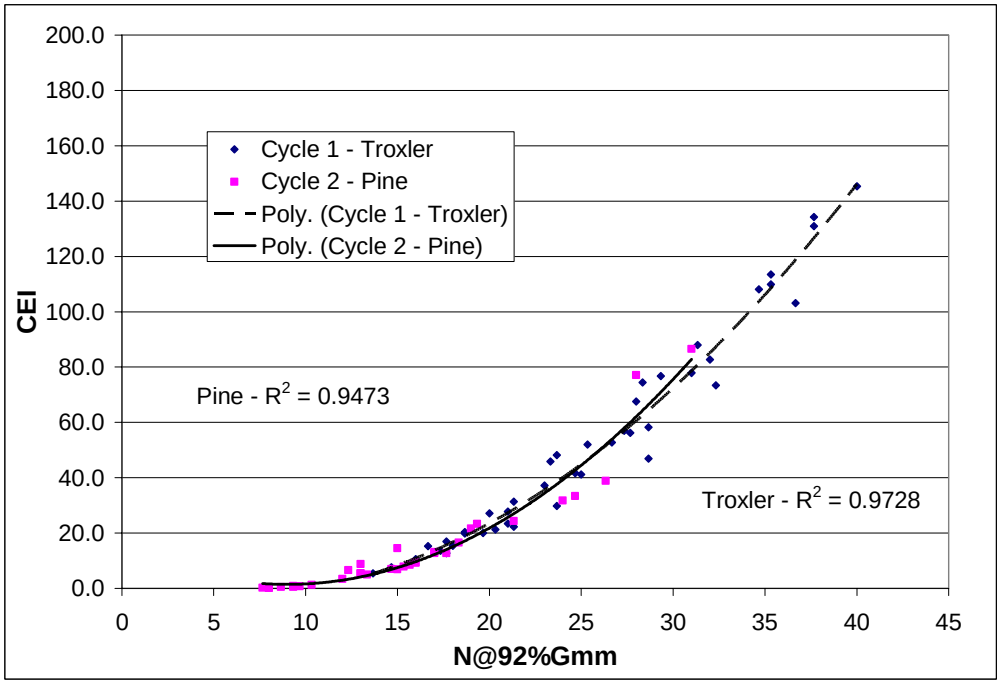

Figure 4.12: Relationship between $N@92\%G^{mm}$ and CEI

4.2.4 Effect of physical properties on the SGC parameters

A multiple analysis of variance (MANOVA) was used to evaluate the effect of physical characteristics (primary aggregate type, NMAS, PG grade, gradation type, and gradation ratios) on SGC parameters ($\%G_{mm}@N_{ini}$, $N@92\%G_{mm}$, CEI, slope, locking point). Because of the limited number of observations (less than 100) this analysis included principal-effects only, and all interactions were omitted. A MANOVA analysis has one or more factors each one with two or more levels and two or more dependent variables. The calculations are extensions of the general linear model approach used for ANOVA and significant terms at alpha = 0.05 are shown in Table 4.2. The asphalt content was included in the analysis as a factor.

For the first response variable, $\%G_{mm}@N_{ini}$, mixtures containing limestone as primary aggregate source tended to be difficult to compact ($\%G_{mm}@N_{ini} = 85.5$). The main differences between limestone and another aggregate type are: tougher aggregate (low values of micro deval below 9%), more angular (F&E 3:1 = 0%, FAA > 45%) and higher content of fine material (% passing 0.075mm sieve above 7%). This confirms that all the properties mentioned above increase the required compactive effort to achieve a specific density.

The same effect was produced by 9.5 mm NMAS mixtures with the lowest value of $\%G_{mm}@N_{ini}$ (86.4). In terms of gradation type, fine-graded mixes were the easiest to compact and SMA mixtures were the most difficult to compact. SMA mixtures are designed to improve resistance to permanent deformation which also requires compaction energy.

For the parameter N@92%G_{mm}, it was found in terms of primary aggregate type that marble-schist mixtures tended to achieve 92% of G_{mm} at the lowest number of gyrations followed by granite mixtures which matched the results obtained for the parameter %G_{mm}@N_{ini}. Marble-schist aggregate is characterized by having flat and elongated particles (F&E 3:1 = 10%) and higher values of micro deval (17%). These properties are related to aggregate degradation and allow denser aggregate packing to be achieved. On the other hand, granite mixtures contain some flat and elongated particles (F&E 3:1 = 7%) and intermediate values of micro deval (8%), but most of these mixtures are fine-graded which may explain their ability to compact easily.

Stiffness of the binder was a significant factor with an interesting result. PG 76 mixtures presented the lowest number of gyrations to reach 92% of G_{mm}. It was followed by PG 67 mixes and finally PG 70 mixes. It was expected that stiffer binders should produce stiffer mixes more difficult to compact. The same behavior was observed for air voids content. On average, PG 76 mixtures presented the lowest air voids content (3.26%) while the remaining mixtures were close to 4% air voids. In addition, it was found that PG 76 mixtures had higher asphalt contents and were designed with that intention which may be the main reason of this behavior.

According to Bahia *(4),* low values of Compaction Energy Index (CEI) indicate that a mixture is easy to compact. In general, marble-schist and granite mixtures were easier to compact than limestone mixes. PG 76 mixtures and fine-graded mixtures tended to be easy to densify as well, according to CEI parameter. This follows the same trend observed for %G_{mm}@N_{ini}.

As mentioned before, higher compaction slope mixtures tend to have higher shear stiffness and lower permanent shear strain. It can be noticed how mixtures with lms/slag as a primary aggregate source had the highest slope (10.6), which means that those mixtures are stiffer and more difficult to compact. The combination lms/slag has more angular particles (CAA = 50%) that makes the mixture difficult to compact and more material passing the 0.075 mm sieve (above 8%) which makes the mixture stiffer.

As expected, finer gradations presented lower compaction slopes (below 7) and coarser gradations presented higher slopes (SMA = 11.6). The highest values obtained for SMA mixtures are due to a combined effect of gradation (coarser gradation) and higher asphalt contents. In terms of number of gyrations to reach the locking point of the mixture, the difference between coarse-graded mixture and SMA mixtures is minor (54.9 and 55.4 respectively) which indicates that the locking point is affected less by asphalt content than the slope. Limestone/slag mixtures had higher locking point (60) which means that this mixes tend to have higher shear stiffness and lower permanent shear strain, while granite/limestone/sand mixtures, as predicted by other parameters such as CEI, $\%G_{mm}@N_{ini}$ and Superpave slope, had a propensity to compact easily.

Table 4.2: Principal effects - MANOVA analysis.

Response variable	Significant terms	Levels	Least-square means (count)
$\%G_{mm}@N_{ini}$	Primary Aggregate Type	Granite	87.7 (21)
		Lms	85.5 (10)
		Marble-Schist	88.1 (3)
		gravel	87.4 (7)
		grn/lms/snd	87.6 (24)
		lms/slag	86.3 (11)
		marine lms	87.6 (4)
	NMAS	9.5 mm	86.4 (18)
		12.5 mm	87.5 (34)
		19.0 mm	87.6 (28)
	Gradation Type	Fine	89.4 (39)
		Intermediate	88.0 (9)
		Coarse	86.3 (24)
		SMA	85.0 (8)
$N@92\%G_{mm}$	Primary Aggregate Type	Granite	21.3 (21)
		Lms	37.5 (10)
		Marble-Schist	17.6 (3)
		gravel	25.4 (7)
		grn/lms/snd	22.5 (24)
		lms/slag	28.3 (11)
		marine lms	24.8 (4)
	PG grade	PG 67	24.6 (34)
		PG 70	28.2 (12)
		PG 76	22.5 (34)
	Gradation Type	Fine	18.6 (39)
		Intermediate	23.6 (9)
		Coarse	31.9 (24)
		SMA	26.2 (8)
Compaction Energy Index (CEI)	Primary Aggregate Type	Granite	44.2 (21)
		Lms	123.2 (10)
		Marble-Schist	38.7 (3)
		gravel	66.9 (7)
		grn/lms/snd	56.1 (24)
		lms/slag	81.5 (11)
		marine lms	55.6 (4)
	PG grade	PG 67	64.9 (34)
		PG 70	88.6 (12)
		PG 76	46.0 (34)
	Gradation Type	Fine	25.8 (39)
		Intermediate	52.9 (9)
		Coarse	92.1 (24)
		SMA	95.3 (8)

Table 4.2 (continued): Principal effects - MANOVA analysis.

Response variable	Significant terms	Levels	Least-square means (count)
SGC Slope	Primary Aggregate Type	Granite	8.27 (21)
		Lms	9.80 (10)
		Marble-Schist	9.00 (3)
		gravel	7.92 (7)
		grn/lms/snd	7.69 (24)
		lms/slag	10.6 (11)
		marine lms	8.43 (4)
	NMAS	9.5 mm	9.51 (18)
		12.5 mm	8.11 (34)
		19.0 mm	8.82 (28)
	Gradation Type	Fine	6.42 (39)
		Intermediate	8.19 (9)
		Coarse	9.04 (24)
		SMA	11.6 (8)
Locking Point	Primary Aggregate Type	Granite	45.8 (21)
		Lms	57.6 (10)
		Marble-Schist	50.1 (3)
		gravel	45.9 (7)
		grn/lms/snd	42.4 (24)
		lms/slag	60.2 (11)
		marine lms	47.0 (4)
	NMAS	9.5 mm	52.8 (18)
		12.5 mm	48.0 (34)
		19.0 mm	48.8 (28)
	PG grade	PG 67	50.8 (34)
		PG 70	51.7 (12)
		PG 76	47.1 (34)
	Gradation Type	Fine	40.6 (39)
		Intermediate	48.6 (9)
		Coarse	54.9 (24)
		SMA	55.4 (8)

4.2.5 Assessment of variability among observations (multivariate statistical analysis)

Since mix properties are related to each other, multivariate statistical techniques not only apply, but also they are indeed needed. Multivariate techniques allow consideration of any existent correlation among variables (both response and predictor), so that their

unique and common effects can be evaluated *(25)*. The following multivariate techniques are considered:

(A) Canonical correlation. In order to gather information on how well composition percentages explain variability on physical properties. Canonical correlation simultaneously correlates several independent variables and several dependent variables.

(B) Factor analysis. In order to evaluate how different mix properties are related to each other, as well as to extract and interpret hidden effects (properties that influence other properties). Principal component analysis extract factors based on the total variance of the factors and it is used to find the fewest number of variables that explain the most variance.

(C) Hierarchical cluster analysis. In order to evaluate how observations can be separated into groups with similar properties, as well as which variables allow for such separation. The purpose of cluster analysis is to reduce a large data set to meaningful subgroups of individuals or objects. The division is accomplished on the basis of similarity of the objects across a set of specific characteristics.

A. Effect of gradation properties and asphalt content on the SGC parameters

Canonical correlation analysis is the study of the linear relations between two sets of variables. It is the multivariate extension of correlation analysis. A canonical correlation analysis was developed in order to evaluate the effect of the gradation parameters (Primary Control Sieve Index, and CA and FA_C ratios) and the asphalt content (AC%) on

the SGC measures parameters of the HMA ($\%G_{mm}@N_{ini}$, $N@92\%G_{mm}$, CEI, $N@96\%G_{mm}$, Slope, and Locking Point). Table 4.3 shows the most significant canonical functions on canonical correlation.

The meaning of the canonical pairs of variables (response variables – independent variables) is evaluated in the following form:

- Canonical set 1; the independent variable correlates with the relative coarseness or fineness of the gradation (PCSI), the asphalt content, the packing characteristics of the coarse portion of the fine aggregate (FA_C Ratio) and the coarse aggregate ratio. The response variable correlates with $\%G_{mm}@N_{ini}$, $N@92\%G_{mm}$, CEI, Slope and Locking Point. Canonical set 1 explains 64.3 % of the total variability. This analysis indicates that coarse mixtures with low CA ratio require stronger fine aggregate structure (higher FA_C ratio) and higher asphalt content to meet the target volumetric properties. Mixtures with these characteristics tend to be difficult to compact in the laboratory.

Table 4.3: Canonical functions on canonical correlation (*).

Canonical pairs (***)	**Higher loadings (**)**				**Accumulated variance among observations explained by response variables, which is reproduced by predictor canonical functions.**
	Predictor variables		**Response variables**		
	Variable	**Loading**	**Variable**	**Loading**	
1	PCSI CA Ratio FA_C Ratio AC, %	-0.89 -0.65 0.78 0.53	%Gmm@Nini N@92%Gmm CEI Slope Locking Point	-0.93 0.76 0.86 0.96 0.87	64.3 %

(*) Even tough there is strong evidence the data corresponds to a non-normal multivariate distribution, how significant the canonical correlation model is gives confidence on results and interpretation. Canonical correlation is highly significant, at 99 % confidence.
(**) Loading refers to the correlation between a common effect (canonical function) and an actual variable.
(***) Common effects on predictor variables correlated to common effects on response variables. Consider every set has a response canonical function, as well as a predictor canonical function.

B. Identification of common effects among parameters

Factor analysis (FA) is an exploratory technique applied to a set of observed variables that seeks to find underlying factors (subsets of variables) from which the observed variables were generated. The factor analyst hopes to identify each factor as representing a specific theoretical factor. Therefore, many of the reports from factor analysis are designed to aid in the interpretation of the factors.

An FA analysis was performed in order to identify common effects. In this case all variables used in canonical correlation were used, including asphalt content. Table 4.4 shows the results of the factorial experiment analysis. It was found that the considered variables do have some common effect; when considering both physical properties and composition percentages, 96% of variance explained by twelve variables can be explained by only two factorials. From these extracted factors, their common effects can be interpreted, allowing establishing hypotheses on hidden effects, as follows:

- Factor 1 has to do with parameters obtained from Superpave densification curve related to shear stiffness and resistance to deformation, and gradation properties which are used to measure compactability. In this case the PCSI, as a measurement of the relative coarseness or fineness of the gradation, affects the shear stiffness of a mixture and its ability to resist permanent deformation. A positive sign of the loading indicates an increase of a value. A positive value of PCSI indicates finer gradations. In general, finer gradations tend to have lower shear stiffness and lower resistance to deformation.

- Factor 2 explains how some parameters used to measure compactability in the laboratory are highly correlated.

Table 4.4: Factorial experiment analysis

Factor	Variables showing higher loading on factorials (*)	Loading (**)	Variance among variables	Accumulated variance among variables
1	PCSI Slope Locking Point Ca Ratio FA_c Ratio	0.88 -0.83 -0.68 -0.69 -0.88	55.8%	55.8%
2	%Gmm@Nini N@92%Gmm CEI	-0.72 0.91 0.76	41.8%	96.6%

(*) Loading refers to the correlation between a common effect (factorial in this case) and an actual variable.
(**) Analysis considering V-rotation. Significant factors are shown.

C. Effect of material properties on the studied parameters

Hierarchical cluster analysis was performed in order to separate observations by similar groups. Cluster separation was performed taking into account physical properties that were not very well explained by canonical correlation analysis and interpretation allowed identifying some hidden effects (see Table 4.5).

Hierarchical clustering pointed out that, in explaining variability among clusters, gradation has a high effect in mixture properties and parameters used to measure compactability. This statement is explained by:

- Cluster 1 includes, basically, un-modified fine-graded mixtures. On average, this group has low values of CEI, slope, locking point and N@92%G_{mm}. This cluster is also characterized by coarse aggregate particles well packed (high CA ratios).

- Cluster 2 is composed by coarse mixtures with intermediate values of CEI, slope, locking point and gradation ratios. In this case, the coarse portion of the fine aggregate controls the particles packing.
- Cluster 3 contains fine-graded and intermediate-graded mixtures. This cluster has the lowest values of CEI and N@92%G_{mm} but intermediate values of slope and locking point. On average, Bailey Method ratios are the same as those for cluster 1. The use of modified asphalt and NMAS of 19.0 mm may be the principal factor of difference.
- Cluster 4 has higher values of CEI, slope, locking point than cluster 2, which indicates that coarse gradations close to the maximum density line and intermediate gradations produce mixes difficult to compact with the SGC.
- Cluster 5 has the highest values of CEI, slope, locking point and air voids, which indicates that this group presents the most difficult mix configuration to compact. Once more, the coarse portion of the fine aggregate controls the particles packing with the highest FAc ratios.

Overall, finer gradations and gradations with PCSI values close to zero tend to increase mixture compactability in the laboratory. In terms of gradation components as indicators of HMA compactability, FA_c ratio has a strong effect in clustering and CA ratio clearly defines SMA mixtures (average CA ratio = 0.2).

CEI, N@92%Gmm, Slope, Locking Point, Primary Control Sieve Index and FA_C ratio are the most important response variables, in order to account for cluster separation. The first four variables are related to mixture performance during densification and represent the applied energy to reach a level of compaction and mixture resistance to

deform. PCSI and FA_C ratio describe gradation properties and how particles are packed together. Both groups of variables are very well related to aggregate geological properties, since every one depends on the aggregate shape and texture.

Table 4.5: Cluster separation and properties

	Cluster*	1		2		3		4		5	
		Mean	St. Dev.	Mean	St. Dev.	Mean	St. Dev.	Mean	St. Dev.	Mean	St. Dev.
Properties	PCSI	8.3	4.9	-4.5	5.2	3.2	5.5	-0.9	3.8	-20.3	3.9
	Lab Voids	4.4	0.7	3.5	0.4	2.8	0.5	3.6	0.7	4.5	1.4
	$\%G_{mm}$ @N_{ini}	89.5	0.6	88.4	0.9	89.7	1.7	85.9	0.7	83.9	2.3
	N@92 $\%G_{mm}$	18.5	4.3	22.5	4.7	13.7	6.0	33.3	4.1	34.6	15.2
	CEI	16.9	11.6	35.6	20.1	12.7	17.2	98.9	25.5	146.5	108.4
	TDI_{92-96}	146.3	34.0	141.0	24.7	93.6	19.6	118.2	16.6	53.7	24.2
	$TDI_{92-Ndes}$	174.8	61.5	235.3	40.1	250.9	62.6	181.3	40.9	74.6	41.0
	N@96 $\%G_{mm}$	84.5	12.1	81.7	12.5	51.6	9.0	87.0	10.8	62.0	20.1
	Slope	5.7	0.5	7.4	0.8	7.1	2.0	9.6	1.0	11.6	0.8
	LockPt.	34.9	3.8	45.1	3.9	41.0	11.3	58.9	4.7	60.1	10.5
	CA Ratio	0.8	0.1	0.4	0.2	0.8	0.2	0.6	0.3	0.2	0.1
	FAc Ratio	0.4	0.1	0.6	0.1	0.4	0.1	0.5	0.1	0.7	0.1
	AC%	5.4	1.1	4.6	0.4	5.2	1.2	6.2	0.8	6.5	1.4
Differences among clusters**	Primary Agg. Type	grn/lms/snd, granite		granite		grn/lms/snd		lms/slag, gravel		Lms, granite	
	Prod NMAS	9.5, 12.5, 19.0		12.5, 19.0		19.0		9.5, 12.5		12.5	
	Asphalt PG Grade	67		67, 76		67, 76		67, 76		69, 81	
	Mod. Type	Neat		NEAT, SBS		NEAT, SBS		NEAT, SBS		SBS	
	Grad. Type	Fine		Coarse		Fine, Intermediate		Coarse, intermediate		SMA	
	Ndes.	80, 100		100		80, 100		100		50, 75	

* Hierarchical cluster separation by Ward's method.
** Those are the most significant differences.

4.3 Field compaction

Due to the well controlled construction operations at the test track, there were not significant differences in as-constructed density for intermediate, fine and coarse-graded mixes (p-value > 0.05, t-test). The only difference can be seen in Figure 4.13 for SMA mixtures (p-value < 0.0.001, t-test), which had the highest density (Test Track cycles 1 and 2). It can be seen in Table 4.6 that the mean densities for fine-graded and intermediate-graded mixes were similar with almost all the sections compacted over 92% of $G_{mm.}$ There were not significant differences in as-constructed density for intermediate, fine, coarse-graded and SMA mixes when comparing them by year of construction (p-value > 0.05, t-test).

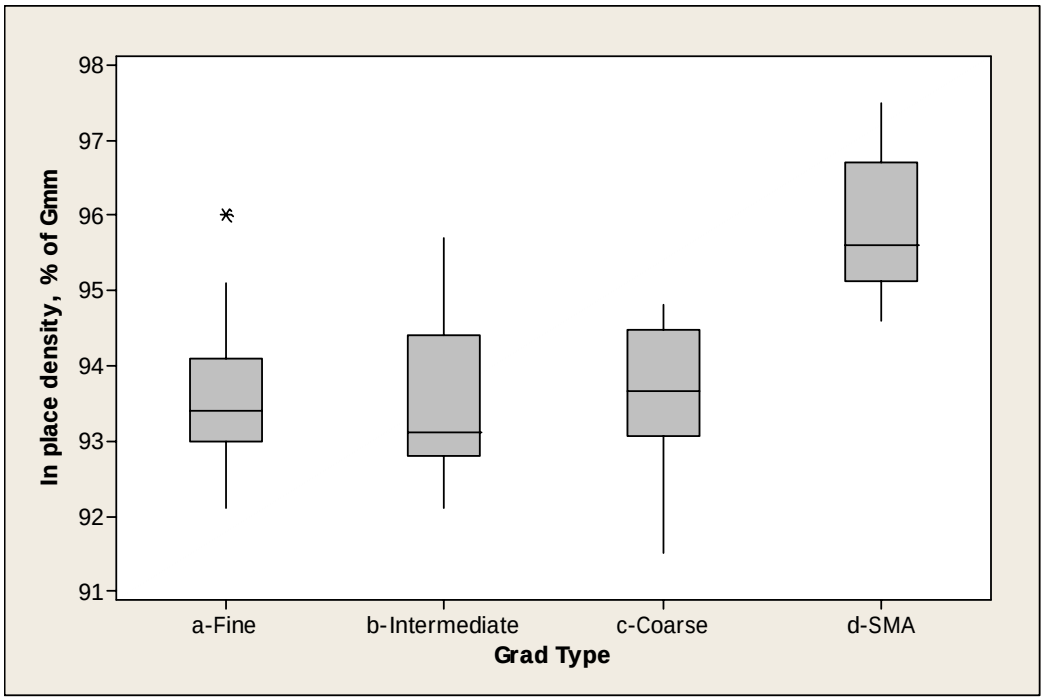

Figure 4.13: Post-construction density level (%G_{mm}) sorted by Gradation Type.

For SMA mixtures placed in 2000, it was found that a few passes of the static roller (2 to 3) produced density levels close to 94% of G_{mm}. This suggests that SMA mixtures were easy to compact in 2000. On the other hand, much more roller passes (5 to 7 static and 3 to 5 pneumatic) were required to achieve density levels near 96% in 2003. This was explained by an increase in the specified density level for SMA mixtures placed in 2003 combined with the reduction in lift thickness compared with mixes placed in 2000.

Table 4.6: Post-construction density level (%G_{mm}) sorted by Gradation Type and Test Track cycle

Gradation Type	Test Track Cycle	Mean density	Minimum	Maximum	Observations
Fine	2000	93.7	92.7	95.1	14
	2003	93.5	92.1	96.0	28
Intermediate	2000	92.9	91.5	94.9	5
	2003	93.5	93.1	93.9	2
Coarse	2000	93.7	91.8	94.8	20
	2003	NA	NA	NA	0
SMA	2000	93.8	92.0	95.0	6
	2003	95.8	93.1	97.5	9

4.3.1 Conceptual hypothesis for explaining expected trends

The following concepts were used to explain expected trends in terms of field compactability:

- Rough surface texture, cubical or block shaped aggregate and highly angular particles will all increase the required compactive effort to achieve a specific density *(8)*.

- Strength of the aggregate particles directly affects the amount of degradation that occurs in the field. Softer aggregates typically degrade more than strong aggregates and allow denser aggregate packing to be achieved *(8)*.
- A continuously graded (dense-graded) aggregate is generally easy to compact *(8)*.
- A mix designed with high dust content is generally more difficult to compact *(6, 8)*.
- Modified asphalt binders tend to have higher shear stiffness and lower permanent shear strain; in other words, they tend to increase resistance to permanent deformation and decrease compactability *(15)*.
- Asphalt binder lubricates the aggregate during compaction and therefore, mixes with low asphalt content are generally difficult to compact because of inadequate lubrication, whereas mixes with high asphalt content will be easier to compact *(6)*.
- According to Bahia *(4)*, it is expected that that mixes with higher CEI tend to be difficult to compact in the field. In addition, coarser mixes are also expected to require more energy applied by the rollers.
- According to Pine *(5)* mixes with higher CA ratios (coarse portion of the gradation highly packed) are more difficult to compact in the field. And as the FAc ratio decreases, compactability of the mixture increases.
- Higher initial mat temperatures require more time to cool down, which means more time available for compaction. On the other hand, if the initial mix temperature is too high, the mix may be tender and difficult to compact until the temperature decreases and the viscosity of the asphalt binder increases *(6, 8)*.

- The desired density is difficult to obtain on thin lifts (layers less than 50 mm) because of the mix's rapid decline in temperature *(8)*.
- Mixes with properties that improve resistance to fatigue and permanent deformation (i.e. higher SGC slopes) require increased compaction effort to obtain a desired density *(8, 15)*.

4.3.2 Analysis of the Accumulated compaction Pressure

Compaction operations at the track were well documented and provide good information about the compactability of the mixtures in the field. These data were used to determine the total compaction energy applied by the rollers during construction.

The total accumulated compaction pressures applied on each mixture were analyzed using some factors that affect field compaction: gradation type (fine, coarse, intermediate, SMA), lift thickness and/or t/NMAS, mix temperature, aggregate size (NMAS) and asphalt grade. Different approaches were used for explaining the variability observed in ACP. The analyses included single comparison using box plots, analysis of pairs using t-test and analysis of variance.

When comparing the total energy applied by the rollers (ACP) in terms of gradation type for the first two cycles, it can be observed that there is not a clear trend as shown in Figure 4.14. This result was confirmed by an ANOVA F-test that showed poor evidence that the ACP differs for gradation type (p-value > 0.05; F-test). For coarse-graded mixes ACP ranges from 300 to 1800 psi, for fine-graded from 400 to 2400 psi, intermediate-graded from 300 to 1400 psi and SMA mixes from 300 to 2000 psi. However, when the data were subdivided also by cycle, differences were observed for

fine-graded and SMA mixes (Figure 4.15). Figure 4.15 shows that greater compaction energy was required for the sections constructed in cycle 2, whereas for cycle 1, coarse-graded mixes required the highest compaction energy followed by fine-graded and intermediate-graded, and SMA mixes required the least (see Appendix B). Observe in Figure 4.15 that comparisons were limited to fine-graded mixes and SMA, and only two values for intermediate-graded mixes found in 2003 were used in the analysis.

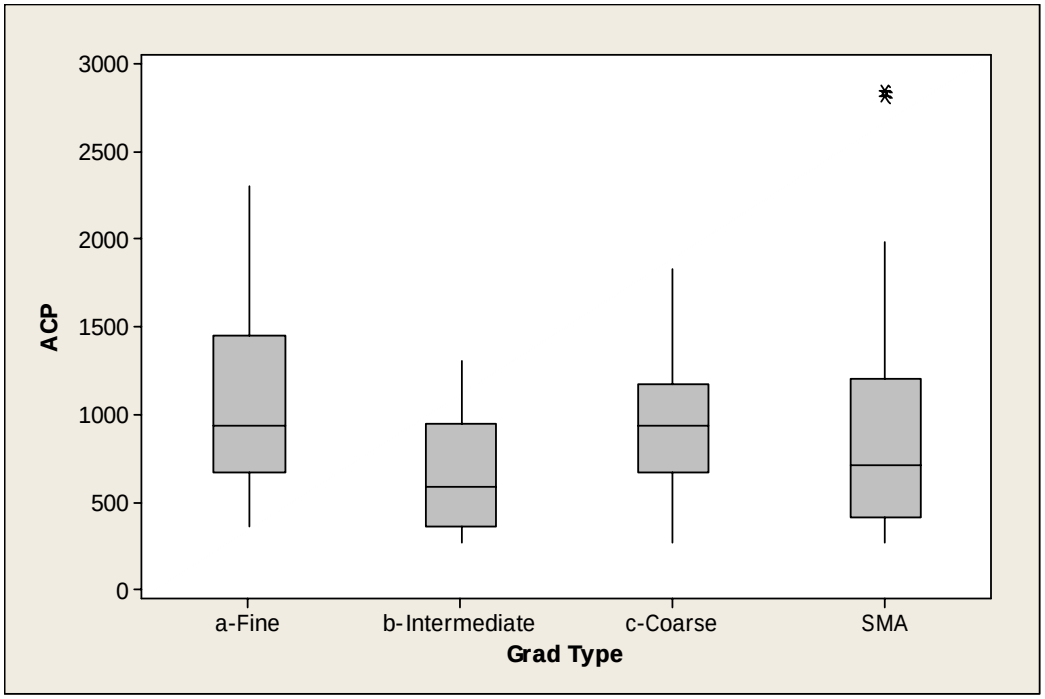

Figure 4.14: ACP sorted by Gradation Type.

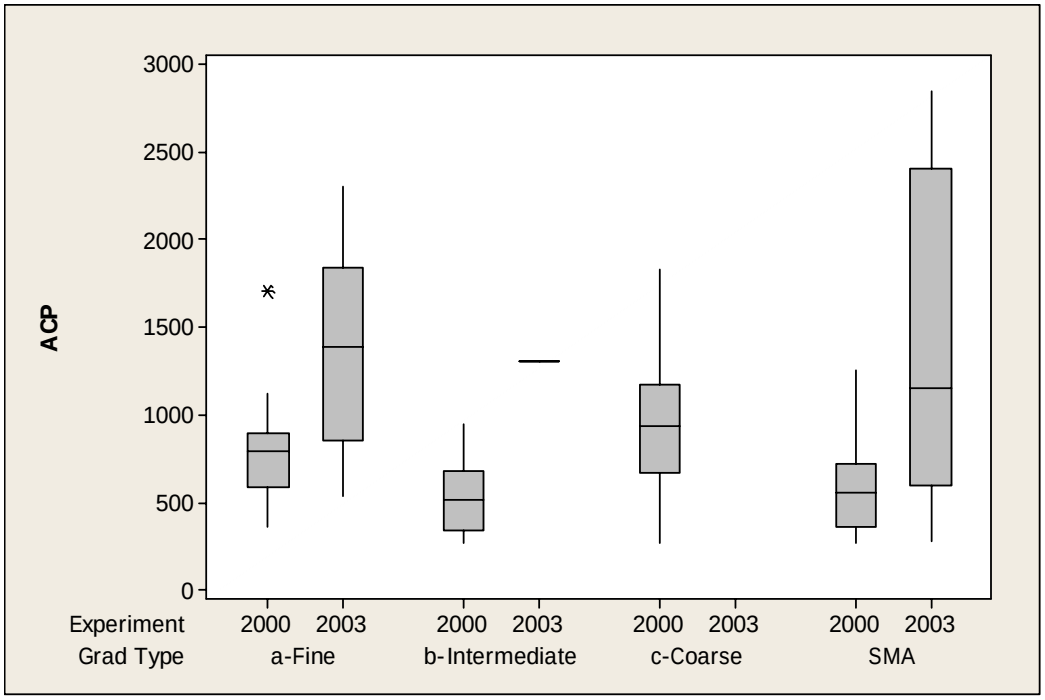

Figure 4.15: ACP sorted by Gradation Type and cycle.

The main reason why 2003 mixes required more compactive effort is observed in Figure 4.16. In 2000 the mean layer thickness was 53 mm, whereas in 2003 the mean thickness was 44 mm. The effect of placing thinner layers (<50 mm) in 2003 decreased the lift temperature and compaction time requiring higher compactive efforts to achieve similar density levels. Figure 4.17 shows the comparison of temperature at different compaction stages for the two cycles (2000 and 2003). It can be seen that the mean laydown temperatures (T1) of the mix were similar for the two cycles. When comparing the temperature at the beginning of the compaction (T2) a significant drop in temperature can be observed for mixes placed in 2003. On average, the compaction process for 2000 mixes started at 250 °F, while the compaction process for 2000 mixes started at 220 °F allowing less time to achieve the desired density. Finally, it can be seen that the rolling

operation ended with temperature (T3) below 175 °F for 2003 mixes. According to some authors *(8)*, below 175 °F little or no gain can be achieved with the application of additional compactive effort.

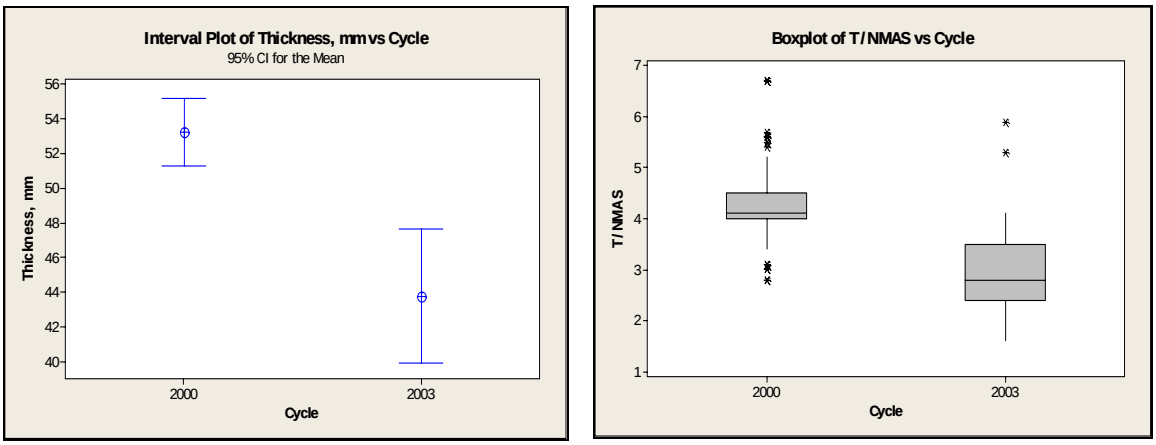

Figure 4.16: Thickness and T/NMAS ratio for each cycle.

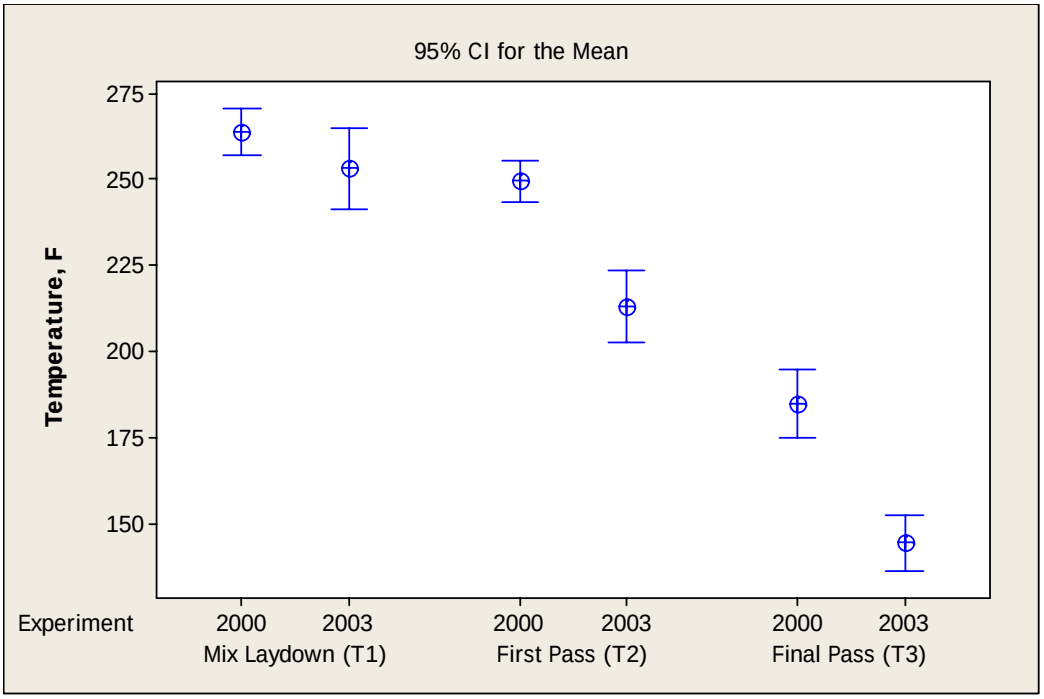

Figure 4.17: Temperature measured at different compaction stages.

An analysis of variance (ANOVA) was performed to determine which factors (NMAS, gradation type, t/NMAS, temperature of mix, PG grade and post construction density level) significantly affected the resulting ACP. Table 4.7 shows the levels for each factors used in this analysis and Table 4.8 provides the ANOVA of ACP. The results show that only t/NMAS and temperature have a significant effect on ACP at a level of significance alpha = 0.05. T/NMAS is the most impacting factor (F-statistic = 7.19).

Figure 4.18 shows the effect of t/NMAS on the total effort applied to the mix; t/NMAS ratios below 3:1 required much more compaction energy. Figure 4.18 also indicates that mixes with temperatures at the first pass of the breakdown roller below 225 °F required more total compaction energy (ACP). Notice how the ACP increases as the post-construction density level increases. This may suggest that more energy was applied to reach a desired density level and may explain some variability observed on the ACP.

Table 4.7: Description of levels per factor used in analysis of variance

	Factor					
	Gradation type	NMAS, mm	t/NMAS	Post construction density level, $\%G_{mm}$	Temperature at first roller pass °F	PG grade
Level	Fine Intermediate Coarse SMA	9.5 12.5 19.0	Low < 3:1 Medium 3:1 – 4:1 High > 4:1	Low < 93 Medium 93 – 94 High > 94	Low < 225 High > 225	67 70 76

Figure 4.19 shows the interaction plot of ACP for the factors t/NMAS and temperature. Notice that for high t/NMAS ratios (above 4:1) the temperature has

minimum effect on the compaction energy. Low t/NMAS ratios (below 3:1) with lower temperature require a substantial increment in compaction energy.

Table 4.8: ANOVA for ACP

Source	Reduced DF	Sum of Squares	Mean Squares	F-Statistic	P-value	Significant at $\alpha = 5\%$
Gradation Type	3	112861.6	37620.55	0.18	0.906	No
NMAS	2	76625.79	38312.89	0.19	0.829	No
Thickness/NMAS (t/NMAS)	2	2086232	1043116	7.19	0.008	Yes
Density level, %Gmm	2	496946.1	248473	1.22	0.302	No
Temperature (T2)	1	1464502	1464502	5.12	0.009	Yes
PG grade	2	681993.8	340996.9	1.67	0.196	No
Error	58					
Total	70					

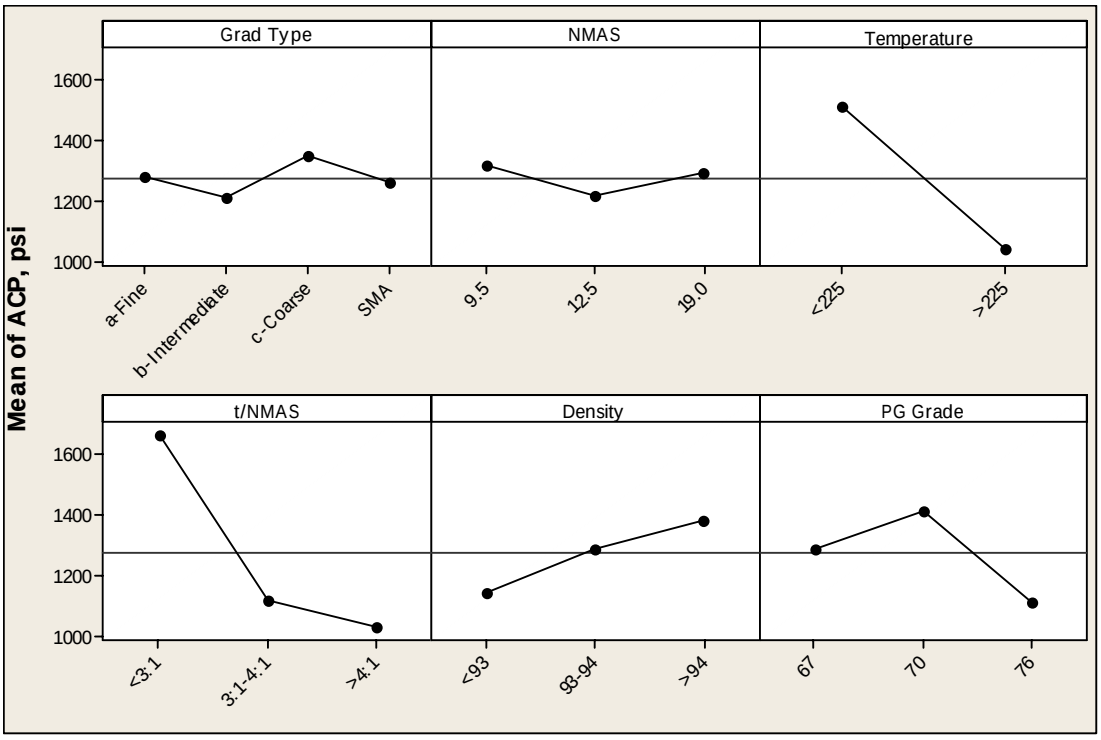

Figure 4.18: Main Effects Plot (fitted means) for ACP.

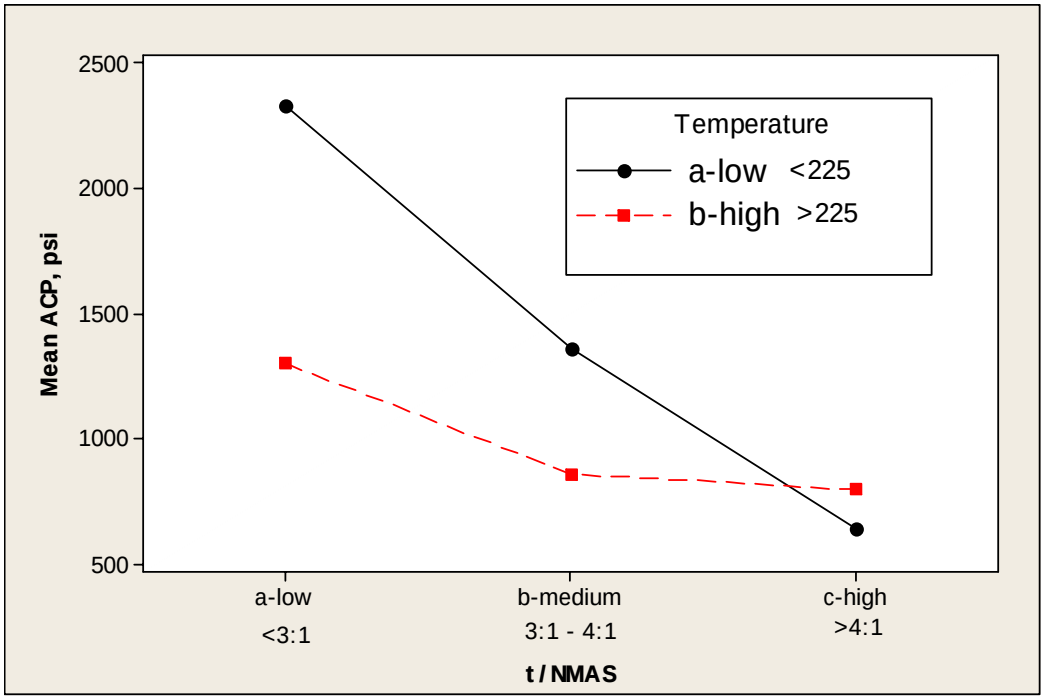

Figure 4.19: Interaction Plot (fitted means) for ACP.

4.3.3 Analysis of pairs

One of the main objectives of the first cycle of the test track was the evaluation of performance for different types of mixtures *(23)*. Several mini experiments were conducted and the evaluation included: fine graded vs. coarse graded mixes, effect of asphalt grade, asphalt content and polymer type and effect of aggregate type. A two-sample t-test for ACP was performed using mixtures from the 2000 experiment. The following subjects were used as comparison factors:

- Binder Grade with two levels: Low (PG 68/70) and High (PG 78/80)
- Asphalt content with levels Low (optimum) and High (optimum + 0.5%)
- Gradation with Coarse and Fine

- Polymer type SBR and SBS
- Aggregate type with granite and others.

Table 4.9 shows the results of the 2-sample t-test. The results show that even though there was no significant difference in ACP at $\alpha = 5\%$ for any factor, the most significant difference (lowest P-value) was obtained for aggregate type followed by gradation. Figure 4.20 shows a better form to understand the trends found in this analysis. A p-value of 0.125 provides suggestive evidence that granite mixes required lower compaction effort than mixes with another aggregate source and fine-graded mixes also required lower compaction effort than coarse-graded mixes. Finally, it can be seen that an increase in asphalt content slightly decreases the required effort.

Table 4.9: Comparison of ACP by various subjects

Factor	Level	Mean	Difference	T-statistic	P-value
Binder Grade	Low	824	27.7	0.22	0.831
	High	796			
Asphalt content	Low	969	189.4	0.79	0.457
	High	780			
Gradation	Coarse	835	215	1.38	0.196
	Fine	620			
Polymer type	SBR	932	-65.5	-0.34	0.75
	SBS	997			
Aggregate type	Granite	606	-224.7	-1.65	0.125
	Other	931			

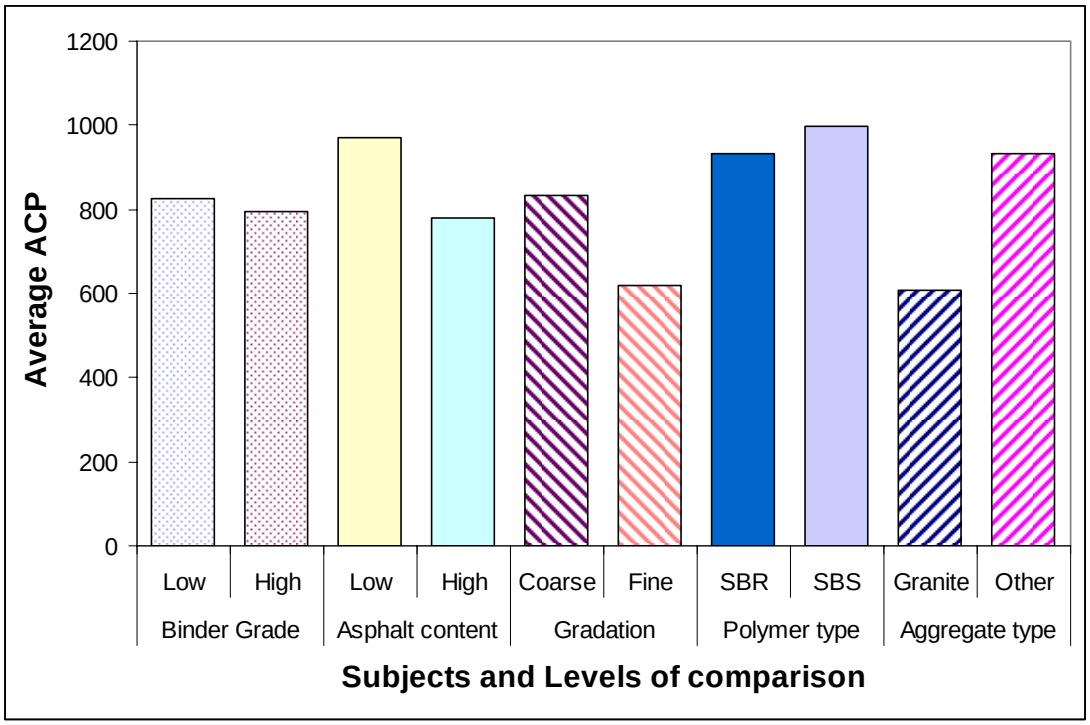

Figure 4.20: Comparison of ACP by various subjects.

A similar analysis was conducted to evaluate the effect of the same subjects on one of the laboratory compactability parameters. In this case, the Compaction Energy Index (CEI) was selected. Table 4.10 shows that gradation was significant at $\alpha = 5\%$ and similar trends as those observed for ACP were found for CEI in terms of aggregate type and asphalt content. Once again a p-value of 0.178 provides suggestive evidence that mixtures contained granite as aggregate source required lower energy to reach 92% of G_{mm} in the SGC than other mixes. Notice that an increase in asphalt content resulted in a slight decrease in CEI (see also Figure 4.21).

Table 4.10: Comparison of CEI by various subjects

Factor	Level	Mean	Difference	T-statistic	P-value
Binder Grade	Low	65	12.1	0.53	0.607
	High	52			
Asphalt content	Low	96.3	20.7	0.73	0.491
	High	75.6			
Gradation	Coarse	81.7	53.2	3.29	0.006
	Fine	28.5			
Polymer type	SBR	59.4	4.66	0.15	0.885
	SBS	54.7			
Aggregate type	Granite	19.4	-48.6	-1.75	0.178
	Other	68			

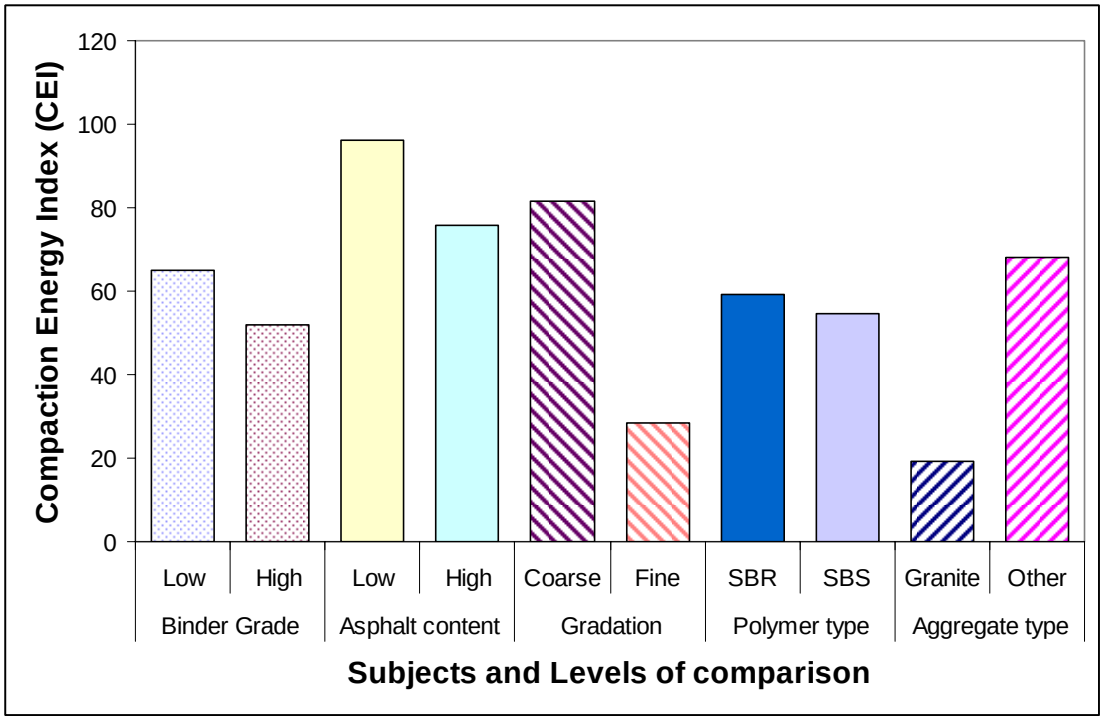

Figure 4.21: Comparison of CEI by various subjects.

4.4 Correlations between ACP and laboratory compaction parameters

Regressions between the field compaction energy (ACP) and laboratory parameters ($\%G_{mm}@N_{ini}$, $N@92\%G_{mm}$, CEI, Slope, Locking Point and Bailey Method ratios), mixture properties (air voids, VMA, VFA, microdeval, FAA, CAA, F&E 3:1, %pass 0.075mm), lift thickness, mix temperature and density level were analyzed. The laboratory measured parameters which yield the best correlations were analyzed further by performing multiple regression analysis with basic mixture properties.

Based on the conceptual hypothesis explained before, it was expected that the total accumulated compaction pressure would increase as the following parameters increased: $\%G_{mm}@N_{ini}$, $N@92\%G_{mm}$, CEI, Slope, Locking Point and CA ratio. In terms of mixture properties, it was expected that the total accumulated compaction pressure would increase as VMA increases, VFA decreases, PG grade increases, asphalt content decreases, micro deval decreases, FAA and CAA increase, F&E 3:1 decreases and the % passing 0.075mm increase. In addition, for low mix temperatures (<225 °F), thin layers (<50 mm) and low t/NMAS ratios (<3:1), an increase in ACP was expected.

As shown in the preceding discussion, there is an important difference in the compactive effort applied to the mixes of the first two test track experiments. When all the combined data were used to correlate ACP and lab compactability parameters, the values of simple linear correlation (R-value) were always near zero (Table 4.11). The factors which have the greatest influence of ACP were grade of the asphalt, temperature, thickness and t/NMAS. Most of the layers placed on the two test track experiments had a thickness near 50 mm as indicated by the oval in Figure 4.22. The best fit line between

ACP and thickness (quadratic model) shows a minimum point of ACP near 65 mm, or in terms of t/NMAS ratio, near 5.0, which may vary depending on gradation type and aggregate size (according to NCHRP 9-27 results).

Table 4.11: Single correlation between ACP and some parameters

PG Grade	0.37
NMAS	0.12
PCSI	-0.06
CA	0.24
FA_c	-0.20
% pass PCS	0.14
% pass 2.36	0.12
% pass 0.075	-0.14
AC%	-0.08
Thickness (mm)	-0.31
Actual PG	0.09
t/NMAS	-0.34
Density	0.08
$\%G_{mm}$@Ni	0.13
N@ $92\%G_{mm}$	-0.14
CEI	-0.10

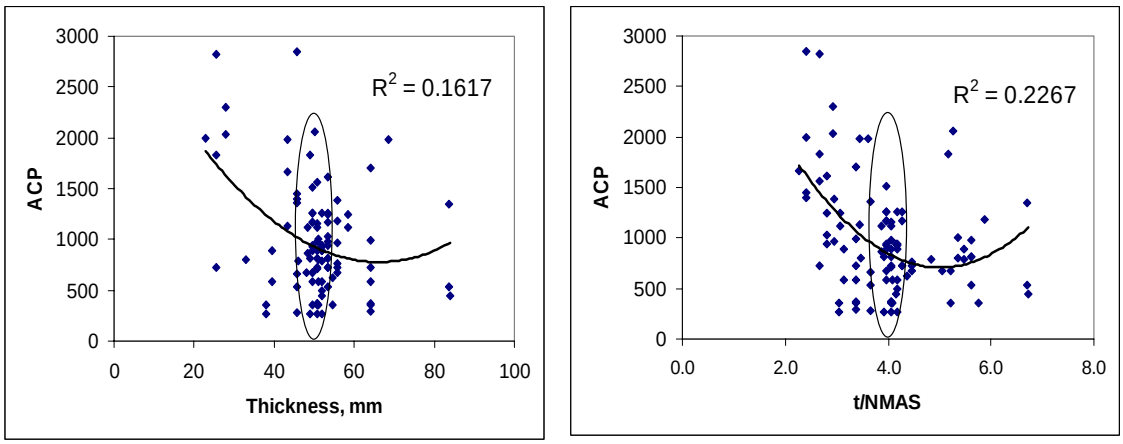

Figure 4.22: Effect of thickness on ACP.

When the data obtained from the 2000 cycle were used to correlate field and lab compactability (see Table 4.12), the majority of the results followed the expected trend and some of them correlated well. Parameters such as N@92%G_{mm} and CEI showed good correlation with ACP (R = 0.68 and 0.67, respectively). As expected, an increment of those parameters produced an increase of the field compaction energy (ACP). Most of these mixes were placed at a thickness of about 50 mm. When the data were limited to mixes placed in one 50 mm lift presented the highest correlation (Figure 4.23, $R^2 = 0.45$). These results indicate that mixes compacted in field with similar thicknesses can be easily correlated to ACP.

Table 4.12: Correlation and expected trend between ACP and compactability parameters including mix properties (Tangents only, cycle 1)

Parameter	Correlation	Expected trend
Density	0.17	correct
% Pass PCS	-0.35	correct
PCSI	0.38	correct
%G_{mm}@N_{ini}	-0.63	correct
N@92%G_{mm}	0.68	correct
CEI	0.67	correct
N@96%G_{mm}	0.38	correct
Slope	0.46	correct
LockPt	0.51	correct
CA Ratio	0.06	inconclusive
FA_c Ratio	-0.11	inconclusive
VMA	0.19	inconclusive
VFA	-0.49	incorrect
CAA	-0.01	inconclusive
F&E 3:1	-0.21	incorrect
FAA	-0.58	incorrect
Micro Deval	0.63	incorrect
AC %	0.21	incorrect
Actual PG	0.22	correct
Temperature	-0.20	correct

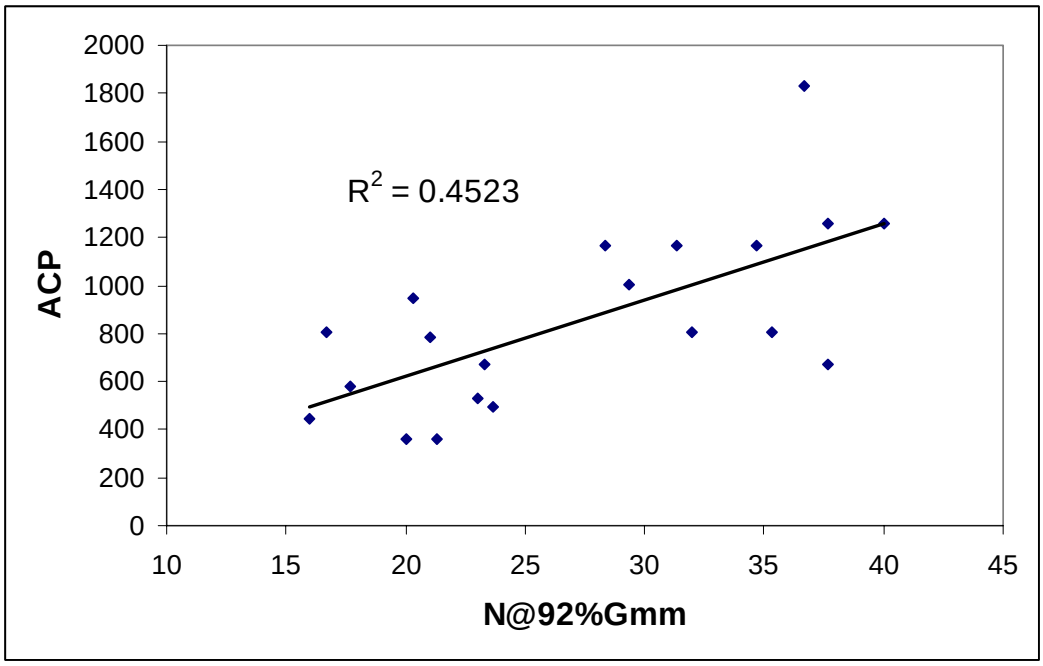

Figure 4.23: Relationship between ACP and N@92%G_{mm}.

Despite these results, the relationship between lab and field compactability is complicated by many other variables which are known to affect compaction. In other words, a simple linear correlation does not adequately describe the relationship. The use of multiple regression analysis was necessary to incorporate the wide variety of mix properties and factors affecting field compactability.

For the multiple regression analysis, the following parameters were used as predictor variables: asphalt content, actual PG grade, compaction slope, Compaction Energy Index (CEI), %G_{mm}@N_{ini}, N@92%G_{mm}, locking point, coarse and fine aggregate ratios, lift temperature, t/NMAS ratio, PCSI, fine aggregate angularity (FAA), VFA and Micro Deval. The best model was selected by choosing the model with the least number of predictor variables, the highest adjusted R^2, Mallow's Cp statistic less than the number

of predictor variables and minimum standard error of the regression. This procedure provides a model with almost all the variables significant at a pre-defined significance level (in this study 5%).

Once the best predictors were determined, a multiple linear regression was performed to determine the coefficients for each predictor. The final model also needed additional residual treatments to account for normality and linearity and only those predictors which followed a logical trend were selected. The final model is shown as follows:

```
SQRTACP = 57.2 - 0.0765 T3 + 1.55 NMAS + 11.5 CA + 2.19 %pass200
                     - 0.767 VFA + 0.0755 N@field                    [18]
```

```
S = 5.55   R-Sq = 54.9%   R-Sq(adj) = 47.6%
```

Predictor	Coef	SE Coef	T	P
Constant	57.25	17.64	3.24	0.002
T3	-0.07652	0.02908	-2.63	0.012
NMAS	1.5546	0.3105	5.01	0.000
CA	11.455	4.498	2.55	0.015
% pass 200	2.1943	0.6330	3.47	0.001
VFA	-0.7668	0.2018	-3.80	0.001
N@field	0.07549	0.05925	2.17	0.051

Where,

SQRTACP = square root of ACP

NMAS = nominal maximum size aggregate size

CA = CA ratio

%pass200 = percent passing 0.075mm sieve

T3 = temperature at the last roller pass

N@field = number of gyrations to reach the post construction density level

For this final analysis the square root of ACP was the response, while NMAS, CA ratio, % passing No 200 sieve, VFA, temperature and the number of gyrations to reach the post construction density level (N@field) were the predictors. The negative sign for temperature shows that the total compactive effort applied to the mixture decreases as the lift temperature increases. Cooler surfaces remove heat from the mat at a faster rate, decreasing the time available for compaction and eventually increasing the compactive effort. It can be observed in this model that, as expected, mixes with higher voids filled with asphalt tend to be more compactable. Equation 18 follows the Bailey Method theory that mixes with higher CA ratios are difficult to compact in the field. The positive sign of %pass200 indicates that higher amounts of material passing the 0.075mm sieve are related to stiffer mixes which tend to be difficult to compact in the field. Finally, the number of gyrations to reach the post construction density level was proportional to the accumulated compaction pressure.

4.5 Compaction of specimens using the SGC at field thickness

The third part of this project included compaction of specimens using the SGC at thicknesses equal to those in the field. The specimens were compacted to meet 92 percent of G_{mm}. One of the objectives of this part of the study was to compare the number of gyrations to reach the post construction density level at lift thickness ($N@92\%G_{mm\text{-}field}$) obtained from these specimens to normal size specimens (115 ± 5 mm) and evaluate the effect of thickness reduction. Initially 25 mixtures were included but only 23 met the required air voids content. Mixtures used in this analysis included a variety of mat

thicknesses from 35 mm to 65 mm and included SMA, coarse, fine, and intermediate gradations (see Table C1 of Appendix C).

A quadratic model was used to fit the relationship between ACP and the number of gyrations to reach 92% of G_{mm} (Figure 4.24) resulting in a poorer correlation (R^2 = 0.21) than was achieved with the standard height specimens, as shown in Figure 4.23. However, when the number of gyrations to reach the as-constructed field density was used, the correlation improved (R^2 = 0.62). Thus, the actual density level achieved with the compaction process is an important factor to take into account.

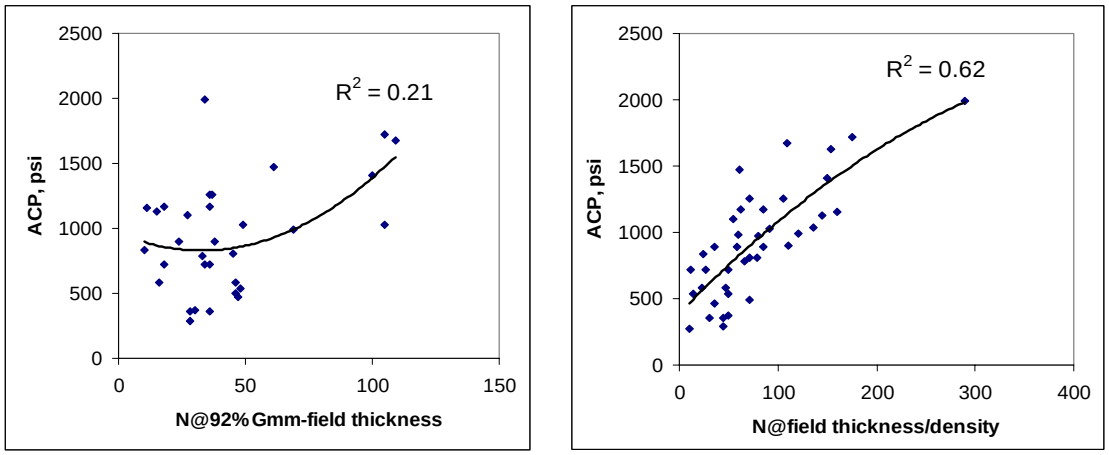

Figure 4.24: Relationship between ACP and number of cycles to reach 92%Gmm and field density.

The majority of the mixes were compacted with a thickness near 50 mm. The effect of reducing the sample high was evaluating by the compaction of samples with a thickness of 100 mm. Figures 4.25 and 4.26 show typical results of the compaction process for 50 mm and 100 mm samples using the Superpave Gyratory Compactor. In Figure 4.25, it can be observed that SMA and fine-graded mixtures required very few gyrations to reach the target of 8% air voids. Meanwhile, coarse and intermediate-graded

mixtures required as much as twice the number of gyrations to reach 92% of G_{mm}. On the other hand, Figure 4.26 shows a smaller difference in the required number of gyrations to reach 8% air voids.

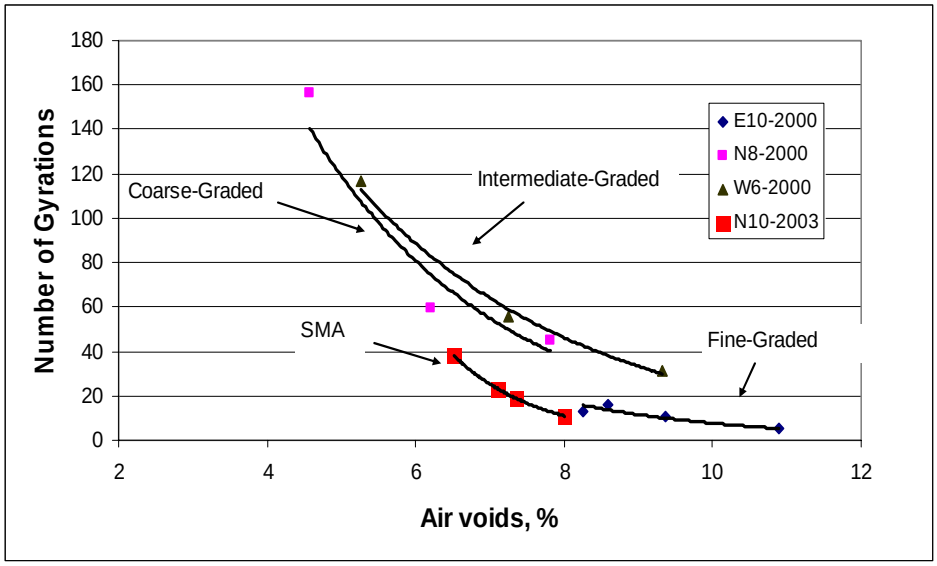

Figure 4.25: Compaction of lab specimens at 50 mm.

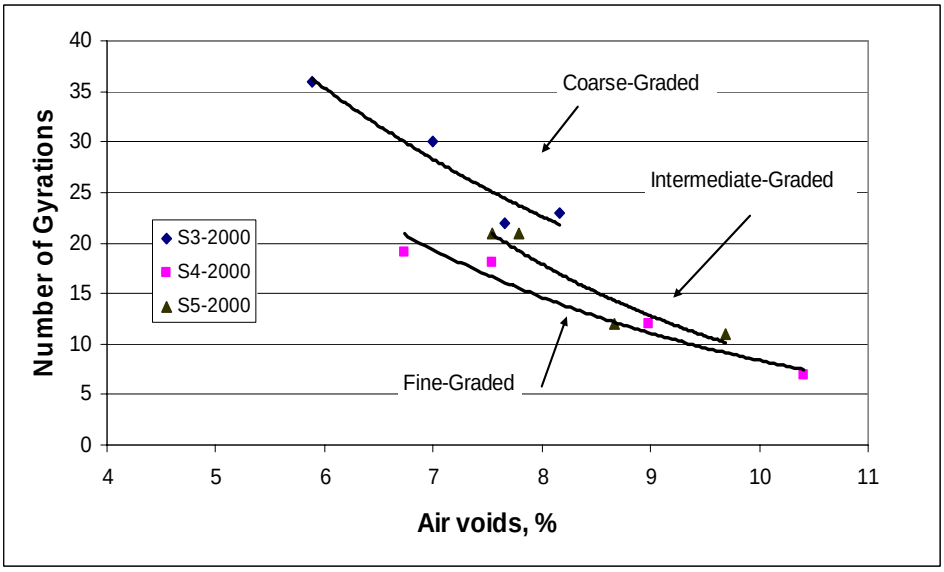

Figure 4.26: Compaction of lab specimens at 100 mm.

As final product of this analysis, by using a quadratic best fit Figure 4.27 shows the effect of reducing the thickness of lab specimens on the number of gyrations to reach 92% G_{mm}. For specimens compacted at almost the design thickness the number of cycles is similar (N@92%Gmm-field / N@92%Gmm-design ratio = 1). Additionally, as the Thickness-design / Thickness-field ratio increases, extra energy is necessary (gyrations) to reach the target density. The best fit line establishes a minimum thickness point near 80 mm where fewer gyrations are needed than the ones obtained from design specimens, but further investigation is required in order to fill the gaps and confirm the results.

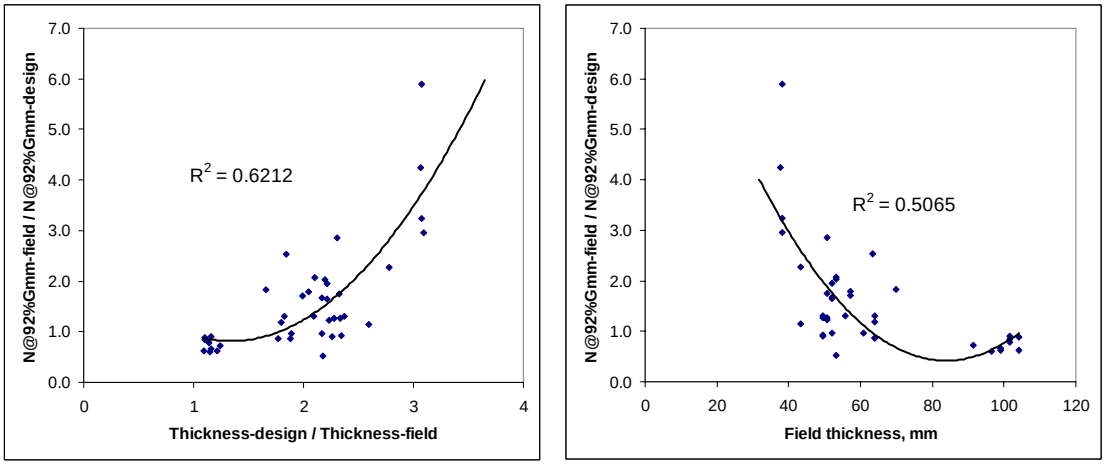

Figure 4.27: Effect of reducing thickness on lab specimens

The use of multiple regression analysis was used to incorporate the wide variety of mix properties and factors affecting field compactability. For this analysis, several parameters obtained from the specimens compacted at lift thickness using the SGC were used as predictor variables: number of gyrations to reach 92% of G_{mm} at lift thickness

(N@92%$G_{mm\text{-}field}$), number of gyrations to reach the post construction density at lift thickness (N@field-density) and locking point at lift thickness. Mix properties such as asphalt content, actual PG grade, coarse and fine aggregate ratios, lift temperature, t/NMAS ratio, PCSI were included in the analysis as well.

The best model was a combination of PCSI, FAc ratio, lift temperature and number of gyrations to reach the post construction density level at lift thickness. These four identified factors were then regressed versus the ACP and the following regression equation was obtained:

```
ACP = 2560 - 19.4 PCSI - 1018 FAc - 6.18 Temp + 4.02 N@density          [19]

S = 181.858   R-Sq = 82.2%   R-Sq(adj) = 78.2%

Predictor     Coef  SE Coef      T      P
Constant    2560.1    574.5   4.46  0.000
PCSI       -19.416    6.931  -2.80  0.012
FAc        -1018.5    428.8  -2.37  0.029
Temp        -6.178    1.941  -3.18  0.005
N@density   4.0250   0.9290   4.33  0.000
```

Where,

ACP = accumulated compaction pressure

PCSI = primary control sieve index

FAc = FAc ratio (Bailey Method)

Temp = temperature at the first roller pass, °F

N@field-density = number of gyrations to reach the post construction density level at lift thickness.

An R^2 of 82.2 indicates that eighty two percent of the variability of ACP can be explained by these four factors. The positive coefficient for N@field-density indicates that ACP increases as the N@field-density increases. The negative coefficient for PCSI

indicates that finer mixes are easy to compact in the field (lower ACP). As the Bailey Method FAc ratio decreases (negative sign) compactability of the mixture in the field increases. As expected, higher mat temperatures required less compactive energy to reach the desired density level.

4.6 Correlations between ACP@92%G_{mm} and lab compaction parameters

The fourth part of this study involved eleven mixtures placed on the 2006 Test Track experiment and twelve mixes placed on the 2003 experiment. These mixes were used to evaluate the field compactability indicator by conducting nuclear density testing and taking temperature readings after each roller pass on each section and obtaining the plot of density versus roller pass. Surface temperatures were obtained with an infrared temperature gun. The purpose of this part was to obtain the field compaction energy at the same level of compaction of laboratory samples and correlate that energy with lab compaction parameters.

The twenty three mixes were used to evaluate the relationship between field compaction energy at 92% of G_{mm} and laboratory compaction parameters. Once again, based on the conceptual hypothesis explained previously, it was expected that the ACP@92%G_{mm} would increase as the following parameters increase: %G_{mm}@N_{ini}, N@92%G_{mm}, CEI, Slope, Locking Point and CA ratio. In terms of mixture properties, it was expected an increase in ACP@92%G_{mm} as the PG grade increases, asphalt content decreases and the % passing 0.075mm increase. In addition, for low mix temperatures

(<225 °F), thin layers (<50 mm) and low t/NMAS ratios (<3:1), an increase in ACP@92%G_{mm} was expected.

As can be seen in Table 4.13, none of the individual laboratory compactability parameters had a strong correlation with ACP@92%G_{mm}. The compactability of a mix in the field can be explained by a strong correlation with lift thickness (R = -0.81) and the negative sign indicates that the compaction energy applied to reach 92% of G_{mm} decreases as the thickness increases for a range of thicknesses between 25 to 80 mm (see Table C2 of Appendix C).

Table 4.13: Correlation and expected trend between ACP@92% of G_{mm} and compactability parameters

Parameter	ACP@92%	Expected trend
PCSI	0.11	Incorrect
CA ratio	-0.08	Inconclusive
FAc ratio	-0.02	Inconclusive
% pass 0.075 mm	-0.07	Inconclusive
AC%	0.08	Inconclusive
Thickness (mm)	-0.81	Correct
Actual PG	0.21	Correct
%G_{mm}@N_{ini}	-0.19	Correct
N@92%G_{mm}	0.23	Correct
CEI	0.04	Inconclusive
Slope	-0.02	Inconclusive
Locking Point	0.11	Correct
NMAS	-0.38	Incorrect
t/NMAS	-0.45	Correct
Temperature	-0.19	Correct

A multiple regression analysis was performed using the following parameters as predictor variables: asphalt content, actual PG grade, compaction slope, Compaction Energy Index (CEI), %G_{mm}@N_{ini}, N@92%G_{mm}, locking point, coarse and fine aggregate ratios, lift temperature, t/NMAS ratio and PCSI. The best model was selected by

choosing the model with the least number of predictor variables, the highest adjusted R^2, Cp less than the number of predictor variables and minimum standard error of the regression. The best model included the ACP@92% G_{mm} as the response, while the interaction temperature*thickness, % passing No 200 sieve, actual PG grade, slope, locking point/Slope ratio, FAc ratio and PCSI square were the predictors (see Equation 20). Note that locking point and compaction slope are determined from normal height SGC specimens.

```
ACP@92% = - 1884 - 730 FAc + 62.1 % pass 200 + 17.8 Actual PG + 57.3 Slope
          + 249 Lp/Slope - 0.0943 T*H - 0.504 PCSI^2                        [20]


S = 95.6737   R-Sq = 92.6%   R-Sq(adj) = 89.1%

Predictor        Coef   SE Coef       T      P
Constant      -1883.6     482.6   -3.90  0.001
FAc            -730.1     315.1   -2.32  0.035
% pass 200      62.08     21.46    2.89  0.011
Actual PG      17.768     4.283    4.15  0.001
Slope           57.34     14.68    3.91  0.001
Lp/Slope       249.45     46.19    5.40  0.000
T*H         -0.094266  0.008095  -11.64  0.000
PCSI^2        -0.5038    0.2084   -2.42  0.029
```

Where,

ACP@92% = accumulated compaction pressure at 92% of G_{mm}

FAc = Fine aggregate coarse ratio (Bailey Method)

%pass200 = percent passing 0.075mm sieve

Actual PG = high temperature grade at failure

Slope = Compaction slope for design specimens

LP/Slope = Locking point / slope ratio for design specimens

PCSI = primary control sieve index

T2*H = lift thickness (mm) multiplied by temperature at the first roller pass, °F

Equation 20 shows that the compactive effort applied to the mixture to reach 92% of G_{mm} decreases as the variable temperature*thickness increases, which is the most significant variable. The positive sign of %pass200 indicates that higher amounts of material passing the 0.075mm sieve are related to stiffer mixes which tend to be difficult to compact in the field. This model also shows that the use of stiffer binders also increases the required compactive effort. It can be seen that the ACP@92% of G_{mm} increases as the locking point/Slope ratio increases. The locking point of the mix (LP 2-1) and the slope are strongly correlated and as these parameters increase the compactability of the mixture decreases. Both variables, slope and locking point, resulted significant when included individually in the model but a multicollinearity problem was detected due to their strong correlation.

As described by the Bailey Method, as the FAc ratio decreases (negative sign) compactability of the mixture in the field increases. Finally, the negative sign of PCSI square indicates that fine-graded mixes and coarse-graded mixes with gradations highly deviated from the maximum density line tend to reach 92% of G_{mm} easily (i.e. SMA and finer mixes).

4.7 Summary of Findings

The main objective of the first part of this study was an evaluation of the SGC parameters (%G_{mm}@N_{ini}, N@92%G_{mm}, CEI, Slope, Locking Point and Bailey Method ratios) to determine compactability of a mix in the laboratory. The results indicated that %G_{mm}@N_{ini}, N@92%G_{mm}, CEI, Slope and Locking Point are highly correlated, as shown

in Table 4.1. Further analysis also indicated that fine-graded mixes are easier to compact compared to coarse-graded. In addition, it was found that the use of highly angular particles, tougher aggregate and mixtures with low asphalt contents tend to increase the required compactive effort to achieve a specific density in the laboratory.

The primary objective of this research was to evaluate a variety of mixture characteristics and determine if they are correlated to compactability in the field. The Accumulated Compaction Pressure (ACP) was introduced as a field compactability measure based on the rolling operation. A strong correlation between ACP and any of the individual laboratory parameters mentioned above was not obtained. It was determined that the ACP was significantly affected by temperature of the mix, lift thickness and the field density level. Several models were developed to correlate laboratory and field compactability. These models took into account temperature, thickness and density to minimize differences between laboratory and field compaction.

Table 4.14 shows a summary of models used to correlate field and laboratory compactability. The first model included Test Track tangent sections placed in 2000. Most of these mixes are characterized for having thicknesses of 50 mm. The parameter that better correlated with ACP at post-construction density level was the number of gyrations to reach 92% of G_{mm} ($R^2 = 0.45$).

Multiple linear regression analyses were used to include all the mixes placed in 2000 and 2003 and try to find a better correlation between field and laboratory compactability. From Table 4.14, it can be seen that the multiple regression did not improve the correlation between field and laboratory compactability ($R^2 = 0.55$). Further

investigation showed that lift thickness and the temperature of the mix measured at the beginning of the compaction process were significant factors that explained most of the variability observed in ACP. This effect can be clearly seen for the second model shown in Table 4.14.

The third model shown in Table 4.14 included the parameter N@field-density obtained from specimens compacted in the SGC at thicknesses similar to those in the field. A better correlation was obtained for this analysis ($R^2 = 0.62$) and it indicates that the actual density level achieved with the compaction process is an important factor to take into account.

Table 4.14: Summary of models used to correlate field and laboratory compactability

Response variable	Variables included in the model	R^2	Characteristics
ACP at field density level	N@92%Gmm	0.45	Test Track tangent sections, first cycle (Figure 4.23)
Square root of ACP at field density level	Temperature NMAS CA ratio %pass 0.075 mm VFA N@field	0.55	Parameters obtained from QC specimens (Equation 18)
ACP at field density level	N@field - thickness/density	0.62	Parameter obtained from specimens compacted in the SGC at thicknesses similar to those in the field (Figure 4.24)
ACP at field density level	PCSI FAc ratio Temperature N@field-density	0.82	Parameters obtained from specimens compacted in the SGC at thicknesses similar to those in the field (Equation 19)
ACP@92%Gmm	FAc ratio PCSI % passing 0.075mm Actual PG Slope Locking point Thickness Temperature	0.92	Parameters obtained from QC specimens (Equation 20)

The fourth model shown in Table 4.14 also included the parameter N@field-density obtained from specimens compacted in the SGC at thicknesses similar to those in the field. A combination of N@field-density, PCSI, FAc ratio and temperature did improve the relationship between field and laboratory compactability ($R^2 = 0.82$). This model suggests that taking an extra step during the mix design process by compacting specimens at thicknesses similar to those to be placed in the field may help predict the required field compactive effort to achieve the desired density.

The first three models were characterized for having a response variable clearly affected by the post-construction density level which differs for each mixture. The last model shown in Table 4.14 used a field compaction energy calculated at a reference density level of 92% of G_{mm} (ACP@92%G_{mm}). The best correlation between field and laboratory compactability was obtained with this model ($R^2 = 0.92$). This model suggests that a combination of laboratory parameters obtained from the original QC specimens (FAc ratio, slope and locking point), mix properties (% passing 0.075mm and actual PG) and factors affecting field compaction (thickness and temperature) may help predict the compactive effort applied by the rollers to achieve a minimum density level of 92%G_{mm}.

4.8 Applicability of the ACP concept for validation purposes

Sixteen surface mixtures placed in different U.S. states as part of the NCHRP 9-27 study were used to compare the results obtained from the analyses of the Test Track mixes. Table 4.15 shows the single correlation value (R-value) calculated for each pair of laboratory parameters used to describe compactability. The shaded cells indicate a better

correlation (R-value > 0.60) between parameters. CEI and $\%G_{mm}@N_{ini}$ have a strong correlation (R = -0.87), slope and $\%G_{mm}@N_{ini}$ have a very strong correlation (R = -0.99), and in this case a poor correlation was found between slope and locking point, contrary to the results obtained for test track mixes that is consistence with the use of much more variable data (see Appendix C).

Table 4.15: Single correlation among laboratory parameters based on NCHRP 9-27 mixtures

	PCSI	**$\%G_{mm}@N_{ini}$**	**$N@92\%G_{mm}$**	**CEI**	**Slope**	**LockPt1**
PCSI	1					
$\%G_{mm}@N_{ini}$	-0.41	1				
$N@92\%G_{mm}$	-0.21	-0.29	1			
CEI	0.20	-0.87	0.68	1		
Slope	0.39	-0.99	0.16	0.80	1	
LockPt1	-0.59	-0.10	0.80	0.40	0.03	1
FAc Ratio	-0.71	0.19	-0.11	-0.19	-0.11	0.27

Accumulated compaction pressure ACP was computed for the sixteen projects and specimens were also compacted in the SGC to meet the 92 percent of G_{mm} and lift thickness. These data were used to compare the results obtained for Equation 19. Figure 4.28 shows the relationship between the actual ACP and predicted ACP for test track mixes and NCHRP 9-27 projects using Equation 18. Notice that this equation provides a relatively good relationship ($R^2 = 0.77$) between actual and predicted ACP for NCHRP projects which present higher construction variability. A slight deviation from the line of equality indicates that Equation 19 underestimated the accumulated compaction pressure. A calibration factor of 1.15 was needed to account for local conditions and make the model applicable to these observations.

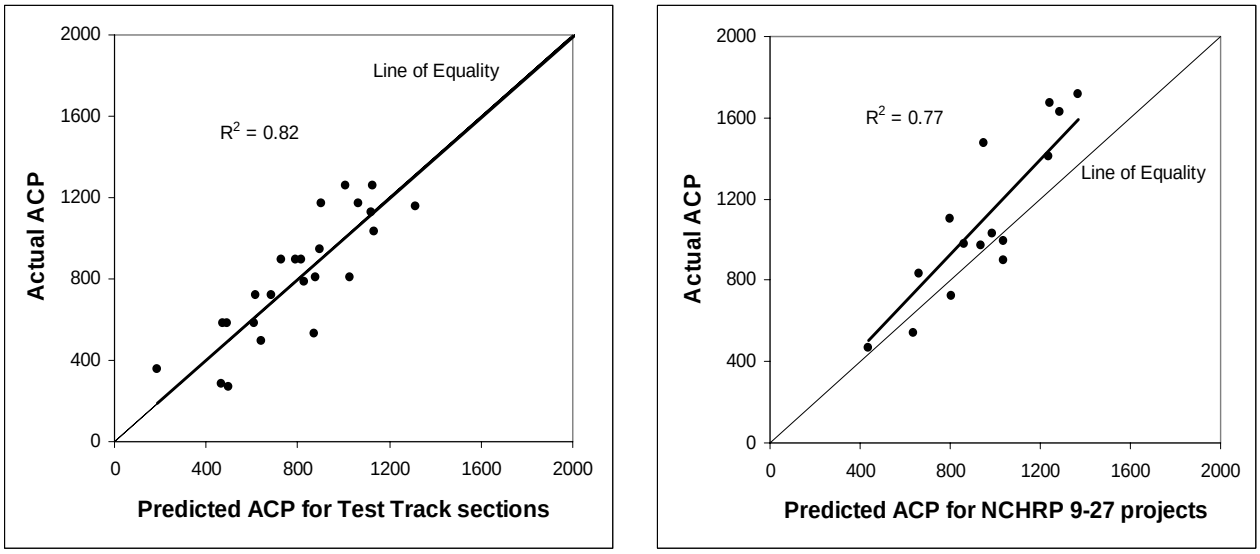

Figure 4.28: Comparison of predicted ACP for test track sections and NCHRP 9-27 projects using Equation 18

CHAPTER 5. CONCLUSIONS AND RECOMMENDATIONS

In terms of parameters used to measure laboratory compactability, it was found that coarse-graded mixtures with low CA ratios require stronger fine aggregate structure (higher FA_C ratio) and higher asphalt content to meet the target volumetric properties. Mixtures with these characteristics tend to be difficult to compact in the laboratory.

Overall, finer gradations and gradations with PCSI values close to zero tended to increase mixture compactability in the laboratory. CEI, N@92%G_{mm}, Slope and Locking Point can be used to represent the applied energy to reach a level of compaction and mixture resistance to deformation. PCSI and FA_C ratio describe gradation properties and how particles are packed together and also can be used as laboratory compactability parameters. This points out that from the selection of an optimum gradation, compactability of a mixture in the SGC may be predicted.

The relationship between laboratory and field compactability is complicated by many other variables which are known to affect compaction. A simple linear correlation was not found to describe that relationship. The use of multiple regression analysis was necessary to incorporate the wide variety of mix properties and factors affecting field compactability. Results showed that field compaction is more affected by t/NMAS ratio and mat temperature.

In general, it was found that mixes placed in 2003 required more compactive effort than mixes placed in 2000. Thinner layers were placed in 2003 (< 50 mm), which led to a reduction in temperature and finally an increase in compaction energy and a reduction in compaction time to achieve the desired density.

The results also suggested that more energy was applied to reach a higher density level and that may explain some variability observed on the ACP. The interaction between temperature and t/NMAS ratio showed that for high t/NMAS ratios (above 4:1) the temperature has minimum effect on the compaction energy and as the t/NMAS ratio decreases lower temperatures required substantially higher compaction energy.

The relationship between compaction effort and thickness or t/NMAS ratio for specimens compacted in the SGC to reach lift thickness showed similar trend to the relationship between ACP and thickness or t/NMAS ratio. In other words, specimens compacted in the SGC are significantly affected by thickness and this is consistent with the results observed in the field.

Future investigation should be addressed to reduce the number of variables and increase the number of observations. The results of this study showed that the data can be grouped mainly by thickness. Keeping the same aggregate source and same rolling pattern may improve the relationship between ACP and lab parameters. Further investigation should also include refinement of the ACP concept.

Current mix design procedures do not provide any specific criteria to estimate achievable roller compacted density. This study can be used as baseline to develop procedures and criteria to identify compaction equipment characteristics and rolling patterns relative to lift thicknesses, mix temperature, and asphalt/aggregate/mixture characteristics that will produce optimum achievable density.

REFERENCES

1. Brown, Decker, Mallick and Bukowski. Superpave Construction Issues and Early Performance Evaluation. Journal of the Association of Asphalt Paving Technologists, Vol. 68, pp. 613-623, 1999.
2. Brown, E. Ray, Hainin, M. Rosli, Cooley, Allen, Hurley, Graham. NCHRP Report 531. Relationships of HMA in-place air voids, lift thickness, and permeability. National Cooperative Highway Research Program. Transportation Research Board, National Research Council, Washington, D. C., 2004.
3. Prowell, B. D., E. R. Brown. NCHRP Project 9-09(1) Verification of Gyration Levels in the Ndesign Table. National Cooperative Highway Research Program. Transportation Research Board, National Research Council, Washington, D. C., 2006.
4. Bahia, Hussain U., Frie mel Timothy P., Peterson, Pehr A., Russell, Jeffery S., and Poehnelt, Brian. Optimization of Constructibility and Resistance to Traffic: A New Design Approach for HMA Using the Superpave Compactor. Asphalt Paving Technology, Journal of the Association of Asphalt Paving Technologists, Vol. 67, pp. 189-232, 1998.
5. Pine, Bill, "The Bailey Method. Achieving volumetrics and HMA Compactability." Heritage Research Group. November 2004.

6. Roberts, F. L. , P. S. Kandhal, E. R. Brown, D-Y, Lee, and T. W. Kennedy, Hot Mix Asphalt Materials, Mixture Design and Construction. Second Edition, NAPA Education Foundation, Lanham, MD, 1996.
7. Scherocman, James A. and Acott, Mike. Hot mix asphalt production, placement, and compaction related to pavement performance. Journal of the Association of Asphalt Paving Technologists, Vol. 58, Nashville, TN, 1989.
8. US Army Corps of Engineers. Hot-Mix Asphalt Paving Handbook 2000. AC 150/5370-14A Appendix 1, 2nd Edition, 2000.
9. Garcia, J., K. Hansen. "HMA Pavement Mix Type Selection Guide." National Asphalt Pavement Association. Information Series 128, 2001.
10. Prowell, B. D., E. R. Brown and M. Huner, Evaluation of the Internal Angle of Gyration of Superpave Gyratory Compactors in Alabama, NCAT 03-04. National Center for Asphalt Technology, 2003.
11. Al-Khaateeb, G., C. Paugh, K. Stuart, T. Harman, and J. D'Angelo. "Target and Tolerance for the Angle of Gyration Used in the Superpave Gyratory Compactor (SGC)." In Transportation Research Record 1789, TRB, National Research Council, Washington, DC. 2002. Pp. 208-215.
12. Prowell, Brian. Verification of the Superpave Gyratory Ndesign Compaction Levels. Doctoral Dissertation. Auburn University, 2006.

13. The Asphalt Institute. Superpave Mix Design (SP-2), Third Edition, 2000.
14. Anderson, R. Michael, Turner, Pamela A., Peterson Robert L. NCHRP Report 478. Relationship of superpave gyratory compaction properties to HMA rutting behavior. National Cooperative Highway Research Program. Transportation Research Board, National Research Council, Washington, D. C., 2002.
15. Anderson, R. M., and H. U. Bahia. "Evaluation and Selection of Aggregate Gradations for Asphalt Mixtures Using Superpave," Transportation Research Record 1583, Transportation Research Board, National Research Council, Washington, DC, 1997.
16. Pine, W. J., Superpave Gyratory Compaction and the Ndesign Table, Internal Report to Illinois Department of Transportation, Illinois, 1997.
17. Vavrik, W. R., and S. H. Carpenter, "Calculating Air Voids at Specified Numbers of Gyrations in Superpave Gyratory Compactor," In Transportation Research Record 1630, Transportation Research Board, National Research Council, Washington, DC, 1998, Pp 117-125.
18. Delage, Kenneth P. The Effect of Fine Aggregate Angularity on Hot Mixture Asphalt Performance. Master Degree Thesis, Department of Civil and Environmental Engineering, University of Wisconsin-Madison, November 2000.
19. M. Guler and H. U. Bahia "Development of a Device for Measuring Shear Resistance of HMA in the Gyratory Compactor." Presented at the meeting of the Transportation Research Board, Paper No. 00-1318, Washington, D.C., January 2000.

20. Vavrik, Pine, Huber, Carpenter and Bailey, “The Bailey Method of Gradation Evaluation,” Proceedings of the Association of Asphalt Paving Technologists, Vol.70, 2001.
21. Grootenboer, H..J. Compaction of Asphalt Road Pavements. University of Twente, Netherlands. H.L. ter Huerne, Enschede, 2004.
22. Bonnot, J., ‘Asphalt analysis, sulfur, mixes, and seal coats’, Transportation Research Record, no.1096, 1986.
23. Brown, Cooley, Hanson, Lynn, Powell, Prowell and Watson. NCAT Test Track Design, Construction, and Performance. NCAT 02-12. National Center for Asphalt Technology, 2002.
24. Devore, Jay L., “Probability and statistics for Engineering and the Sciences.” Fifth Edition, 2000.
25. Johnson, Richard and Wichern, Dean. “Applied Multivariate Statistical Analysis”, Fifth Edition, 2002.
26. Minitab Reference Manual, Release 10 for Windows, Minitab Inc., State College, PA, 1994.

APPENDIX A

MATERIAL PROPERTIES

Table A.1: Mixture properties

Quad	Sec*	Cycle**	Sublot	Initial field density $\%G_{mm}$	Lab. Air Voids %	VMA %	VFA %	Asphalt Content %	% Pass PCS***
E	1	1	S	94.0	3.41	16	79	5.3	54
E	2	1	S	94.7	2.78	12	77	4.7	29
E	3	1	S	93.5	3.89	12	68	4.8	29
E	4	1+2	S	93.8	3.73	12	70	4.7	29
E	5	1+2	S	92.7	3.63	13	73	5.1	40
E	6	1+2	S	92.9	4.09	13	69	5	37
E	7	1+2	S	93.2	3.53	13	72	4.8	38
E	8	1+2	S	92.7	4.25	16	73	5.6	51
E	9	1+2	S	92.9	4.66	16	70	5.4	49
E	10	1	S	93.0	3.58	15	77	5.8	51
N	1	1	S	95.1	2.38	13	81	7.4	52
N	2	1	S	94.7	2.11	13	84	7.8	50
N	3	1	S	94.1	2.41	13	81	7.6	51
N	4	1	S	93.4	3.75	12	69	6.8	52
N	5	1	S	93.8	3.86	13	71	6.9	38
N	6	1	S	94.4	3.61	13	72	6.8	37
N	7	1	S	93.9	2.45	13	81	6.9	36
N	8	1	S	94.7	4.15	13	72	6.6	37
N	9	1	S	94.5	3.19	12	74	6.7	40
N	10	1	S	94.7	3.53	13	74	6.8	34
N	11	1+2	S	93.1	3.48	11	70	4.3	37
S	1	1	S	94.8	2.71	14	80	5	36
S	2	1+2	S	93.8	4.90	14	65	6	41
S	3	1+2	S	92.7	3.29	13	75	5.6	43
S	4	1	S	94.3	2.04	13	84	5.3	46
S	5	1	S	94.9	3.56	14	76	5.6	45
S	6	1+2	S	92.9	4.50	x	x	6.2	53
S	7	1+2	S	93.2	3.30	x	x	6.6	34
S	8	1+2	S	91.8	2.48	12	80	4.2	38
S	9	1+2	S	93.4	3.93	14	72	4.7	36
S	10	1+2	S	93.7	3.07	15	79	5.2	52
S	11	1+2	S	93.2	3.23	13	75	3.9	47

* Cycle 1 = 2000 Test track experiment, cycle 1+2 = 2000 and 2003, cycle 2 = 2003 only.
** S = surface mixture, B = binder or bottom mixture.
*** PCS = Primary Control Sieve

Table A.1 (continued): Mixture properties

Quad	Sec*	Cycle**	Sublot	Initial field density $\%G_{mm}$	Lab. Air Voids %	VMA %	VFA %	Asphalt Content %	% Pass PCS***
W	6	1	S	92.1	2.59	x	x	6.2	45
W	9	1	S	93.6	3.91	x	x	5	33
W	10	1+2	S	93.3	3.77	x	x	5	33
E	1	2	S	96.4	4.62	17	73	6.3	23
E	2	2	S	94.8	3.73	14	73	7.8	50
E	3	2	S	93.2	3.55	13	73	8.2	54
N	1	2	S	92.8	4.39	18	76	6.2	63
N	3	2	S	92.8	5.65	17	67	6.1	63
N	4	2	S	93.4	5.53	19	71	6.1	61
N	5	2	S	93.3	5.43	19	71	6.1	61
N	6	2	S	93.7	5.00	19	74	6.2	62
N	9	2	S	95.1	5.03	17	70	6.6	17
N	10	2	S	95.6	4.28	17	75	6.2	17
N	13	2	S	94.6	2.90	16	82	5.9	21
S	1	2	S	95.6	2.05	16	87	5.1	25
S	5	2	S	93.1	2.88	14	79	5.6	43
W	2	2	S	96.8	5.03	19	74	9.7	22
W	3	2	S	92.1	2.75	14	80	6.2	51
W	6	2	S	92.2	4.01	16	75	6.1	50
W	9	2	S	93.4	3.87	18	78	5.8	61
S	1	1	B	93.7	3.26	x	x	5	32
S	2	1+2	B	93.0	4.76	x	x	4.9	46
S	3	1+2	B	92.8	3.82	x	x	4.2	47
S	4	1	B	93.6	4.43	x	x	4.1	48
S	5	1	B	91.5	3.26	x	x	4	53
S	11	1+2	B	94.6	2.28	x	x	3.6	38
N	11	1+2	B	92.7	3.23	x	x	4.1	46

* Cycle 1 = 2000 Test track experiment, cycle 1+2 = 2000 and 2003, cycle 2 = 2003 only.
** S = surface mixture, B = binder or bottom mixture.
*** PCS = Primary Control Sieve

Table A.1 (continued): Mixture properties

Quad	Sec*	Cycle**	Sublot	Initial field density $\%G_{mm}$	Lab. Air Voids %	VMA %	VFA %	Asphalt Content %	% Pass PCS***
N	2	2	B	93.9	4.79	14	66	4.3	51
N	3	2	B	93.3	4.66	14	67	4.3	51
N	3	2	B	93.7	3.06	13	76	4.5	53
N	3	2	B	93.0	5.06	16	68	4.3	57
N	3	2	B	94.6	4.02	15	73	4.6	50
N	4	2	B	92.9	4.67	15	69	4.3	52
N	4	2	B	93.2	3.35	14	76	4.4	51
N	5	2	B	92.9	4.29	15	71	4.3	52
N	5	2	B	92.8	3.02	14	78	4.4	51
N	5	2	B	93.2	3.27	15	78	4.7	49
N	6	2	B	94.1	4.88	15	67	4.6	52
N	6	2	B	93.4	3.12	14	78	4.5	52
N	6	2	B	96.0	2.92	14	79	5	53
N	7	2	B	94.3	4.59	15	69	4.6	52
N	7	2	B	93.3	3.07	14	78	4.5	52
N	7	2	B	95.0	2.88	14	79	5	53
N	8	2	B	93.0	4.80	15	68	4.6	52
N	8	2	B	93.0	2.59	13	80	4.5	52
N	9	2	B	95.2	5.85	18	68	6.2	15
N	10	2	B	97.5	6.20	19	67	6.3	18
N	13	2	B	93.9	3.09	11	72	4.3	42
S	1	2	B	95.7	1.81	12	85	4.9	43

* Cycle 1 = 2000 Test track experiment, cycle 1+2 = 2000 and 2003, cycle 2 = 2003 only.
** S = surface mixture, B = binder or bottom mixture.
*** PCS = Primary Control Sieve

Table A.2: Gradations of 2000 and 2003 test track experiment

Quad	Sec	Cycle	Sub lot	Percentage Passing (%)										
				1"	3/4"	1/2"	3/8"	No. 4	No. 8	No. 16	No. 30	No. 50	No. 100	No. 200
E	1	1	S	100	100	99	92	73	54	38	25	14	9	7.4
E	2	1	S	100	100	96	74	41	29	22	18	12	7	4.1
E	3	1	S	100	100	94	73	41	29	23	18	12	7	4.2
E	4	1+2	S	100	100	95	75	42	29	23	18	13	8	4.6
E	5	1+2	S	100	100	98	83	54	40	30	24	16	9	5.1
E	6	1+2	S	100	100	96	81	52	37	28	22	15	8	4.3
E	7	1+2	S	100	100	97	83	53	38	29	22	16	9	5.2
E	8	1+2	S	100	100	98	86	66	51	38	28	18	10	5.2
E	9	1+2	S	100	100	97	85	64	49	36	27	18	10	5.2
E	10	1	S	100	100	97	87	67	51	38	29	19	10	5.6
N	1	1	S	100	100	100	92	69	52	33	22	15	10	6.7
N	2	1	S	100	100	99	90	66	50	33	22	16	11	7.6
N	3	1	S	100	100	99	91	68	51	33	22	15	10	6.5
N	4	1	S	100	100	99	91	68	52	35	23	15	9	6.0
N	5	1	S	100	100	99	84	52	38	26	18	14	11	8.3
N	6	1	S	100	100	99	85	54	37	25	17	13	10	8.2
N	7	1	S	100	100	98	83	52	36	24	17	13	10	7.8
N	8	1	S	100	100	99	85	55	37	24	17	13	10	7.5
N	9	1	S	100	100	99	87	57	40	26	19	14	11	8.8
N	10	1	S	100	100	98	84	51	34	23	17	13	10	7.7
N	11	1+2	S	100	100	97	80	52	37	30	24	18	11	7.2
N	12	1+2	S	100	100	96	73	32	23	21	19	17	14	11.8
N	13	1	S	100	100	99	74	30	25	23	21	17	13	11.5
W	1	1+2	S	100	100	95	68	28	20	18	16	14	12	9.7
W	2	1	S	100	100	98	77	35	24	17	15	13	12	10.7
W	3	1	S	100	100	98	68	19	13	11	10	9	8	6.8
W	4	1+2	S	100	100	95	66	23	14	13	12	11	10	8.6
W	5	1+2	S	100	100	95	67	22	15	12	11	11	10	8.5
W	6	1	S	100	100	99	89	65	45	28	18	13	10	7.8
W	7	1+2	S	100	100	95	74	32	23	18	15	12	9	5.9
W	8	1	S	100	100	99	80	33	25	22	20	18	15	12.9
W	9	1	S	100	100	96	80	51	34	22	16	12	9	6.7
W	10	1+2	S	100	100	96	81	51	33	22	16	12	9	6.5

Table A.2 (continued): Gradations of 2000 and 2003 test track experiment

Quad	Sec	Cycle	Sub lot	Percentage Passing (%)										
				1"	3/4"	1/2"	3/8"	No. 4	No. 8	No. 16	No. 30	No. 50	No. 100	No. 200
S	1	1	S	100	100	95	86	54	36	28	21	15	9	5.5
S	2	1+2	S	100	100	100	96	67	41	29	22	15	10	8.4
S	3	1+2	S	100	100	100	100	70	43	29	21	15	11	8.9
S	4	1	S	100	100	98	88	63	46	33	23	13	9	7.8
S	5	1	S	100	100	95	82	61	45	33	22	10	7	5.0
S	6	1+2	S	100	100	95	87	74	53	41	33	24	12	5.9
S	7	1+2	S	100	100	96	88	71	34	25	20	16	10	6.2
S	8	1+2	S	100	100	100	93	58	38	25	19	15	12	7.8
S	9	1+2	S	100	100	93	82	53	36	27	20	14	9	5.7
S	10	1+2	S	100	100	95	88	69	52	38	27	19	11	6.6
S	11	1+2	S	100	100	100	92	62	47	30	22	17	13	7.5
S	12	1+2	S	100	100	97	82	63	46	32	23	16	10	7.0
S	13	1+2	S	100	100	93	80	68	50	37	27	19	11	6.6
E	1	2	S	100	100	91	69	35	23	17	14	12	11	10.0
E	2	2	S	100	100	96	93	73	55	44	37	24	10	5.1
E	3	2	S	100	100	96	92	73	54	43	36	24	10	5.3
N	1	2	S	100	100	100	100	81	63	51	38	20	12	7.0
N	2	2	S	100	100	100	100	80	63	51	38	21	12	6.6
N	3	2	S	100	100	100	100	80	63	51	38	21	12	6.6
N	4	2	S	100	100	100	100	81	61	49	37	21	12	6.7
N	5	2	S	100	100	100	100	81	61	49	37	21	12	6.7
N	6	2	S	100	100	100	100	81	62	50	37	21	12	6.8
N	7	2	S	100	100	100	100	49	24	20	17	14	12	9.2
N	8	2	S	100	100	100	100	49	24	20	17	14	12	9.2
N	9	2	S	100	100	97	83	37	17	13	12	11	10	8.6
N	10	2	S	100	100	95	87	30	21	17	15	14	13	11.5
N	13	2	S	100	100	95	71	32	21	18	16	15	14	12.1
W	2	2	S	100	100	88	54	22	17	14	13	12	11	9.7
W	3	2	S	100	100	100	100	79	51	39	29	21	14	8.7
W	6	2	S	100	100	100	100	98	75	50	35	22	15	11.3
W	8	2	S	100	100	100	96	40	25	19	15	13	10	7.5
W	9	2	S	100	100	100	98	83	61	43	32	23	15	7.5
S	1	2	S	100	99	92	74	33	25	24	22	19	16	13.0
S	4	2	S	100	100	95	78	19	5	3	3	2	2	1.6
S	5	2	S	100	100	96	87	66	43	30	21	10	7	5.5

Table A.2 (continued): Gradations of 2000 and 2003 test track experiment

Quad	Sec	Cycle	Sub lot	Percentage Passing (%)										
				1"	3/4"	1/2"	3/8"	No. 4	No. 8	No. 16	No. 30	No. 50	No. 100	No. 200
S	1	1	B	100	97	66	48	32	24	20	16	11	7	4.1
S	2	1	B	100	100	86	69	46	30	23	19	11	7	5.5
S	3	1	B	100	97	86	80	47	27	20	16	12	9	7.3
S	4	1	B	100	99	88	69	48	38	30	24	15	9	6.5
S	5	1	B	100	95	83	73	53	36	27	21	15	12	8.7
S	11	1	B	100	100	86	70	38	26	18	14	12	10	7.2
N	11	1	B	100	100	81	70	46	34	27	21	15	10	6.3
N	5	2	B	100	92	82	72	52	44	37	28	15	9	5.5
N	5	2	B	100	92	82	71	51	42	34	24	13	7	5.1
N	5	2	B	100	92	79	66	49	43	36	26	14	8	5.5
N	6	2	B	100	93	82	71	52	45	39	30	16	9	5.7
N	6	2	B	100	96	85	74	52	43	35	24	14	9	5.6
N	6	2	B	100	90	78	71	53	44	36	27	15	9	5.7
N	7	2	B	100	93	82	71	52	45	39	30	16	9	5.7
N	7	2	B	100	96	85	74	52	43	35	24	14	9	5.6
N	7	2	B	100	90	78	71	53	44	36	27	15	9	5.7
N	8	2	B	100	93	82	71	52	45	39	30	16	9	5.7
N	8	2	B	100	96	85	74	52	43	35	24	14	9	5.6
N	9	2	B	100	100	96	85	32	15	11	10	10	9	8.2
N	10	2	B	100	100	94	84	27	18	15	13	12	11	10.2
N	13	2	B	100	100	80	68	42	29	24	20	14	9	5.3
N	2	2	B	100	92	82	72	51	43	37	29	16	9	5.6
S	1	2	B	100	100	81	68	43	31	25	21	15	10	5.9
N	3	2	B	100	92	82	72	51	43	37	29	16	9	5.6
N	3	2	B	100	93	84	74	53	43	35	24	14	9	5.5
N	3	2	B	100	100	84	75	57	48	42	33	20	11	6.7
N	3	2	B	100	90	79	68	50	44	39	30	16	9	5.6
N	4	2	B	100	92	82	72	52	44	37	28	15	9	5.5
N	4	2	B	100	92	82	71	51	42	34	24	13	7	5.1

Table A.3: Parameters obtained from Densification Curve

Quad	Sec	Cycle	$\%G_{mm}$ @N_{ini}	N@92 $\%G_{mm}$	CEI	TDI 92-96	TDI	N@96 $\%G_{mm}$	Slope	Lock. Pt.
E	1	1	89.2	20	20.0	147	237.9	79	6.78	43
E	2	1	88.8	19	20.4	107.3	282.5	63	7.66	48
E	3	1	87.3	28	56.3	128	183.9	96	7.99	49
E	4	1+2	87.9	25	41.7	159.6	203.9	89	7.64	47
E	5	1+2	89.4	18	15.4	165.4	238.1	84	6.33	40
E	6	1+2	89.0	21	23.5	201.5	201.5	100	6.27	42
E	7	1+2	89.5	17	13.7	156.5	245.6	81	6.32	38
E	8	1+2	89.8	18	12.8	205.1	205.1	100	5.44	33
E	9	1+2	89.2	21	22.3	172.2	172.2	100	5.55	37
E	10	1	90.4	14	5.5	167	262.7	80	5.48	35
N	1	1	88.1	21	31.3	90.7	285.9	61	8.68	51
N	2	1	88.2	20	27.1	84.3	306.6	57	8.84	56
N	3	1	87.9	23	37.2	91.2	270.5	65	8.85	60
N	4	1	86.5	32	82.7	140	174.3	92	8.90	57
N	5	1	85.0	38	130.9	133.8	153.1	95	10.17	63
N	6	1	84.8	38	134.3	115.2	162.8	91	10.56	64
N	7	1	86.1	28	74.5	88.3	247.9	69	10.43	61
N	8	1	84.9	40	145.3	136	136.0	98	9.99	62
N	9	1	85.9	31	87.9	114.3	201.7	81	9.95	61
N	10	1	85.5	35	108.1	120.6	174.3	89	10.03	64
N	11	1+2	89.9	16	10.6	147	258.4	77	6.08	37
S	1	1	89.4	17	15.2	104.2	300.5	59	7.23	42
S	2	1+2	86.4	37	103.1	119	119.0	100	7.92	51
S	3	1+2	86.3	29	76.8	119.9	207.2	81	9.51	56
S	4	1	89.5	18	17.0	100.3	403.2	60	7.39	46
S	5	1	89.5	20	21.3	201.2	287.8	102	6.06	38
S	6	1+2	88.9	24	29.8	170.8	170.8	100	6.04	40
S	7	1+2	85.4	35	113.5	111.8	182.4	86	10.27	59
S	8	1+2	87.1	23	45.9	90.2	276.6	62	9.53	54
S	9	1+2	88.1	25	41.2	156.7	193.9	93	7.30	44
S	10	1+2	90.1	15	7.6	128	282.8	68	6.20	40
S	11	1+2	88.5	21	27.8	127.5	249.6	75	7.51	47
W	6	1	86.5	28	67.6	94	239.9	71	9.98	61
W	9	1	86.8	31	77.9	137.3	178.4	88	8.45	47
W	10	1+2	87.4	27	52.8	156.2	197.8	91	8.02	47
E	1	2	84.2	26	70.7	49.4	49.4	49	12.14	50
E	2	2	89.5	18	16.5	158.5	231.0	84	6.18	39
E	3	2	89.6	17	13.1	158.5	245.6	82	6.27	36
N	1	2	89.3	17	12.7	149.1	149.1	80	5.95	38
N	3	2	88.3	26	38.9	76.8	76.8	80	5.75	37
N	4	2	88.4	25	33.4	84.4	84.4	80	5.73	33

Table A.3 (continued): Parameters obtained from Densification Curve

Quad	Sec	Cycle	%Gmm @N_{ini}	N@92 %G_{mm}	CEI	TDI $_{92\text{-}96}$	TDI	N@96 %G_{mm}	Slope	Lock. Pt.
N	5	2	88.5	24	31.7	90.3	90.3	80	5.78	36
N	6	2	88.7	21	24.3	111.3	111.3	80	5.96	34
N	9	2	82.0	43	208.1	54.6	54.6	75	12.60	74
N	10	2	84.1	33	111.4	91.3	91.3	75	11.29	66
N	13	2	87.2	15	14.5	49.5	112.8	37	10.72	49
S	1	2	87.4	13	8.8	38.9	142.7	30	11.42	47
S	5	2	89.7	13	5.5	85.3	212.5	48	7.21	43
W	2	2	83.0	49	239.8	88	88.0	80	10.89	59
W	3	2	85.8	28	77.2	95.7	238.6	71	10.43	58
W	6	2	86.0	31	86.6	171.5	171.5	80	9.06	53
W	9	2	89.2	13	5.4	97.3	97.3	47	7.56	43
S	1	1	87.3	25	51.97	123.4	226.46	78	8.63	50
S	2	1+2	87.3	32	73.43	134.6	136.37	100	7.23	48
S	3	1+2	85.6	35	109.93	132.2	164.24	94	9.65	60
S	4	1	88.7	29	46.88	208.7	208.69	125	6.03	34
S	5	1	87.8	27	57.04	156	288.17	94	7.83	49
S	11	1+2	86.9	24	48.24	83.3	282.42	61	9.85	58
N	11	1+2	89.0	19	19.95	129.5	259.85	71	7.08	45
N	2	2	89.8	16	9.28	133.5	135.52	80	5.08	32
N	3	2	90.0	15	7.96	144.4	144.40	80	5.08	31
N	3	2	91.0	9	0.86	104.6	244.66	49	5.59	31
N	3	2	89.6	18	12.71	120.5	120.49	80	5.02	31
N	3	2	90.6	12	3.45	140	188.57	69	5.11	30
N	4	2	90.0	15	6.83	144.1	144.10	80	5.07	29
N	4	2	90.8	10	1.24	117.1	224.51	57	5.50	32
N	5	2	90.3	13	5.00	167.9	167.87	79	5.15	32
N	5	2	91.0	10	0.83	99.7	238.47	50	5.63	34
N	5	2	91.0	9	0.54	133.1	231.56	54	5.41	32
N	6	2	89.8	16	8.48	132.3	132.33	80	5.02	31
N	6	2	91.4	8	0.10	103.2	248.60	49	5.19	27
N	6	2	91.4	8	0.34	91.5	258.60	45	5.34	33
N	7	2	90.0	15	6.96	146.4	146.42	80	5.14	32
N	7	2	91.3	9	0.49	107.1	245.64	50	5.31	26
N	7	2	91.5	8	0.21	92.2	261.75	45	5.28	32
N	8	2	89.8	16	9.31	134.7	134.65	80	5.07	32
N	8	2	91.5	8	0.21	78.6	275.86	40	5.56	32
N	9	2	80.9	49	280.10	30.3	30.30	75	12.87	71
N	10	2	82.5	49	238.91	27.3	27.32	75	11.00	65
N	13	2	88.6	19	23.31	124	258.60	71	7.61	44
S	1	2	87.8	12	6.69	35.3	150.92	29	11.24	48

Table A.4: Gradation parameters as indicators of compactability

Quad	Sec	Cycle	Sublot	PCSI*	CA Ratio	FAc Ratio
E	1	1	S	7	0.81	0.36
E	2	1	S	-10	0.20	0.62
E	3	1	S	-10	0.20	0.62
E	4	1+2	S	-10	0.22	0.62
E	5	1+2	S	1	0.60	0.38
E	6	1+2	S	-2	0.31	0.59
E	7	1+2	S	-1	0.32	0.58
E	8	1+2	S	12	0.77	0.36
E	9	1+2	S	10	0.69	0.37
E	10	1	S	12	0.69	0.34
N	1	1	S	5	0.58	0.45
N	2	1	S	3	0.65	0.50
N	3	1	S	4	0.61	0.45
N	4	1	S	5	0.71	0.39
N	5	1	S	-1	0.29	0.47
N	6	1	S	-2	0.37	0.46
N	7	1	S	-3	0.33	0.47
N	8	1	S	-2	0.40	0.46
N	9	1	S	1	0.50	0.58
N	10	1	S	-5	0.35	0.50
N	11	1+2	S	-2	0.31	0.65
N	12	1+2	S	-16	0.13	0.83
N	13	1	S	-14	0.07	0.84
S	1	1	S	-3	0.39	0.58
S	2	1+2	S	-6	0.79	0.54
S	3	1+2	S	-4	0.90	0.49
S	4	1	S	7	0.77	0.39
S	5	1	S	6	0.92	0.32
S	6	1+2	S	14	0.67	0.36
S	8	1+2	S	-9	0.48	0.50
S	9	1+2	S	-3	0.36	0.56
S	10	1+2	S	13	0.79	0.41
S	11	1+2	S	0	0.47	0.59
S	12	1+2	S	7	0.64	0.43
S	13	1+2	S	11	0.77	0.41

* PCSI = Primary control Sieve Index

Table A.4 (continued): Gradation parameters as indicators of compactability

Quad	Sec	Cycle	Sublot	PCSI*	CA Ratio	FAc Ratio
W	1	1+2	S	-19	0.11	0.80
W	2	1	S	-15	0.17	0.63
W	6	1	S	6	0.59	0.56
W	7	1+2	S	-16	0.13	0.65
W	8	1	S	-14	0.12	0.80
W	9	1	S	-5	0.35	0.47
W	10	1+2	S	-6	0.37	0.48
E	1	2	S	-16	0.18	0.61
E	2	2	S	8	0.64	0.27
E	3	2	S	7	0.64	0.28
N	1	2	S	16	1.08	0.32
N	2	2	S	16	1.08	0.32
N	3	2	S	16	1.08	0.32
N	4	2	S	14	1.00	0.32
N	5	2	S	14	1.00	0.32
N	6	2	S	15	1.08	0.32
N	7	2	S	-23	0.49	0.71
N	8	2	S	-23	0.49	0.71
N	9	2	S	-22	0.32	0.71
N	10	2	S	-18	0.13	0.71
N	13	2	S	-18	0.16	0.76
S	1	2	S	-14	0.12	0.88
S	5	2	S	4	0.69	0.33
W	3	2	S	4	0.83	0.48
W	8	2	S	-22	0.25	0.60
W	9	2	S	14	0.61	0.47
S	1	2	B	-15	0.31	0.63
S	2	2	B	-1	0.74	0.50
S	3	2	B	0	0.57	0.56
S	4	2	B	1	0.80	0.50
S	5	2	B	6	0.53	0.56
S	11	2	B	-9	1.07	0.47
N	11	2	B	-1	0.80	0.59
N	12	2	B	2	0.62	0.57
S	8	2	B	-8	1.03	0.46

* PCSI = Primary control Sieve Index

Table A.4 (continued): Gradation parameters as indicators of compactability

Quad	Sec	Cycle	Sublot	PCSI*	CA Ratio	FAc Ratio
W	3	2	B	-10	0.20	0.62
W	4	2	B	-21	0.08	0.72
W	5	2	B	-20	0.08	0.74
W	7	2	B	-22	0.06	0.71
S	1	2	B	-4	0.78	0.58
N	2	2	B	4	0.75	0.43
N	3	2	B	4	0.75	0.43
N	3	3	B	6	0.80	0.40
N	3	4	B	10	0.67	0.48
N	3	5	B	3	0.83	0.41
N	4	2	B	5	0.88	0.41
N	4	3	B	4	0.89	0.38
N	5	2	B	5	0.88	0.41
N	5	3	B	4	0.89	0.38
N	5	4	B	2	1.17	0.39
N	6	2	B	5	0.86	0.41
N	6	3	B	5	0.89	0.40
N	6	4	B	6	0.89	0.42
N	7	2	B	5	0.86	0.41
N	7	3	B	5	0.89	0.40
N	7	4	B	6	0.89	0.42
N	8	2	B	5	0.86	0.41
N	8	3	B	5	0.89	0.40
N	9	2	B	-24	0.25	0.67
N	10	2	B	-21	0.12	0.72
N	13	2	B	-5	0.81	0.57
E	1	2	B	-17	0.22	0.59
E	3	2	B	8	0.73	0.31
N	1	2	B	5	1.13	0.46
N	1	3	B	2	0.78	0.39
N	2	3	B	6	0.80	0.40
N	4	4	B	2	1.17	0.39
N	4	5	B	2	0.86	0.44
N	8	4	B	7	0.89	0.38
w	2	2	B	-21	0.06	0.72

* PCSI = Primary control Sieve Index

Table A.5: Aggregate properties, Cycles I and II

Quad	Sec	Cycle	Primary Agg. Type	CAA	LA Abrasion	Micro Deval	FAA
E	1	1	quartzite	35.4	26.0	4.92	46.1
E	2	1	granite	46.8	26.7	8.00	47.7
E	3	1	granite	46.8	26.9	8.00	47.6
E	4	1	granite	46.8	26.9	8.00	47.6
E	5	1	granite	47.0	27.8	8.00	47.7
E	6	1	granite	47.0	27.8	8.00	47.7
E	7	1	granite	47.0	27.8	8.00	47.7
E	8	1	granite	46.8	26.6	8.00	48.2
E	9	1	granite	46.8	26.6	8.00	48.2
E	10	1	granite	46.8	26.6	8.00	48.2
N	1	1	lms/slag	50.1	39.0	15.00	45.0
N	2	1	lms/slag	50.1	39.0	15.00	45.0
N	3	1	lms/slag	50.1	39.0	15.00	45.0
N	4	1	lms/slag	50.1	39.0	15.00	45.0
N	5	1	lms/slag	50.1	39.0	15.00	44.2
N	6	1	lms/slag	50.1	39.0	15.00	44.2
N	7	1	lms/slag	50.1	39.0	15.00	44.2
N	8	1	lms/slag	50.1	39.0	15.00	44.2
N	9	1	lms/slag	50.1	39.0	15.00	44.2
N	10	1	lms/slag	50.1	39.0	15.00	44.2
N	11	1	granite	46.5	25.0	8.00	47.6
N	12	1	granite	47.0	27.8	8.00	47.7
N	13	1	gravel	38.6	13.4	4.00	39.7
W	1	1	granite	NA	NA	NA	NA
W	2	1	lms/slag	NA	NA	NA	NA
W	3	1	lms/slag	NA	NA	NA	NA
W	4	1	granite	NA	NA	NA	NA
W	5	1	granite	NA	NA	NA	NA
W	6	1	lms/slag	50.1	39.0	15.00	44.3
W	7	1	granite	NA	NA	NA	NA
W	8	1	sndstn/lms/slag	NA	NA	NA	NA
W	9	1	gravel	35.3	28.5	5.60	44.6
W	10	1	gravel	35.3	28.5	5.60	44.6
S	1	1	granite	45.5	45.8	12.98	48.3

Table A.5 (continued): Aggregate properties, Cycles I and II

Quad	Sec	Cycle	Primary Agg. Type	CAA	LA Abrasion	Micro Deval	FAA
S	2	1	gravel	38.6	13.4	4.00	39.7
S	3	1	gvl/lms	37.3	15.3	5.29	43.8
S	4	1	limestone	47.2	12.0	4.00	42.2
S	5	1	gravel	37.9	14.0	2.00	44.6
S	6	1	lms/RAP	23.6	14.2	0.49	44.1
S	7	1	lms/RAP	13.2	7.9	0.27	44.0
S	8	1	mar. schist	47.9	22.0	17.00	50.1
S	9	1	granite	47.5	7.8	1.34	48.3
S	10	1	granite	47.5	9.7	1.67	48.2
S	11	1	mar. schist	47.9	22.0	17.00	50.1
S	12	1	lms	NA	NA	NA	NA
S	13	1	granite	49.6	21.1	0.75	45.1
E	1	2	lms	17.6	8.5	45.3	49.0
E	2	2	marine lms	38.3	36.5	36.4	47.6
E	3	2	marine lms	38.3	36.5	36.4	47.6
N	1	2	grn/lms/snd	30.3	10.8	45.9	44.1
N	2	2	grn/lms/snd	30.3	10.8	45.9	44.1
N	3	2	grn/lms/snd	30.3	10.8	45.9	44.1
N	4	2	grn/lms/snd	30.3	10.8	45.9	44.1
N	5	2	grn/lms/snd	30.3	10.8	45.9	44.1
N	6	2	grn/lms/snd	30.3	10.8	45.9	44.1
N	7	2	granite	33.5	9.9	47.4	46.1
N	8	2	granite	33.5	9.9	47.4	46.1
N	9	2	lms	37.3	17.5	47.5	43.8
N	10	2	lms/chert	23.9	8.8	47.3	44.4
N	13	2	granite	32.3	4.2	48.1	51.9
W	2	2	porph/lms	23.9	7.2	46.6	47.0
W	3	2	lms	36.6	29.3	48.2	48.5
W	6	2	lms/gvl/snd	NA	NA	NA	46.7
W	8	2	granite	26.8	8.6	47.6	43.4
W	9	2	granite	28.4	11.6	51.1	42.3
S	1	2	granite	27.9	12.1	47.3	49.3
S	4	2	lms	18.9	9.1	47.9	44.2
S	5	2	gvl/lms/snd	15.8	3.1	43.9	42.5

APPENDIX B

COMPACTION INFORMATION

Table B.1: ACP for 2000 sections

Quad	Sec	Sublot	Number of Roller Passes			T1*	T2**	T3***	Accumulated Compaction Pressure
			Vibratory	Static	Rubber				
E	1	4	2	4	2	279	242	152	786
E	8	4	4	0	0	203	203	179	720
E	9	4	4	2	0	253	246	159	895
E	10	4	4	0	0	259	233	204	720
N	1	4	2	1	0	223	215	111	358
N	2	4	2	1	0	258	258	128	358
N	3	4	2	3	0	229	218	140	533
N	4	4	4	1	0	222	219	160	807
N	5	4	3	2	0	239	234	220	670
N	6	4	6	1	0	238	228	174	1256
N	7	4	6	0	0	240	240	220	1169
N	8	4	6	1	0	241	231	140	1256
N	9	4	6	0	0	227	214	180	1169
N	10	4	6	0	0	234	231	198	1169
N	11	4	2	2	0	295	280	174	445
N	12	4	2	0	0	320	293	285	271
N	13	4	2	1	0	248	235	156	358
S	1	4	4	1	0	270	270	156	807
S	2	4	7	5	0	285	262	184	1830
S	3	4	3	2	4	249	244	124	1002
S	4	4	3	1	0	275	269	221	583
S	5	4	5	0	0	275	228	187	945
S	6	4	3	0	0	278	253	233	495
S	7	4	4	1	0	279	237	163	807
S	8	4	3	2	0	281	266	173	670
S	9	4	2	0	0	274	258	246	271
S	10	4	4	2	0	243	230	137	895
S	11	4	2	4	2	294	277	151	786
S	12	4	2	4	6	308	265	148	1118
S	13	4	2	4	6	297	292	219	1118
W	1	4	3	1	0	282	278	172	583
W	2	4	4	0	0	248	224	196	720
W	3	4	4	3	0	249	233	200	982
W	4	4	4	0	0	280	246	215	720
W	5	4	3	3	0	276	205	156	757
W	6	4	3	1	0	268	255	215	583
W	7	4	2	1	0	295	276	238	358
W	8	4	1	3	0	304	288	269	374

*T1 = Temperature in °F degress behind the paver
**T2 = Temperature at first pass
***T3 = Temperature at the end of compaction

Table B.1 (continued): ACP for 2000 sections

Quad	Sec	Sublot	Number of Roller Passes			T1*	T2**	T3***	Accumulated Compaction Pressure
			Vibratory	Static	Rubber				
W	9	4	4	2	0	284	263	153	895
W	10	4	4	2	0	276	258	160	895
E	1	2	4	2	0	290	269	148	895
N	1	2	3	2	0	237	237	166	670
N	2	2	2	4	0	241	232	224	620
N	3	2	4	3	0	236	213	139	982
N	4	2	4	1	0	227	209	144	807
N	5	2	3	3	0	225	224	149	757
N	6	2	3	5	0	199	199	160	932
N	7	2	3	5	0	221	221	133	932
N	8	2	5	0	0	251	251	216	945
N	9	2	6	4	0	218	218	132	1518
N	10	2	6	1	0	232	218	164	1256
N	11	2	3	1	0	243	237	220	583
N	12	2	3	1	5	244	209	138	998
S	1	2	1	3	0	290	279	186	374
S	2	2	1	2	0	302	288	264	287
S	3	2	4	0	0	287	281	256	720
S	4	2	2	5	12	312	276	179	1703
S	5	2	2	1	0	293	293	219	358
S	6	2	2	0	8	279	279	173	935
S	7	2	4	3	0	288	261	144	982
S	8	2	5	0	0	300	280	249	945
S	9	2	2	1	0	278	220	200	358
S	10	2	3	1	0	275	264	160	583
S	11	2	5	1	0	288	270	176	1032
S	12	2	2	4	3	271	251	178	869
S	13	2	1	3	0	284	284	267	374
W	1	2	6	1	0	298	270	185	1256
W	2	2	2	5	0	281	263	214	707
W	3	2	6	2	0	298	273	175	1344
W	4	2	2	3	0	290	279	235	533
W	5	2	2	2	0	286	284	254	445
W	6	2	2	0	0	268	266	254	271
W	7	2	4	0	0	280	272	252	720
W	8	2	2	0	0	271	249	244	271
W	9	2	2	1	0	263	263	201	358
W	10	2	3	2	0	260	256	189	670

*T1 = Temperature in °F degress behind the paver
**T2 = Temperature at first pass
***T3 = Temperature at the end of compaction

Table B.2: ACP for 2003 sections

Quad	Sec	Sublot	Number of Roller Passes			T1*	T2**	T3***	Accumulated Compaction Pressure
			Vibratory	Static	Rubber				
E	1	1	2	3	0	281	251	187	529
E	1	2	1	6	0	253	209	176	659
E	2	1	3	2	17	248	217	130	2056
E	3	2	6	1	0	244	168	143	1178
N	1	1	2	6	0	162	150	129	806
N	1	2	4	3	8	275	228	141	1610
N	1	3	1	4	6	280	196	166	972
N	2	1	5	10	6	238	191	109	2300
N	2	3	1	5	10	298	242	173	1397
N	3	2	4	4	5	167	150	132	1453
N	3	3	5	3	10	237	236	175	1984
N	3	4	1	4	2	263	260	165	640
N	3	5	2	7	14	212	212	125	2061
N	4	1	8	0	4	295	214	120	1834
N	4	2	5	4	5	258	230	133	1662
N	4	3	3	4	5	285	194	165	1245
N	4	4	1	2	3	297	200	151	538
N	4	5	1	8	12	275	206	115	1840
N	5	1	5	4	9	194	168	117	1994
N	5	3	5	2	6	230	216	154	1560
N	5	4	3	6	5	318	318	117	1430
N	6	1	4	4	12	216	162	96	2034
N	6	2	2	4	6	251	226	166	1119
N	6	3	3	1	10	262	226	151	1382
N	6	4	2	2	2	248	248	183	602
N	7	1	9	3	10	223	205	113	2818
N	7	3	4	0	7	196	153	128	1249
N	7	4	1	4	7	260	236	184	1055
N	8	4	1	5	0	278	275	155	567
N	9	1	6	3	0	278	249	169	1363
N	10	1	5	3	0	280	245	159	1154
N	10	2	9	3	0	266	223	142	278
N	13	1	2	3	0	290	222	173	1988
N	13	2	2	6	6	212	212	123	1304
S	5	1	1	6	0	273	208	156	659
S	1	1	4	5	0	265	226	147	1131
W	2	1	14	14	0	272	247	121	4047
W	2	2	10	10	0	252	236	115	2844
W	3	1	0	5	4	286	207	138	795
W	9	1	1	4	3	230	158	109	723

*T1 = Temperature in °F degress behind the paver
**T2 = Temperature at first pass
***T3 = Temperature at the end of compaction

APPENDIX C

INFORMATION OF FIELD AND LABORATORY STUDY

Table C.1: Specimens compacted at field thickness

Quad	Prod NMAS	Initial density	PCSI	Field Thickness, mm	ACP	t/NMAS	N@density	N@92 t/field
E1-2000	9.5	94.0	7	52	786.0	5.48	66	33
E8-2000	12.5	92.7	12	53	720.0	4.27	50	36
E10-2000	12.5	93.0	12	56	720.0	4.47	27	18
N1-2000	9.5	95.1	5	50	358.1	5.21	44	28
N3-2000	9.5	94.1	4	53	532.7	5.61	50	30
N4-2000	9.5	93.4	5	53	807.3	5.61	79	35
N6-2000	12.5	94.4	-2	52	1256.4	4.17	71	36
N7-2000	12.5	93.9	-3	50	1169.1	3.96	62	36
N8-2000	12.5	94.7	-2	50	1256.4	3.96	105	37
N10-2000	12.5	94.7	-5	53	1169.1	4.27	85	18
N11-2000	12.5	93.1	-2	104	445.4	8.33	15	10
S1-2000	12.5	94.8	-3	99	807.3	7.92	29	11
S3-2000	9.5	92.7	-4	102	1002.0	10.69	26	23
S4-2000	12.5	94.3	7	102	582.7	8.13	28	15
S5-2000	12.5	94.9	6	104	944.6	8.33	47	18
S6-2000	12.5	92.9	14	52	495.4	4.17	71	46
S7-2000	12.5	93.2	-5	51	807.3	4.06	71	45
S8-2000	9.5	91.8	-1	97	670.0	10.16	13	14
S11-2000	9.5	93.2	0	91	786.0	9.63	21	15
W6-2000	12.5	92.1	6	52	582.7	4.17	47	46
W9-2000	12.5	93.6	-5	51	894.6	4.06	59	38
W10-2000	12.5	93.3	-6	50	894.6	3.96	35	24
N11B-2000	19	92.7	-1	64	582.7	3.37	23	16
S1B-2000	19	93.7	-15	64	374.1	3.37	49	30
S2B-2000	19	93	-1	64	286.8	3.37	44	28
S5B-2000	19	91.5	6	64	358.1	3.37	30	36
S11B-2000	19	94.6	-9	53	1031.8	2.81	136	49
N10-2003	12.5	95.6	-18	51	1154.1	4.06	160	11
N13-2003	12.5	94.6	-18	43	1987.7	3.46	290	34
S1-2003	12.5	95.6	-14	43	1130.7	3.46	145	15

Table C.2: Properties of mixes for field study

Cycle	Qua.	Sec.	CA Ratio	FAc Ratio	% pass 200	AC%	Thick. (mm)	Actual PG	$\%G_{mm}$ @Nini	N @ 92% G_{mm}	CEI
2003	E	1	0.18	0.61	10	6.3	46	78	84.2	26	70.7
	N	1	1.13	0.46	5.8	4.5	53	81	89.3	17	12.7
	N	4	0.88	0.41	5.5	4.3	43	81	90.0	15	6.83
	N	5	1.00	0.32	6.7	6.1	23	81	88.5	24	31.7
	N	6	1.08	0.32	6.8	6.2	28	70	88.7	21	24.3
	S	1	0.12	0.88	13.0	5.1	43	78	87.4	13	8.8
	N	9	0.32	0.71	8.6	6.6	46	74	82.0	43	208
	N	10	0.13	0.71	11.5	6.2	51	74	84.1	33	111.4
	W	3	0.83	0.48	8.7	6.2	33	69	85.8	28	77.2
	W	9	0.25	0.60	7.5	5.8	25	69	89.2	13	5.4
	E	3	0.73	0.31	6	7.9	56	78	89.6	17	13.1
	E	2	0.64	0.27	5.1	7.8	50	69	89.5	18	16.5
2006	N	1	0.81	0.46	8.7	5.7	47	67	91.4	9	0.36
	N	2	0.81	0.49	9.6	5.3	45	76	91.1	10	0.99
	N	5	1.02	0.35	6.8	6.2	50	67	91.3	7	0.77
	N	10	0.83	0.42	5.6	4.4	44	70	84.9	48	187
	E	5	1.07	0.39	6.2	5.2	54	67	91.0	8	1.39
	E	6	1.08	0.40	7.3	5.1	51	76	91.0	8	1.47
	E	7	1.09	0.39	7.2	5.2	54	76	90.8	8	2.25
	S	2	0.58	0.32	6.0	7.0	41	76	89.5	13	9.46
	W	3	1.01	0.38	7.5	6.1	50	67	92.5	5	0.03
	W	4	1.05	0.38	7.6	6.0	56	76	92.1	5	0.02
	W	5	1.00	0.44	8.3	5.1	52	70	91.8	6	0.03

Table C.2 (continued): Properties of mixes for field study

Cycle	Quad	Sec.	NMAS	PCSI	Slope	LockP	ACP	ACP@92 %G_{mm}	Temp 1st pass, F	Temp. Behind Paver, F
2003	E	1	12.5	-16	12.14	50	553	144	251	281
	N	1	19	5	5.95	38	1606	353	228	275
	N	4	19	5	5.07	29	1707	350	230	258
	N	5	9.5	14	5.78	36	2067	1200	168	NA
	N	6	9.5	15	5.96	34	1373	750	162	216
	S	1	12.5	-14	11.42	47	1126	314	226	265
	N	9	12.5	-22	12.60	74	1357	328	249	278
	N	10	12.5	-18	11.29	66	923	353	245	280
	W	3	9.5	4	10.43	58	934	840	221	286
	W	9	9.5	14	7.56	43	843	750	158	230
	E	3	9.5	8	6.27	36	1217	353	168	244
	E	2	9.5	8	6.18	39	1965	216	217	248
2006	N	1	12.5	12	5.95	37	1805	406	198	215
	N	2	12.5	11	5.93	33	1306	445	246	254
	N	5	12.5	15	6.27	33	770	125	212	264
	N	10	19	-6	9.01	57	875	410	263	277
	E	5	12.5	3	6.17	34	1060	118	195	240
	E	6	12.5	8	6.17	35	1570	465	183	276
	E	7	12.5	9	6.26	35	1570	545	199	266
	S	2	9.5	1	7.40	43	1850	765	215	230
	W	3	12.5	15	5.82	33	705	48	240	247
	W	4	12.5	15	5.99	34	595	47	225	260
	W	5	12.5	7	6.28	32	595	99	205	275

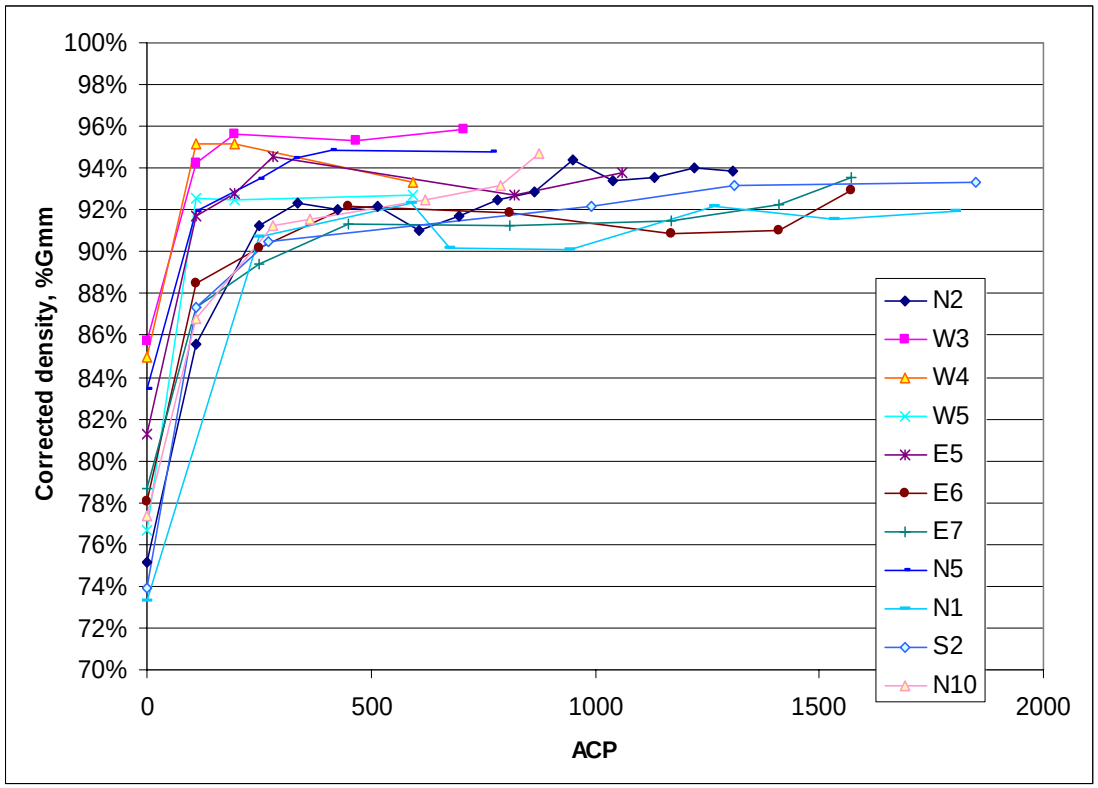

Figure C1: Change in density level as function of compaction pressure for mixes placed in 2006

Table C.3a: Laboratory and field properties for NCHRP 9-27 projects

Project	Prod NMAS	PG Grade	Grad Type	Ndes	Lab Voids	AC %	%Gmm @Ni	N@ 92% Gmm	CEI	Slope	LockPt
VA-1	9.5	70-22	Fine	65	4.55	5.5	89.1	18	17.3	6.6	39
VA-2	19.0	64-22	Coarse	65	4.36	4.7	86.1	27	64.0	9.8	55
VA-3	9.5	64-22	Coarse	65	3.10	5.5	87.8	18	21.7	9.4	60
NC-1	9.5	70-22	Fine	100	5.08	6.9	87.9	31	60.3	6.5	41
CO-1	12.5	58-28	Coarse	75	2.15	6.2	88.1	16	15.1	9.5	51
MO-1	19.0	64-22	Coarse	100	5.53	4.2	82.7	62	339.6	10.3	65
MO-2	19.0	64-22	Coarse	100	4.35	4.5	82.8	49	250.0	11.7	69
UT-2	19.0	64-34	Coarse	125	3.18	4.6	85.9	36	128.4	9.5	56
AL-1	25.0	76-22	SMA	50	1.82	5	89.3	10	2.5	9.7	41
AL-2	25.0	67-22	Fine	100	4.70	3.5	52.5	26	521.8	39.1	40
AL-4	19.0	76-22	Coarse	100	3.55	4.1	87.1	27	57.9	8.5	51
AL-5	12.5	67-22	Coarse	86	2.77	5.5	91.6	8	0.1	5.2	36
FL-2	12.5	64-22	Fine	75	3.37	4.4	91.5	8	0.5	5.0	27
GA-1	12.5	67-22	Coarse	75	3.07	4.7	87.7	19	26.2	9.0	48
GA-2	9.5	67-22	Fine	75	2.38	5.4	89.8	12	4.3	7.6	42
MS-1	12.5	67-22	Fine	80	2.93	4.8	87.7	20	27.6	8.6	50

Table C.3b: Laboratory and field properties for NCHRP 9-27 projects

Project	PCSI	CA	FAc	Initial density	Temp	Field Thickness, mm	ACP	t/NMAS	N@density
VA-1	5	0.64	0.29	91.7	250	38.10	1031	4.0	91
VA-2	-6	1.06	0.47	93.5	265	63.50	991	3.3	121
VA-3	-14	0.41	0.58	91	265	38.10	901	4.0	110
NC-1	14	0.93	0.24	90.6	230	31.80	1407	3.3	150
CO-1	0	0.61	0.55	94.4	230	57.20	1103	4.6	55
MO-1	-10	0.66	0.40	90.5	250	50.80	1673	2.7	109
MO-2	-3	0.87	0.32	93.4	250	101.60	1490	5.3	65
UT-2	-6	1.46	0.46	92.8	250	38.10	1718	2.0	175
AL-1	-10	0.00	0.57	94.4	260	60.90	832	2.4	24
AL-2	17	0.85	0.32	90.7	260	69.90	468	2.8	36
AL-4	1	0.60	0.40	88.5	250	57.20	450	3.0	14
AL-5	-2	0.44	0.56	91.3	230	38.10	970	3.0	80
FL-2	7	1.40	0.24	90	230	37.50	720	3.0	11
GA-1	-3	0.43	0.49	91.3	230	38.10	1475	3.0	61
GA-2	3	0.66	0.41	91.2	230	31.80	1628	3.3	154
MS-1	4	0.86	0.23	92	265	38.10	979	3.0	60

Table C.4: Field compaction information for NCHRP 9-27 projects

Project	Nearest City	Pavement	Date	Weather	Mix Temp behind paver	thickness/ NMAS	Asphalt Grade	TAC	Breakdown Roller	Breakdown Passes	Intermediate Roller	Intermediate Passes	Finish Roller	Finish Passes	T166 %Gmm Achieved
AL-4	Troy	over PCC	10/3/2002	90, little to no wind	315	3	76-22	120+	IR DD110	1, hi amp., hi freq., 2 static			IR DD90	2, static	88.5%
AL-3	Opelika	interstate hwy	8/9/2002	60-65, night, slight breeze	290	2	76-22	8	Dynapac	5 to 6, vib.	Dynapac	4, vib.	Cowin, ST105	1, static	89.8%
FL-2	Marianna	county road	7/9/2002	90, humid, cloudy	255	3	64-22	23	IR DD110	4 static					90.0%
MO-1	Kansas City	over PCC	8/20/2002	70, clear, night		2.7	64-22		IR DD130 in echelon	5, hi amp., hi freq.	IR PT220R pneumatic	5	IR DD90	2 static	90.5%
NC-1	New Bern	2-lane state highway	5/29/2002	80, sunny, no wind	285	3.3	70-22	19	IR DD110HF	4 to 5, hi amp., hi freq.	CAT CB634C	3, hi amp., hi freq.	Hamm HD12	2 static	90.6%
AL-2	Prattville	new lane	8/29/2002	80, overcast	295	2.8	67-22	50	IR DD110	2, hi amp., hi freq., one static			IR DD90	2 static	90.7%
VA-3	Floyd	2-lane county hwy	5/23/2002	70-75, sunny	265	4	64-22	27	IR DD110HF	2 to 3, hi amp., hi freq.	IR DD110HF	2 to 3, hi amp., hi freq.	Dynapac	2 static	91.0%
GA-2	Macon	state hwy	6/23/2002	90, clear		3.3	67-22		IR DD 90	3, med. amp., med. freq., 2 static	pneumatic	15	IR DD90	6	91.2%
GA-1	Junction City	state hwy	6/19/2002	85, humid, mostly cloudy		3	67-22		IR DD130	2, med. amp, med. freq., 4 static	IR PT-125 pneumatic	7	IR DD90	7, static	91.3%
AL-5	Banks	US hwy	6/26/2002	95, partly cloudy	282	3	64-22	28	IR DD90	2, med. amp, med. freq., 3 static			Dynapac	6	91.3%
VA-1	Roanoke	2-lane county road	5/21/2002	70, overcast drizzle	310	4.0	70-22	19	IR DD90	2 to 3, hi amp., hi freq.		2 to 3 static	IR DD90	3 static	91.7%
MS-1	Starkville	new highway	#########	65, clear		3	67-22		CAT CB 634C in echelon	4 vib, 1 static	PS-150B pneumatic		Dynapac CC42	static	92.0%
UT-2	Fillmore	interstate hwy	8/8/2002	90-95, sunny, windy	300	3	64-34	24	IR DD130	4, hi amp., hi freq.	IR Propac 100DA	3 static, 2 vib.	IR DD103	4 to 5, med. amp., med. freq.	92.8%
MO-2	Joplin	new highway	8/23/2002	95, sunny, no wind	315	4.1	64-22	120+	IR DD130	3 to 4, hi amp., hi freq.	IR PT240R pneumatic	8		2 lo vib, 1 static	93.4%
VA-2	Blacksburg	new highway	5/22/2002	60, sunny	300	3.3	64-22	63	IR DD110HF	4 to 5, hi amp., hi freq.			IR DD90 HF	4 to 5 static	93.5%
UT-1	North Glendale	granular base	8/5/2002	90-95, mostly sunny, windy		3	64-34		CAT CB 634C	vib.	CAT PS360B pneumatic		CAT CB634C	static	93.6%
FL-1	Jacksonville	agg base interstate shoulder	5/16/2002	90, sunny, windy	300	5.1	RA295	58	CAT CB 634C	4 to 5, static	IR DD125	six static	IR DD110	4 to 5 static	93.9%
CO-1	Pagosa Springs	unbound base	8/13/2002	80, sunny, light wind	255	4.6	58-28	10	IR DD130	3, hi amp., hi freq.	CAT PS360B pneumatic	4 to 5	IR DD130	2 static	94.4%
CO-2	Silverthorne	existing hwy	8/14/2002	75, sunny, 15-20 mph winds	285	5.3	64-28	24	CAT CB 634C	3, med. amp., hi freq.			CAT CB634C	3 to 4, static	94.4%
AL-1	Opelika	interstate hwy	7/23/2002	80-85, mostly sunny, slight breeze	315	2.4	76-22	64	Dynapac CC522		Dynapac CC522		IR ST105	3 to 4, static	94.4%

TAC: time available for compaction, minutes